

**Functional characterization of DNA dealkylation repair
protein AlkB from *Escherichia coli*
and use of indenone derivatives as inhibitors of AlkB and
human AlkB homologue 3 (AlkBH3)**

Richa Nigam

A Dissertation Submitted to
Indian Institute of Technology Hyderabad
In Partial Fulfillment of the Requirements for
The Degree of Doctor of Philosophy



भारतीय प्रौद्योगिकी संस्थान हैदराबाद
Indian Institute of Technology Hyderabad

Department of Biotechnology

November, 2018

Contents

Declaration	vi
Approval Sheet.....	vii
Acknowledgements	viii
Abstract	x
Synopsis	xii
List of abbreviations.....	xxii
Chapter 1: Introduction	1
1.1 Alkylation damage to DNA	1
1.2 DNA damaging agents	3
1.3 Cellular defence against alkylation damage	3
1.4 Molecular mechanism of DNA dealkylation repair	5
1.5. Human homologs of AlkB	7
1.6 AlkBH3 and cancer	13
1.7 Inhibition of AlkBH3	16
1.8 Indenone derivatives as AlkBH3 inhibitor	23
1.9 Significance and specific objectives	25
1.9.1 Specific objectives	28
1.10 Reference	29
Chapter 2: Functional characterization of <i>E. coli</i> DNA repair protein AlkB.....	53
2.1 Introduction	53
2.2 Materials and method.....	55
2.2.1 cloning.....	55
2.2.2 Purification of recombinant proteins	55
2.2.3 N3meC containing oligonucleotide substrate	56
2.2.4 Preparation of methylated DNA substrate	57
2.2.5 Preparation of Acetoacetanillide	57
2.2.6 Preparation of Ammonium acetate.....	57
2.2.7 10X demethylation assay buffer.....	57
2.2.8 Demethylation assay by direct detection of formaldehyde	58
2.2.9 Preparation of formaldehyde standard curve	59
2.2.10 Demethylation assay by FDH coupled indirect detection of formaldehyde.....	59
2.2.11 Enzyme kinetic analysis	59

2.3 Results and discussion.....	60
2.3.1 SSB facilitated repair of longer ssDNA by AlkB	61
2.3.2 FDH coupled indirect assay to confirm SSB promotes AlkB activity	66
2.3.3 AlkB enzyme kinetics in presence of SSB.....	69
2.4 References	75
Chapter 3: Interaction of AlkB with SSB.....	79
3.1 Introduction	79
3.2 Materials and method.....	80
3.2.1 cloning.....	80
3.2.2 <i>In vitro</i> GST pull down assay.....	82
3.2.2.1 Purification of recombinant His-AlkB protein.....	82
3.2.2.2 Preparation of glutathion sepharose bead-bound GST-SSB	83
3.2.2.3 Interaction of glutathion bead-bound GST-SSB and His-AlkB	84
3.2.2.4 SDS-PAGE.....	84
3.2.2.5 Western blotting	85
3.2.3 Isothermal titration calorimetry(ITC).....	86
3.2.3.1 Purification of tagless AlkB	86
3.2.3.2 The Peptide ligand for ITC	87
3.2.3.3 ITC experiment	87
3.2.4 CD-spectroscopy	87
3.2.4.1 Preparation of protein.....	87
3.2.4.2 CD-experiment	88
3.2.5 Yeast two-hybrid analysis of SSB-AlkB interaction.....	88
3.2.5.1 Yeast strain.....	88
3.2.5.2 Media preparation	89
3.2.5.3 Yeast transformation	89
3.2.5.4 Yeast two-hybrid analysis	90
3.2.5.5 HIS3 selection for interaction positive cells	91
3.2.5.6 Colony lift filter assay using lacZ reporter.....	91
3.3 Results and discussion.....	92
3.3.1 Characterization of direct interaction of AlkB with SSB by yeast-two-hybrid assay	92
3.3.2 Verification of SSB-AlkB interaction <i>in vitro</i>	94
3.3.3 Examination of the strength of SSB-AlkB interaction	96
3.4 References	101
Chapter 4: Screening and evaluation of indenone derivatives as AlkB inhibitors	104
4.1 Introduction	104
4.2 Materials and method.....	105

4.2.1 cloning.....	105
4.2.2 Purification of recombinant AlkB	105
4.2.3 Preparation of methylated DNA substrate	105
4.2.4 Screening of Indenone analogs for AlkB inhibition.....	106
4.2.5 Determination of IC ₅₀	106
4.2.6 CD-spectroscopy	107
4.2.7 Isothermal titration calorimetry (ITC).....	108
4.2.8 Enzyme kinetics	108
4.2.9 Molecular docking	109
4.2.10 Cell survival assay.....	109
4.2.11 Effect of compound 3o on MMS sensitivity	110
4.3 Results and discussion.....	110
4.3.1 Evaluation of Indenone compounds as inhibitor of DNA demethylation repair protein AlkB.....	110
4.3.2 Conformational and binding analysis of AlkB and 3o	114
4.3.3 Mechanism of inhibition of AlkB	117
4.3.4 Prediction of binding pocket	119
4.3.5 Inhibition of AlkB by 3o significantly enhances cell death.....	121
4.4 References	124
Chapter 5: Screening and evaluation of indenone derivatives as potential inhibitors of human AlkBH3	126
5.1 Introduction.....	126
5.2 Materials and method.....	127
5.2.1 cloning.....	127
5.2.2 Purification of proteins.....	127
5.2.3 Preparation of methylated DNA substrate	128
5.2.4 Preparation of double stranded DNA substrate.....	128
5.2.5 <i>In vitro</i> screening.....	128
5.2.6 Determination of IC ₅₀	129
5.2.7 CD-spectroscopy	129
5.2.8 Isothermal titration calorimetry (ITC).....	130
5.2.9 Enzyme kinetics	130
5.2.10 Molecular docking	131
5.2.11 Cytotoxicity analysis.....	132
5.2.12 Effect of AlkBH3 inhibition on cell proliferation.....	132
5.2.13 MMS sensitivity of A549 cells	136
5.3 Results and discussion.....	136
5.3.1 Evaluation of Indenone compounds as inhibitor of DNA repair by human AlkBH3	136

5.3.2 Conformational and binding analysis of AlkBH3 inhibitor 5c	138
5.3.3 Mechanism of inhibition of AlkBH3	142
5.3.4 Compound 5c inhibits proliferation of human lung adenocarcinoma A549 cells in dose dependent manner and sensitizes to alkylating agent MMS	145
5.4 References	155

Declaration

I declare that this written submission represents my ideas in my own words, and where others' ideas or words have been included, I have adequately cited and referenced the original sources. I also declare that I have adhered to all principles of academic honesty and integrity and have not misrepresented or fabricated or falsified any idea/data/fact/source in my submission. I understand that any violation of the above will be a cause for disciplinary action by the Institute and can also evoke penal action from the sources that have thus not been properly cited, or from whom proper permission has not been taken when needed.



Richa Nigam

BO14RESCH01003

Approval Sheet


This thesis entitled **Functional characterization of DNA dealkylation repair protein AlkB from *Escherichia coli* and use of indenone derivatives as inhibitors of AlkB and human AlkB homologue 3 (AlkBH3)** by Richa Nigam is approved for the degree of Doctor of Philosophy from IIT Hyderabad.

Das
25/03/2019

Prof. Amit Kumar Das
Department of Biotechnology
IIT Kharagpur
Examiner



Dr. Thenmalarchelvi Rathinavelan
Department of Biotechnology
IIT Hyderabad
Internal Examiner



Dr. Anindya Roy
Department of Biotechnology
IIT Hyderabad
Adviser/Guide



Prof. Faiz Ahmed Khan
Department of Chemistry
IIT Hyderabad
Chairman

Acknowledgements

First and foremost, I would like to express my sincere gratitude to my supervisor Dr. Anindya Roy for the continuous support of my Ph. D research, for his patience, motivation, and immense knowledge. His guidance helped me in all the time of research and writing of this thesis. I could not have imagined having a better advisor and mentor for my Ph. D study.

Besides my supervisor, I would also like to thank the doctoral committee members; Prof. Faiz Ahmed Khan (Professor, Department of Chemistry, IIT Hyderabad) and Dr. Thenmalarchelvi Rathinavelan (Associate Professor and HOD, Department of Biotechnology, IIT Hyderabad) for their insightful comments and encouragement.

My sincere gratitude to our collaborators; Dr. Prolay Das (Associate Professor, Dept. of Chemistry, IIT Patna) and Dr. Subha Narayan Rath (Associate Professor, Dept. of Biomedical Engineering, IIT Hyderabad) who gave access to their research facility and helped in shaping this research work.

I would also like to thank Prof. U. B. Desai, Director, Indian Institute of Technology Hyderabad for providing the infrastructure and sophisticated instruments to accomplish the research work. I am also grateful to MHRD for the fellowship during my PhD tenure.

I thank my fellow lab mates Dr. Gururaj, Dr. Naveena, Mukul, Monisha, Deepa for their valuable inputs in the course of this study.

Last but not the least, I am grateful to my parents for their constant encouragement and support.

Dedicated to

My Husband

Abstract

DNA alkylation damage, emanating from the exposure to environmental alkylating agents or produced by certain endogenous metabolic processes, affects cell viability and genomic stability. Fe(II)/2-oxoglutarate-dependent dioxygenase enzymes, such as *Escherichia coli* (*E. coli*) AlkB is involved in protecting DNA from alkylation damage. Previous studies have shown that AlkB preferentially removes alkyl DNA adducts from single-stranded DNA (ssDNA). Notably, ssDNA produced during DNA replication and recombination, remains bound to *E. coli* single-stranded DNA binding protein SSB and it is not known whether AlkB can repair methyl adduct present in SSB-coated DNA. Therefore, AlkB-mediated DNA repair using SSB-bound DNA as substrate is studied in the present thesis. By using *in vitro* repair reaction, it is found that AlkB can efficiently remove N3-methyl Cytosine (N3meC) adducts inasmuch as DNA length is shorter than 20 nucleotides. However, when longer N3meC-containing oligonucleotides were used as the substrate, efficiency of AlkB catalyzed reaction is found to be abated compared to SSB-bound DNA substrate of identical length. It is also observed here that truncated SSB containing only the DNA binding domain can support the stimulation of AlkB activity, suggesting the importance of SSB-DNA interaction for AlkB function. Using 70-mer oligonucleotide containing single N3meC, it is demonstrated that SSB-AlkB interaction promotes faster repair of the methyl DNA adducts.

Intrinsically disordered regions (IDRs) of proteins often regulate function through interactions with folded domains. *E. coli* single-stranded DNA binding protein SSB binds and stabilizes ssDNA. The N-terminal of SSB contains characteristic oligonucleotide/oligosaccharide-binding (OB) fold which binds ssDNA tightly but non-specifically. SSB also forms complexes with large number proteins via the C-terminal interaction domain consisting mostly of acidic amino

acid residues. The amino acid residues located between the OB-fold and C-terminal acidic domain are known to constitute an intrinsically disordered region (IDR) and no functional significance has been attributed to this region. Although SSB is known to bind many DNA repair protein, it is not known whether it binds to DNA dealkylation repair protein AlkB. Therefore, AlkB-SSB interaction is characterized in detail in this thesis. It is demonstrated by *in vitro* pull-down and yeast two-hybrid analysis that SSB binds to AlkB via the IDR. The site of contact is found to be the residues 152-169 of SSB. The present study also reveals that unlike most of the SSB-binding proteins which utilize C-terminal acidic domain for interaction, IDR of SSB is necessary and sufficient for AlkB interaction.

The human homologue of AlkB, AlkB homologue 3 (AlkBH3), is also a member of the dioxygenase family of enzymes involved in DNA dealkylation repair. Because of its role in promoting tumor cell proliferation and metastasis of cancer, extensive efforts are being directed in developing selective inhibitors for AlkBH3. The present thesis also reports screening and evaluation of panel of arylated indenone derivatives as new class of inhibitors of AlkB and AlkBH3 DNA repair activity. The indenone-derived AlkB and AlkBH3 inhibitors are found to display specific binding and competitive mode of inhibition. It is demonstrated that AlkB inhibitor has the ability to sensitize cells to methyl methane sulfonate (MMS) that mainly produce DNA alkylation damage and AlkBH3 inhibitor can prevent the proliferation of lung cancer cell line and enhance sensitivity to MMS.

SYNOPSIS

Thesis title: “Functional characterization of DNA dealkylation repair protein AlkB from *Escherichia coli* and use of indenone derivatives as inhibitors of AlkB and human AlkB homologue 3 (AlkBH3)”

Name of the student: Richa Nigam

Roll No: BO14RESCH01003

Degree for which submitted: PhD

Department: Biotechnology

Thesis Supervisor: Dr. Anindya Roy

Introduction

Exposure to environmental or endogenous alkylating agents induces DNA alkylation damages that are known to affect genomic stability, cellular viability and cause multiple diseases such as cancer and aging. Alkylating agents from the environment such as tobacco-specific nitrosamines and chemotherapeutic drugs or endogenous alkylating agents such as S-adenosylmethionine (SAM) can form cytotoxic or mutagenic lesions. DNA damaging alkylating agents are divided into two categories based on the mechanism of alkylation reaction. S_N1 type alkylating agents such as N-methyl-N'-nitro-N-nitrosoguanidine (MNNG) act indirectly by forming a carbocation intermediate and generates mutagenic lesion on both nitrogen and oxygen in DNA such as O⁶-methylguanine and cytotoxic N³-methyladenine. S_N2 type alkylating agents, such as Methyl methanesulfonate (MMS) act directly and produces alkyl adducts predominantly at DNA base nitrogens such as N¹-methyladenine (1meA) and N³-methylcytosine (3meC). N-alkylated DNA adducts m1A and 3meC in single stranded DNA and RNA are repaired by *Escherichia coli*

AlkB which belongs to the family of iron (Fe II) and 2-oxoglutarate-dependent dioxygenases. AlkB catalyzed demethylation reaction is coupled to the oxidative decarboxylation of 2-oxoglutarate (α -ketoglutarate) to succinate and CO_2 resulting in hydroxylation of methyl group. The hydroxymethyl group is unstable and spontaneously released as formaldehyde restoring 1meA and 3meC (Figure 1).

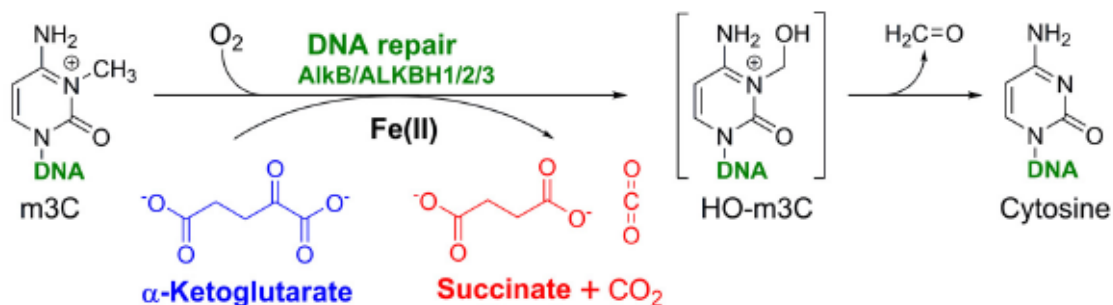


Figure 1. DNA repair reaction catalyzed by AlkB family of enzymes

AlkB preferentially repairs methyl adducts from single stranded DNA. Bacterial single stranded DNA (ssDNA) regions are usually stabilized by binding to single stranded DNA binding protein (SSB.) *E. coli* SSB is a tetrameric protein and each monomer has two domains: the characteristic OB-domain (Oligonucleotide/oligosaccharide Binding) that binds ssDNA and structurally disordered C-terminal domain (CTD). CTD of SSB is known to bind several proteins involved in DNA repair, recombination and replication. The CTD is subdivided into two regions the intrinsically disordered linker region (IDL) and the acidic tip formed by last 8-10 amino acids. The acidic tip is conserved whereas IDL has low sequence complexity and is enriched with a large number of proline, glycine, and glutamine residues. The acidic tip was considered to be essential for protein-protein interaction but recent reports have shown that the linker region also facilitates SSB interaction with other proteins. Homologues of AlkB have been identified across the species from bacteria to mammals and has eight human

homologues (AlkBH1-8). AlkB and its homologues share a common structural feature, known as double-stranded β -helical (DSBH) fold or jelly-roll fold, composed of eight β -strands that form two four-stranded antiparallel β -sheets. This DSBH fold contains conserved sequence motif HXD/E(X)_nH for metal binding. AlkB homologue-3 (AlkBH3), like AlkB, preferentially repairs m1A and 3meC base lesions in ssDNA and RNA.

The present work entitled as “**Functional characterization of DNA dealkylation repair protein AlkB from *Escherichia coli* and use of indenone derivatives as inhibitors of AlkB and human AlkB homologue 3 (AlkBH3)**” has been divided into **5 chapters**. Chapter 1 is General Introduction and focuses on the background of the study and review of the literature. Chapters 2-5 have three sections, namely Introduction, Materials and Methods and Results and Discussions. Overall, this thesis deals with the biochemical and functional characterization of DNA repair protein AlkB. It describes how DNA repair reaction was reconstituted *in vitro* and experiments were carried out to determine its mode of action, especially with respect to the varying length of the substrate. The study also investigates AlkB’s affinity towards SSB and identifies a novel interaction domain on SSB. The present work also elaborates indenone derivatives as a new class of inhibitors against AlkB and AlkBH3. The mechanisms of inhibition, mode of binding and cellular effect were studied extensively.

Chapter 1 is the **General Introduction** which embodies the brief review of the literature dedicated to the AlkB and its human homologue AlkBH3 and their structural features. It mainly describes how substrate specificity of AlkB family of enzymes is regulated. Since AlkB preferentially repairs ssDNA, it also encounters SSB which wraps the ssDNA. Chapter 1 also reviews recent literature on SSB and its interaction partners. The chapter also focuses on AlkB and AlkBH3 inhibitors

reported so far. Based on the structural studies of AlkB and AlkBH3 docking analysis were performed with all the inhibitors reported in the literature to analyze the mode of binding. The chapter also reviews the literature on the mechanism of inhibition, binding affinity and cellular effects of AlkB and AlkBH3 inhibitors.

The significance of the work has been elaborated in this chapter. AlkBH3 has been extensively studied for its role in promoting tumour cell proliferation and metastasis of cancer. Several studies have shown a high level of AlkBH3 expression in non-small-cell lung cancer, prostate cancer, pancreatic cancer and renal cell carcinoma. Knockdown of AlkBH3 in these cells resulted in reduced proliferation. Extensive efforts are being made for developing selective inhibitors for AlkBH3 as therapeutically desirable lead molecules. AlkBH3 inhibitors can be potentially used in combination therapy with chemotherapy agents allowing a reduction in the amount of cytotoxic alkylating agents used in cancer chemotherapy.

Chapter 2 describes **functional characterization of *E. coli* DNA dealkylation repair protein AlkB**. The objectives of this chapter were to characterize DNA-demethylation activity of AlkB with substrates of different lengths and determine the role of SSB in the AlkB-mediated repair of ssDNA substrate. Most of the studies on AlkB activity have analyzed short oligonucleotide substrates or long stretches of ssDNA in a protein-free environment. Since ssDNA generated during DNA replication or repair always remains bound by SSB, SSB-bound ssDNA was studied in this chapter to characterize AlkB activity. In order to study the demethylation activity of AlkB, oligonucleotides of varying lengths 10-70mer containing single 3meC were used as substrates. Demethylation activity was determined by direct repair assay where the formaldehyde released reacts with acetoacetanillide and ammonia forming a fluorescent compound with emission at 465 nm. It was observed that the AlkB can efficiently repair the shorter

oligonucleotide substrates (10mer oligonucleotides), but the repair activity was diminished for longer substrate (70mer oligonucleotides). However, when the complex of longer oligonucleotide DNA bound by SSB was used as a substrate in AlkB demethylation reaction, the repair activity was efficient. It was also observed that the presence or absence of SSB did not alter the AlkB demethylation activity with shorter length substrates. These observations were consistent with the previous reports, which showed that ssDNA shorter than 20 nucleotides failed to bind SSB. To mimic the cellular conditions, the repair reaction was also reconstituted with MMS damaged M13 DNA having numerous randomly located methyl adducts as a substrate for AlkB. When the repair activity was monitored in the presence and absence of SSB, it was found that AlkB activity was significantly higher with SSB bound M13 DNA compared to the free M13 DNA. These results were further confirmed by another method wherein formaldehyde generation was detected via the activity of Formaldehyde dehydrogenase (FDH). In order to examine whether SSB-DNA interaction is required for stimulation of AlkB activity, C-terminal truncated SSB having only DNA binding domain was used to form SSB-DNA complex. This complex was then used as substrate for AlkB repair reaction. It was found that the truncated SSB could also facilitate the repair activity of AlkB. To further explore the mechanism of stimulation of AlkB mediated DNA repair by SSB, kinetics of AlkB catalyzed reaction using 70-mer substrate was studied. Two different 70mer substrates were used to study kinetics, one having single me3C positioned at the terminal and the other having internally located me3C. It was observed that the presence of SSB was dispensable for terminally located methyl adduct repair and no change in kinetic parameters was observed. However, for the internally located damaged residue, it was observed that AlkB was able to repair but with a higher K_M . Addition of SSB significantly stimulated the repair activity and K_M was reduced

considerably. From these studies, it was concluded that as the length of the ssDNA increases, the catalytic efficiency of AlkB decreases. Since the longer stretch of ssDNA is always bound by SSB, AlkB readily repairs such SSB-bound DNA

Chapter 3 focuses on the **interaction of AlkB with SSB**. The objective of this chapter was to characterize the protein-protein interaction between AlkB and SSB. Several sequential deletion constructs of SSB were generated to study AlkB-SSB interaction by the yeast-two-hybrid assay. The direct interactions of proteins were investigated by expression of the reporter genes *HIS3* and *lacZ*. It was observed that the C-terminal domain of SSB interacts directly with AlkB. The site of interaction was mapped between amino acid residues 152–169 of SSB located in the intrinsically disordered linker region. To verify the results of the yeast-two-hybrid assay, SSB-AlkB interaction was studied using in-vitro GST pull-down assay. The results showed that his-tagged AlkB protein was bound to GST-SSB and the site of interaction was found to be amino acid residues 152–169 of SSB belonging to the IDL region. The strength of SSB-AlkB interaction was then studied in presence of increasing ionic strength. It was observed that the interaction of AlkB and SSB was lost at high NaCl concentrations. It was also observed that there is weak interaction between AlkB and SSB. Based on the conclusion from chapter 1, this interaction was also studied in the presence of ssDNA. It was observed that AlkB-SSB interaction was more resistant to high salt NaCl concentrations in presence of DNA suggesting that the presence of ssDNA renders stability to SSB-AlkB complex. To gain further insight into AlkB-SSB interaction, the effect of NaCl was studied on conformation of AlkB and SSB. By CD spectra analysis of SSB it was observed that it remains unchanged at a high salt concentration in agreement with the published reports. The CD spectra analysis of AlkB at lower and higher salt concentrations showed very little conformational change. To further determine the strength of the

interaction between residues 152–169 of SSB and AlkB, thermodynamic parameters were measured by ITC. The synthetic SSB peptide used for ITC was first analyzed by CD spectroscopy to confirm the conformation of the peptide. It was observed that AlkB binds to the SSB peptide weakly with a micromolar dissociation constant.

Chapter 4 describes **Screening and evaluation of indenone derivatives as AlkB inhibitors**. The objective of this chapter was to screen and evaluate a library of 17 indenone derivatives for their potential AlkB inhibition property. The library of indenone derivatives was synthesized in collaboration with Prof. Faiz Ahmed Khan's research group, Department of chemistry, IIT Hyderabad. The indenone compounds were screened using direct repair assay where the formaldehyde release was monitored using purified recombinant AlkB. 40 mer oligonucleotide containing single 3meC was used as a substrate. It was found that a compound **3o** was able to inhibit AlkB activity significantly and the activity of human AlkBH3 remained unaltered in presence of **3o**, suggesting the specificity of **3o** to AlkB. The binding affinity of compound **3o** with respect to AlkB was evaluated using ITC. The ITC data revealed the binding between **3o** and AlkB to be tight with dissociation constant 3.3 μM . The complex formation between AlkB and compound **3o** was also evaluated using CD spectra analysis to find out if there is any local energy change in the overall conformation of AlkB upon **3o** binding. The results indicated slight alterations in the helical content and an alteration of characteristic double-stranded β -helix conformation of AlkB when bound to **3o**. The mechanism of inhibition of AlkB by **3o** was determined by studying the steady-state enzyme kinetics of AlkB in presence of **3o**. For this, the initial velocities of AlkB ~~was~~ were determined and fitted to double-reciprocal Lineweaver-Burk plot. No change in V_{max} was observed in the presence of **3o**, indicating a competitive mode of inhibition for the DNA substrate. The mode of inhibition with respect to co-substrate 2OG was found to be

a mixed type of inhibition. We further analyzed the binding conformation of **3o** using molecular docking. Docking study showed that **3o** interacted with the DNA binding residues of AlkB presumably occupying the DNA binding pocket and blocking AlkB-DNA interaction. To examine whether the compound **3o** can inhibit *E. coli* AlkB function *in vivo*, the proliferation of *E. coli* cells was studied in the presence of compound **3o** and MMS. It was observed that growth of wild-type *E. coli* was more affected by the presence of MMS and **3o** than in the presence of MMS alone. The study in this chapter revealed compounds **3o** to be competitive inhibitors of AlkB-catalyzed demethylation of DNA. This compound exhibited selective binding properties and able to modulate the function of AlkB when present *in vitro* as well as *in vivo*.

Chapter 5 describes **Screening and evaluation of Indenones as potential inhibitors of human AlkBH3**. The objective of this chapter was to screen and evaluate another library of indenone derivatives for inhibition of human AlkBH3. The library of 27 indenone derivatives was synthesized by Prof. Faiz Ahmed Khan's research group, department of chemistry, IIT Hyderabad. In order to screen the library of 27 indenone derivatives for their inhibitory effect on the activity of human AlkBH3, direct repair assay was used. 40-mer oligonucleotide containing single 3meC was used as substrate for the purified recombinant AlkBH3. After initial screening, three compounds (namely, **5c**, **8f** and **10a**) were found to have some inhibitory effect on the human AlkBH3 activity. To determine the inhibitory potential of these three compounds IC-50 was calculated and the compound **5c** was selected as the best hit and characterized further. Next, the ability of the compound **5c** to form a complex with AlkBH3 was studied by using CD spectroscopy and ITC. Comparison of CD spectra of AlkBH3 and **5c**-bound AlkBH3 indicated that there are subtle conformational changes induced by **5c** binding which might involve only

a few residues from a larger and structured domain, most probably the jelly roll fold where active site is located. Then, the binding affinity of **5c** to AlkBH3 was determined by ITC. The data revealed tight binding between **5c** and AlkBH3 with dissociation constant 7.8 μ M. Mechanism of inhibition of the compound **5c** was determined by studying the steady-state enzyme kinetics. For this, the initial velocity of AlkBH3 was determined in the presence of increasing concentrations of compound **5c**. The results indicated unchanged V_{max} which is a characteristic feature of a competitive inhibitor. With respect to 2OG, the compound **5c** showed a mixed type inhibitor. In order to get a better understanding of **5c**-AlkBH3 interaction, molecular docking studies were performed. Docking analysis demonstrated that **5c** binding site lies in close proximity of the active site and it interacts with catalytically important residues of AlkBH3. Human AlkBH3 is overexpressed in non-small cell lung adenocarcinoma cell line A549 and AlkBH3 gene silencing inhibited A549 cell survival. In order to test the *in vivo* effect of **5c** as AlkBH3 inhibitor, A549 cells were treated with increasing concentration of **5c** and cell survival was monitored using MTT assay. It was found that **5c** treatment indeed affected the viability and proliferation of A549 cells. Interestingly, MMS sensitivity of A549 cells was significantly increased in the presence of **5c**, suggesting that compound **5c** could be an inhibitor for AlkBH3. Thus, this chapter clearly established that the compound **5c** could inhibit the function of AlkBH3 *in vitro* and *in vivo* and exhibited modest binding properties.

List of Abbreviations

DNA	:	Deoxyribonucleic acid
N1meA	:	N1-methyl adenine
N3meA	:	N3-methyl adenine
N6meA	:	N6-methyl adenine
N7meA	:	N7-methyl adenine
N3meT	:	N3-methyl Thymine
N1meG	:	N1-methyl Guanine
N2meG	:	N2-methyl Guanine
N3meG	:	N3-methyl Guanine
N7meG	:	N7-methyl Guanine
N1meC	:	N1-methyl Cytosine
N3meC	:	N3-methyl Cytosine
N4meC	:	N4-methyl Cytosine
O6meG	:	O6-methyl Guanine
O2meT	:	O6- methyl Thymine
O4meT	:	O4-methyl Thymine
O2meC	:	O2-methyl Cytosine
RNA	:	Ribonucleic acid
MGMT	:	O6-methyl guanine DNA methyltransferase
SAM	:	s- adenosyl-L-methionine
DNMT	:	DNA-methyltransferase
ϵ A	:	Etheno adenine
ϵ C	:	Etheno cytosine
MMS	:	Methyl methanesulphonate
2OG	:	2-oxo glutarate
DSBH	:	Double-stranded β -helix
ASPH	:	Asparaginyl hydroxylase
BER	:	Base excision repair
PCNA	:	Proliferating Cell Nuclear Antigen
RRM	:	RNA-recognition motif
VEGF	:	Vascular endothelial growth factor
RNAi	:	RNA interference

RCC	:	Renal Cell carcinoma
NOG	:	N-oxalylGlycine
DON	:	6-Diazo-5-oxo-L-norleucine
BPTES	:	Bis-2-(5-phenylacetamide-1,3,4-thiadiazol-2-yl)ethyl sulfide
2HG	:	2-hydroxyglutarate
TCA	:	Tri carboxylic acid cycle
IDH	:	Iso-citrate dehydrogenase
PARP	:	poly ADP ribose polymerase
SSB	:	Single-strand DNA-binding protein
DTIC	:	Trade name for Dacarbazine
E coli	:	Escherichia coli
OB	:	oligonucleotide/oligosaccharide-binding
IDL	:	Intrinsically Disordered linker
NaCl	:	Sodium chloride
IPTG	:	Isopropyl β -D-1-thiogalactopyranoside
HCl	:	Hydro chloric acid
Rpm	:	revolution per minute
TE	:	Tris-EDTA
EDTA	:	Ethylenediaminetetraacetic acid
RFU	:	Relative fluorescence unit
Nm	:	Nano metre
NAD	:	Nicotinamide adenine dinucleotide
CTD	:	Carboxy terminal Domain
FDH	:	Format dehydrogenase
V _{max}	:	maximum velocity
K _m	:	Michaelis constant
GST	:	Glutathione S-transferase
Ni-NTA	:	Nickel - nitrilotriacetic acid
PBS	:	Phosphate buffer saline
HRP	:	Horseradish peroxidase
ITC	:	Isothermal titration calorimetry
CD	:	Circular Dichroism
UV	:	Ultraviolet
DOB	:	Drop out base

SD	:	Syntheticdefined
β -gal	:	β -galactosidase
w/o	:	without
IDR	:	Intrinsically disordered region
Kd	:	Dissociation constant
V/v	:	volume/volume
V _o	:	Initial velocity
OD	:	Optical density
IC ₅₀	:	Inhibitory concentration
DMEM	:	Dulbecco's Modified Eagle Medium
MTT	:	3-(4,5-Dimethylthiazol-2-Yl)-2,5-Diphenyltetrazolium Bromide
DMSO	:	Dimethyl sulfoxide

Chapter 1: Introduction

1.1 Alkylation damage to DNA

DNA is exposed to harmful alkylation damage by endogenous and exogenous agents at all times. Alkylating agents from the environment such as tobacco-specific nitrosamines and chemotherapeutic drugs used in cancer treatment such as Temozolomide, Melphalan causes alkylation damage in the DNA[1]. Alkylating agents can react with 16 different sites of the DNA bases [2]as well as with phosphate backbone of DNA generating methyl phosphoesters (MTE)[3] (**Table 1**). Alkylating agents can introduce methyl or ethyl groups at all of the available nitrogen and oxygen atoms in DNA bases, producing fifteen different types of base modifications [2]. Among these, N7-methylguanine (N7meG), 3-methyladenine (N3meA) and O6-methylguanine (O6meG), are specific to the double-stranded DNA [4]. Whilst N7-methylguanine is relatively harmless, N3meA has a strong toxic effect [4]. The methyl group of N3meA protrudes into the minor groove of the double helix, which is normally free of methyl groups (the methyl groups of thymine and 5 methylcytosines are in the major groove) [5]. N3meA efficiently blocks RNA polymerase and replicative DNA polymerases resulting in a strong cytotoxic but low mutagenic effect [6]. The low mutagenicity observed may be due to trans-lesion synthesis by DNA polymerases [7] . O6meG is highly mutagenic and directly demethylated by O6-methylguanine-DNA methyltransferase (MGMT) [8]. This protein transfers the methyl group to a Cystein residue within the active site resulting in self-inactivation [8]. In single-stranded DNA (ssDNA), N1-methyladenine (N1meA) and N3- methylcytosine (N3meC) lesions are mostly

observed as all the other nitrogen lone pairs required for nucleophilic attack are occupied with hydrogen bonding in double-stranded DNA[9]. These lesions are cytotoxic but less mutagenic as they are unable to base pair but able to block DNA replication [1, 9, 10].

Table 1: Alkylation adducts caused by DNA damaging agents

S. No.	Alkylated base	Fe(II)/2OG dioxygenase involved in repair	Reference
1.	N1meA	AlkB, AlkBH2, AlkBH3, AlkBH1	[6, 11, 12]
2.	N3meA	-	
3.	N6meA	AlkBH1, AlkBH5, FTO	[13-15]
4.	N7meA	-	
5.	N3meT	AlkB, AlkBH2, AlkBH3, FTO	[6, 11, 12] [16, 17]
6.	N1meG	AlkB, AlkBH1, AlkBH3	[6, 11, 12] [16]
7.	N2meG	AlkB	[18]
8.	N3meG	-	
9.	N7meG	-	
10.	N1meC	-	
11..	N3meC	AlkB, AlkBH1, AlkBH2, AlkBH3	[6, 11, 12]
12.	N4meC	AlkB	[18]
13.	O6meG	-	
14.	O2meT	-	
15.	O4meT	-	
16.	O2meC	-	
17	Phosphate tri-ester	-	

1.2 DNA damaging agents

Endogenous sources of alkylation damage come from many types of reactive byproducts generated from biochemical reactions inside cells. The enzyme cofactor S-adenosylmethionine (SAM) is the methyl donor in many biomethylation pathways and is produced in cells in high concentrations ranging from 20 μM to 50 μM [19, 20]. This molecule can methylate DNA at a rate characteristic of weak alkylating agents [21, 22]. The peroxidation of lipids in the cell membranes by free radical byproducts of cellular metabolism can create alkylating agents that damage DNA. The main lesions produced by this mechanism are ethenoadenine (ϵA) and ethencytosine (ϵC) [23]. The genomic DNA also gets methylated at N3 position of cytosine by non-specific demethylation activity of DNA methyltransferases (DNMTs) [24]. DNMT3a and 3b have been revealed as one of the major endogenous source of N3meC lesions as these enzymes introduce 3000-5000 N3meC bases per genome [24]. Cells are also exposed to DNA damaging alkylating agents that occur in the environment and endogenously generated byproducts of cellular oxidative metabolism that leads to the damage in the genome. Some alkylating agents such as naphthyridinomycin and cyanocycline-A are used in cancer chemotherapy [25, 26]. Simple methylating agents, such methyl methane sulphonate (MMS), methylate DNA resulting N7meG and N3meA [27]. MMS also methylate single-stranded DNA and results in N1-meA and N3meC [10].

1.3 Cellular defense against alkylation damage

To cope with the alkylation damage to DNA caused by endogenous as well as exogenous alkylating agents and to maintain the genome integrity, cells have evolved repair pathways against alkylation specific DNA damage. In *E coli*,

resistance to alkylation damage is orchestrated by an increased expression of four genes, namely, *ada*, *alkB*, *alkA*, and *aidB*, collectively called ‘*ada regulon*’ [28] . This coordinated response of cells to the alkylation damage is called the adaptive response or ‘*ada response*’ and their induction provides protection against alkylation damage to DNA[29]. The enzyme which has been known to be involved in repair of N1meA and N3meC is known as alkylation repair protein-B (AlkB) in *E. coli* [16]. AlkB is a Fe(II)-2-oxoglutarate(2OG)-dependent dioxygenase which catalyzes the demethylation reaction. AlkB-catalyzed reaction mechanism is initiated by the oxidative decarboxylation of 2OG to succinate and CO₂ resulting in the removal of the methyl group from N1meA and N3meC [28, 30]. The methyl group is hydroxylated and spontaneously released as formaldehyde [31, 32]. AlkB deficient *E. coli* cells are prone to the accumulation alkylated lesions in the DNA. The AlkB deficient *E. coli* cells also show hypersensitivity towards alkylating agents [33].

E.coli AlkB is a 216 amino acids protein which has a characteristic double stranded beta helix (DSBH) protein fold that involves eight beta strands forming two four-stranded antiparallel β -sheets [34, 35]. AlkB structure consists of 3 well-defined regions: (1) a catalytic core in the carboxy-terminal domain, (2) a nucleotide recognition lid and (3) N-terminal extension. As shown in **Figure 1**, AlkB has the characteristic H131..D133....H187 triad which is important for the coordination of Fe atom in the catalytic core [34] . In addition to the characteristic HDH triad, AlkB also has the RXXXXXXR motif where the first arginine residue is involved in the coordination of Fe atom while the other arginine is involved in AlkB-specific substrate binding[36]. The carboxylate moiety of 2OG forms salt bridge with R204 and R210 residues of AlkB protein[36]. The N-terminal 1-90 amino acids of AlkB

constitute the nucleotide recognition lid. In the absence of DNA, this lid is flexible and allow access to the wide range of alkyl adducts containing substrate [37]. In the open conformation of AlkB, the damaged base binds to a hydrophobic cavity where it is held by the base stacking interaction with H131 and W69 from the nucleotide recognition lid [37]. In the absence of bound substrate, Y76 flips away from active site thereby allowing the damaged base to access the catalytic core [37]. The T51-Y55 loop shifts about 2.5Å from the active site upon binding of the substrate. In the closed conformation, the Y76 residue interacts with the damaged base and clamps it into the positions for the catalysis [37].

1.4 Molecular mechanism of DNA dealkylation repair

E. coli AlkB catalyzes oxidative demethylation reaction which requires Fe(II) and 2OG as cofactor and co-substrate, respectively. Detailed mutational and structural studies have revealed molecular mechanism of AlkB catalyzed reaction. It promotes the two-electron oxidation of the substrate coupled with decarboxylation of 2OG to form succinate and CO₂ leading to demethylation of the damaged base the restoration of undamaged base in the DNA. For Substrate binding, W69 and H131 stack against the damaged base and facilitate substrate recognition by forming π - π interactions. W76 forms hydrogen bond interactions to the two phosphates 5' of the methylated base which holds the substrate to the active site. AlkB modifies the DNA backbone around the alkylated base so that the alkylated base is flipped out into the active site and the two flanking bases are “squeezed” and stacked together. This base flipping mechanism is a characteristic feature of AlkB [38].

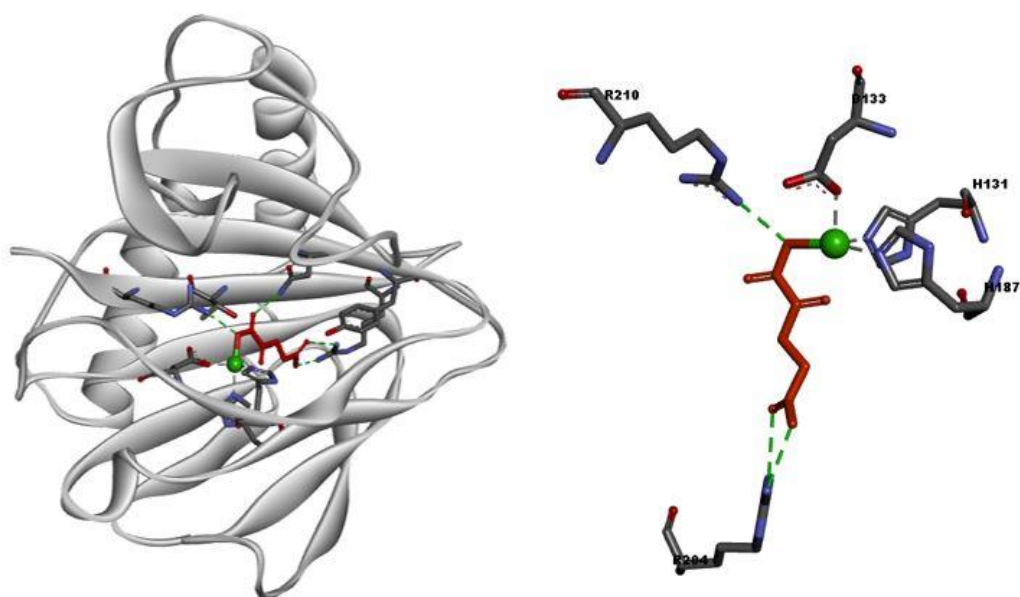
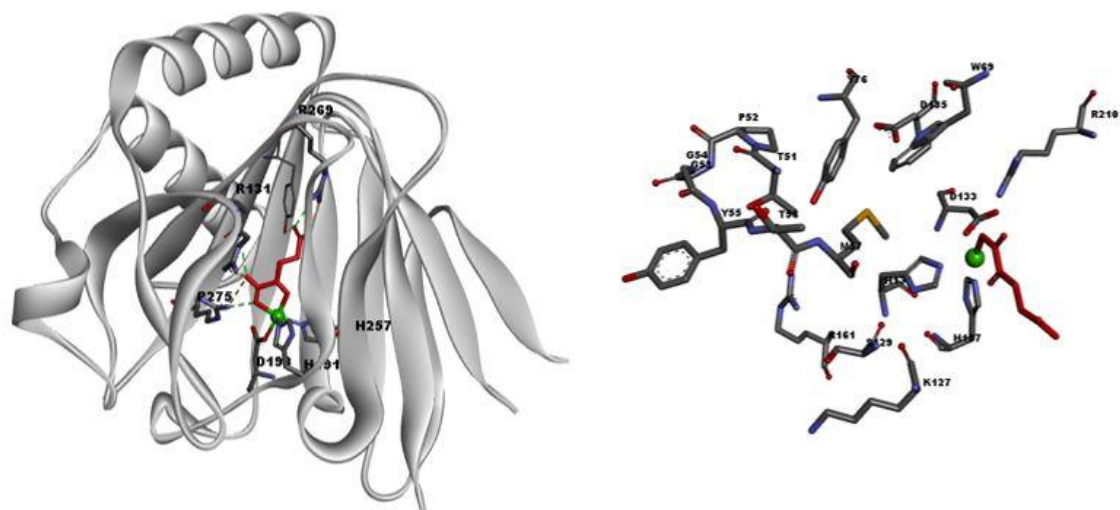
A**B**

Figure 1. Structure of AlkB and AlkBH3 showing active site residues. (A) The active site iron is co-ordinated by amino acid residues H131, D133 and H187. R210 and R204 are involved in interaction with 2OG. (B) The active site of AlkBH3 is co-ordinated by H191, D193 and H257. 2OG is co-ordinated by R131, R269 and R275.

Active site iron has a five-coordinate geometry: it is coordinated by H131, H187 and D133. The other two coordination sites are occupied by C1 carboxyl and C2 keto group of 2OG, respectively. C-5 carboxyl of 2OG hydrogen bonds to Y122 and N206 and thus held at the active site. This coordinated iron is utilized to activate the dioxygen molecule for oxidation of inert C-H bond [38] .

1.5 Human homologs of AlkB

The human Fe(II)-2OG-dependent dioxygenase family consists of over 60 members sharing conserved structural feature of AlkB, such as DSBH fold and HDH triad, necessary for iron and cofactor binding. All the members of this family also share the common mechanism of hydroxylation of their specific substrates [39, 40]. Apart from DNA dealkylation repair, Fe(II)-2OG-dependent dioxygenase are involved in range of metabolic processes viz (a) hydroxylation of Asp/Asn residues in epidermal growth factor-like domains, ankyrin repeat domains of the asparaginyl hydroxylase(ASPH) FIH, and splicing regulatory proteins (the lysyl-hydroxylase JMJD6), (b) antibiotic biosynthesis in prokaryotes (c) oxygen sensing in humans, (d) fatty acid metabolism and (e) chromatin modification and modification of proteins via demethylation of lysine residues [41]. Sequence analysis revealed that there are nine Fe(II)-2OG-dependent dioxygenase that are similar to *E.coli* AlkB and are known as AlkBH1-9 [42] [43].

AlkBH1 was the first discovered AlkB homologue in humans. Protein sequence homology showed that AlkBH1 is structurally closest to AlkB among all the human homologues of AlkB [44]. The structural features also indicated that the protein is longer than AlkB by 71 amino acids in the N-terminus and 42 amino acids in the C-terminus[45]. The subcellular localization of AlkBH1 remains controversial

to date. Ougland *et al* showed that AlkBH1 is localized in the nucleus of human embryonic stem cells while Westby *et al* have reported AlkBH1 as a mitochondrial protein [46, 47]. Six different enzymatic activities of AlkBH1 have been reported in the literature. AlkBH1 has been reported to have weak N3meC demethylation activity in ssDNA and RNA. It does not repair other methylated bases such as N1meA double-stranded DNA [47]. AlkBH1 has been also reported to have a tRNA binding domain and demethylates N1meA at position 58 tRNA (N1meA58). It has been proposed that demethylation of N1meA58 by AlkBH1 signals degradation of tRNA, thus regulating the level of tRNA-iMet in the cells[14]. AlkBH1 also modifies the wobble base in the mitochondrial tRNA^{met} by oxidizing 5-methyl cytosine to generate 5-formylcytosine in the mitochondria [48]. These studies showed that apart from DNA repair, AlkBH1 also plays a direct role in mitochondrial translation regulation [49]. AlkBH1 has also been reported to demethylate Histone H2A [46]. Knockout studies have shown that *ALKBH1*^{-/-} mice die at an embryonic stage. It has been reported that AlkBH1 regulates stemness by interacting with key transcription factors OCT4, NANOG and SOX2 which are essential for embryonic development[50]. Knockdown of *ALKBH1* enhances the pluripotency markers and delay the induction of early differentiation genes. Mouse study from Pan *et al* have also emphasized the role of AlkBH1 in transcriptional regulation and showed that AlkBH1 knockout leads to trophoblast lineage defects[51]. Another study reported enzyme activity of AlkBH1 in demethylation of N6meA of DNA in the mouse embryonic stem cells. AlkBH1 deficient cells accumulate N6meA which leads to silencing of X-chromosome genes and delayed differentiation[52, 53]. Osteogenic differentiation in human mesenchymal stem cells

is regulated by AlkBH1 mediated demethylation of N6meA. Depletion of AlkBH1 leads to accumulation of N6meA resulting in transcriptional silencing[52]. AlkBH1 has also been reported to have DNA Apurinic/aprimidinic lyase (AP lyase) activity[54]. The Ap-lyase activity is conserved across species[55]. The AP-lyase activity is independent of the Fe^{II}/2OG and the catalytic site differs from the HDH triad [54, 56, 57]. AlkBH1 AP-lyase activity is mediated via β -elimination reaction. However, AlkBH1 does not play any role in the BER pathway [58]. It has been reported that K133 is a catalytically important residue with respect to AP lyase activity; K154 and K182 are located within 5Å of serine residues S136, S147, and S181 which could be essential residues for AP-lyase activity[45]. Crystallographic studies are required to determine precisely the AP lyase activity site in AlkBH1.

Two human homologues, AlkBH2 and AlkBH3 were identified to have biochemical activity similar to AlkB[59, 60]. Human AlkBH2 repairs methylation damage preferentially in double-stranded DNA. It has very low activity on the ssDNA or RNA[61]. It has been reported to be mostly a housekeeping gene maintaining the genome integrity by repairing the methylation adducts N1meA and N3meC[35, 61] [16]. AlkBH2 has been found to have a rather promiscuous substrate specificity. It can demethylate a number of methyl adducts such as N1meA, N3meC and a number of etheno adducts in the genomic DNA by the base flipping mechanism[62]. It has been reported that AlkBH2 colocalizes in the nucleus where it interacts with PCNA in the replication fork during S-phase of the cell cycle[63, 64]. AlkBH2 interacts with PCNA using a specific interaction motif identified on PCNA as AlkBH2-PCNA-interaction motif [65, 66]. Studies on mouse models have shown that AlkBH2^{-/-} mice are more sensitive to MMS induced cytotoxicity.

Mutation frequency also increases significantly in *AlkBH2*^{-/-} [67]. However, knockout studies have also shown that knockout of *AlkBH2* or *AlkBH3* neither affect the viability nor lead to any significant phenotype [68]. Mice study has shown that *AlkBH2* knockout results in accumulation of methyl adducts in the genome, substantiating that *AlkBH2* is essential for genome maintenance [69]. Overexpression of *AlkBH2* has been reported in glioblastoma which made the cells resistant to chemotherapeutic agent temozolomide [70]. There have been reports of mutated forms of *AlkBH2* expressing in certain brain tumor samples, colon cancer, and bladder cancer [71-74]. Rosic *et al* have found that DNMT3a and DNMT3b and have co-evolved with *AlkBH2* among the eukaryotes. *AlkBH2* is involved in repair of N3meC adducts generated non-specifically by DNMT3a and 3b. Loss of *AlkBH2* leads to accumulation of N3meC in the genome [24].

AlkBH3 is another human homologue of *AlkB* which has biochemical (DNA demethylation) activity similar to *AlkB*. *AlkBH3* repair methylation damage primarily N1meA and N3meC from ssDNA and RNA as efficiently as *AlkB*. There are subtle differences in the substrate preference of *AlkB*, *AlkBH2*, and *AlkBH3* arising from the different amino acid residues present in their substrate binding pocket [16, 60]. *AlkBH3* have been found to be the only human *AlkB* homologue which can reactivate the phage mRNA by demethylation of the methylated residues [75]. *AlkBH3* has been found to be co-localizing in the cytoplasm as well as the nucleus and does not exhibit any cell cycle-dependent variation in sub-cellular localization [59, 64]. *AlkBH3* interacts with 3'-5' helicase ASCC3 [76]. *AlkBH3* has been also reported to repair N6meA in tRNA. It was found that tRNA modified by *AlkBH3* help in increasing translation efficiency [77]. Mouse knockout study showed that

absence of AlkBH3 did not result in any significant phenotype, but it was found that the triple knockout of AlkBH2, AlkBH3, and DNA glycosylase AAG caused a synergistic phenotype in inflammation-associated colon cancer suggesting the possibility of overlapping substrate specificity [71]. AlkBH3 overexpression has been associated with poor prognosis in a wide array of cancers. The relevance of AlkBH3 with cancer cell proliferation has been discussed in detail in section 1.6.

AlkBH4 has been recently identified as Fe(II)-2OG dependent dioxygenase based on structural conservation but the substrate specificity and biological functions remain largely unknown[78]. Protein-protein interaction study has shown that AlkBH4 interacts with proteins involved in chromatin regulation and transcription[79]. AlkBH4^{-/-} mice were found to be embryonic lethal[80]. AlkBH4 has been found to be involved in demethylation of K84 in actin and play some role in actin-myosin regulation dynamics. AlkBH4 co-localizes with the actomyosin-based contractile ring and mid-body via association with methylated actin[15]. AlkBH4 knockout studies also revealed that it is essential for the completion of meiosis. AlkBH4 knockout leads to leads to the insufficient establishment of the synaptonemal complex [15, 80]. The detailed study of the enzymatic function of AlkBH4 *in vitro* and *in vivo* is not yet reported.

AlkBH5 is a hydroxylase which catalyzes demethylation of N6meA methyl group from RNA[81]. AlkBH5 is co-localized in the nucleus. AlkBH5^{-/-} mice display impaired male fertility resulting from compromised spermatogenesis, aberrant apoptosis, and altered gene expression in the testes[81, 82]. Human AlkBH5 has been reported to be induced under hypoxia and has been suggested to

have a direct interaction with Hypoxia-Inducible factor (HIF) in MCF-7, U2OS and IMR-32 cells[83].

AlkBH6 has been found to be localized in the nucleus as well cytoplasm in normal human tissues [84] . The *in vitro* enzyme activity, substrate specificity and *in vivo* significance of AlkBH6 has not been characterized to date.

AlkBH7 has been reported as a mitochondrial protein with a conserved mitochondrial localization signal. AlkBH7 has been associated with programmed necrosis [85, 86] . Programmed necrosis refers to the programmed cell death which is mediated by receptor-interacting protein kinase-1 and 3; and is independent of caspase mediated cell death signaling pathway [87]. It has been observed that AlkBH7 knockout makes the cells resistant to cell death which is induced by alkylating agents namely, MMS [85] . Knockout of AlkBH7 in mouse models leads to obesity indicating that AlkBH7 plays a role in fatty acid metabolism [88]. The substrate specificity and *in vitro* activity of AlkBH7 is yet to be characterized.

AlkBH8 has been characterized as Fe(II)/2OG dependent dioxygenases with tRNA methyltransferase domain [89]. Along with the conserved HDH triad, AlkBH8 also possesses an RNA recognition motif (RRM) and methyltransferase domain. methyltransferase domain of AlkBH8 catalyzes the methylation of 5-carboxymethyluridine to 5-methoxycarbonylmethyluridine in tRNAs with UPyN (Py = C/U) as an anticodon triplet sequence, whereas the AlkB domain catalyzes the hydroxylation of 5-methoxycarbonyl methyluridine to S-5-(methoxycarbonyl hydroxymethyl)uridine specifically in tRNAGly (UCC)[90-93].

AlkBH9 is also known as fat and obesity associated protein (FTO). AlkBH9/FTO has been characterized to have RNA demethylation activity. It has

been known to hydroxylate N3meT and N3meU in the mRNA [17, 94]. Recent reports have shown that N6meA is the major substrate for FTO[95]. Mouse model studies have shown that FTO knockout leads to reduced adipose tissues and enhanced metabolism[96]. Genome-wide association studies have shown that there is a strong link between FTO polymorphism and type II diabetes and obesity [96-100]. Extensive efforts are being made to identify small molecule inhibitors for FTO. In summary, it can be said that most of the human AlkB homologues are multi-functional and there are many more functions likely to be discovered for these proteins besides the nucleic acid repair or regulation of epigenetic methylations activity reported so far.

1.6 AlkBH3 and Cancer

Of the nine AlkB homologs AlkBH2 and AlkBH3 have been well established to have DNA repair activity similar to AlkB. AlkBH3 has been primarily associated with repair of methylation damage in single-stranded DNA and RNA [16] . AlkBH3 has been known to be up-regulated in several cancers [101] . AlkBH3 is highly expressed and associated with poor prognosis in several types of cancers. It has been shown that AlkBH3 binds to the promoter of genes important for transcriptional regulation[102]. It has been proposed to be essential for maintaining the genomic integrity of cancer cells.[102]

AlkBH3 is initially identified as one of the Prostate cancer antigen as it is overexpressed in androgen-independent prostate cancer cells and cancer survival is dependent on AlkBH3 expression [103, 104] . RNAi mediated knockdown of AlkBH3 in prostate cancer cell lines PC-3 has resulted in the induction of apoptosis [104]. It is overexpressed in Castration-resistant and hormone-independent

prostate cancer [105]. AlkBH3 knockdown also inhibited anchorage-independent cell growth of prostate cancer cell line DU145 [105]. The *in vivo* gene silencing also lead to reduced tumorigenesis via decreased Akt activity and hence reduced PI3K-Akt pathway [105]. Effort to design an AlkBH3 inhibitor has led to the discovery of HUHS015, as a small molecule inhibitor for AlkBH3 [106].

AlkBH3 is also overexpressed in pancreatic cancer and promotes cancer cell proliferation [107]. Like prostate cancer, high level of AlkBH3 in pancreatic cancer is associated with poor prognosis. RNAi mediated silencing of AlkBH3 in PANC-1 cells reduces VEGF expression and leads to suppression of cell proliferation [107]. AlkBH3 plays an important role in the progression of human urothelial carcinoma. AlkBH3 is overexpressed in KU7 urothelial carcinoma cell line. RNAi mediated knockdown of AlkBH3 in KU7 cells leads to cell cycle arrest in G1 phase. In these cells, AlkBH3 acts as an upstream molecule to NOX-2-ROS and Tweak/VGEF signaling thus promoting tumor survival and angiogenesis [108].

AlkBH3 was found to be contributing significantly to cancer cell survival and proliferation of lung adenocarcinoma [109]. It has also been proposed as the therapeutic target for lung adenocarcinoma and squamous cell carcinoma [109]. Mouse model studies have shown that RNAi mediated silencing of AlkBH3 in non-small cell lung cancer cells A549 leads to reduced proliferation. Knockdown of AlkBH3 inhibits cancer proliferation by inducing cell cycle arrest at G2/M phase leading to senescence or induction of apoptosis[109]. The phenotype induced by AlkBH3 knockout in lung cancer cell lines depends on the *TP53* status of cells. In the cell lines with wild-type *TP53* (e.g., A549 or NCI-H1650), AlkBH3 knockdown

leads to cell cycle arrest; while AlkBH3 silencing leads to apoptosis in cell lines expressing mutated p53 [110].

AlkBH3 has also been associated with renal cell carcinoma (RCC) which is the most common type of kidney cancer [111]. High level of AlkBH3 in RCC cell line CAKI-1 are related to tumor metastasis and progression. Knockdown of AlkBH3 by siRNA resulted in the induction of apoptosis and reduced cancer cell proliferation. The high AlkBH3 expression is also linked to poor prognosis [111]. AlkBH3 was found to be inactivated in breast cancer patients [112]. The promoter region of AlkBH3 was found to undergo aberrant methylation in the CpG Island resulting in gene silencing. Higher levels of promoter methylation were associated with reduced patient survival [112]. Both AlkBH2 and AlkBH3 were found to be mutated in glioma patients. AlkBH2 I141V mutation and AlkBH3 D189N mutations were found in patient samples. These mutant proteins were overexpressed in brain tumor samples. Overexpression might be responsible for repairing the DNA damage caused by therapeutic alkylating agents during chemotherapy thereby reducing the efficiency of therapy.[72] AlkBH3 was also found to be overexpressed and involved in carcinogenesis in colorectal cancer. The significance of AlkBH3 overexpression in the prognosis of cancer has not been elaborately studied yet[113]. Candidate gene study has found AlKBH3 as one of the genes associated with papillary thyroid cancer[114]. AlkBH3 has also been associated with hepatocellular carcinoma. High expression of AlkBH3 was found in patient samples with poor prognosis[115].

Alkylating agents are extensively used as chemotherapeutic agents, which damage the DNA and cause replication fork stalling ultimately leading to loss of genome integrity and cell death. AlkbH3 assists in cell survival and cancer

proliferation. Being a DNA repair protein, it associated with replication fork and repairs the methylation damage caused by chemotherapeutic agents. Since the cancer cell proliferation is dependent on AlkBH3 overexpression, AlkBH3 can be a potential anti-cancer therapeutic target.

1.7 Inhibition of AlkBH3

As described in the previous section, AlkBH3 has been extensively studied as a regulatory gene involved in promoting tumor cell proliferation and metastasis of cancer. Extensive efforts have been directed towards developing selective inhibitors for AlkBH3 (**Table 2**). AlkBH3 inhibitors can be potentially used in combination therapy with alkylating agents; which can be significantly effective in reducing the amount of alkylating agents used in cancer chemotherapy. There have been multiple approaches towards designing inhibitors of AlkBH3. One stream of studies has been entirely focused on the biochemical mechanism of action of molecule, its chemical characterization, and its binding parameters. However, the *in vivo* significance of inhibition remains lagging and there is no data relating to the *in vivo* activity of the molecule. Cell permeability, toxicity and other *in vivo* parameters of the molecule remain unaccounted. Another approach for inhibitor design has been focused on the pre-clinical inhibition studies of AlkBH3. Extensive studies have been carried out using cell lines and mouse models to study the *in vivo* effect of the lead molecule, however, the biochemical parameters for enzyme-ligand binding have not been studied. Although the molecule shows *in vivo* tumor growth inhibition, the mechanism of action, affinity of the molecule, binding pocket, and other biochemical parameters remain unknown, hence limiting the possibility of improvement and design of other analogs with more efficiency. It appears that a

combined approach towards designing of AlkBH3 inhibitors is lacking. A combined study should include studying the biochemical parameters such as the mechanism of action, binding affinity, binding pocket in the protein cavity as well as *in vivo* study as the guiding principle for design of the small molecules. The inhibitor should be then studied using cell lines and mouse models to understand the pharmacokinetics and pharmacodynamics.

One major concern while designing inhibitors for this class of enzymes is the selectivity of small molecule inhibitors. Due to the similar catalytic mechanism followed by this large family of enzymes, targeting one of the enzymes selectively is a difficult task. There have been very few studies with a combined approach where AlkBH3 has been targeted selectively. In order to achieve specificity, the emphasis should be on targeting the substrate binding pocket as the site for inhibitor binding. The substrate binding pocket for each member of the AlkB family has been attributed to unique properties so that different proteins bind to a wide range of substrates. Those amino acid residues should be targeted to selectively inhibit these enzymes[116].

The crystal structure of AlkBH3 shows that the iron is coordinated by H191, D193 and H257 (**Figure 1B**). The substrate binding pocket of AlkBH3 is more polar compared to AlkB and AlkBH2. There is a hairpin loop extended by three amino acid residues R122, E123 and D124 which makes the DNA binding groove comparatively more negatively charged (**Figure 2**). This unique feature of AlkBH3 is also defined as RED fist [117, 118]. These unique characteristics of the enzyme could be targeted so as to achieve selective inhibition. However, one of the factors hindering the design of AlkBH3 inhibitor is the fact that the crystal structure of

AlkBH3 lacks the N-terminal 69 residues. Multiple Sequence alignment of AlkBH3 sequence across species shows that the N-terminal region of AlkBH3 is highly conserved. The well-defined nucleotide recognition lid in AlkB is formed by the first 90 amino acid residues. No such feature has been defined in the truncated AlkBH3 structure. AlkBH3 N-terminal 69 amino acids could be functionally important. Secondly, there is no AlkBH3 structure with a bound DNA substrate available, unlike AlkB and AlkBH2. Availability of substrate-bound structure reveals crucial information about the interacting residues, their three-dimensional geometry, and overall protein folding and provide an insight into designing inhibitors.

Several generic Fe(II)-2OG-dependent dioxygenase inhibitors have been identified that compete 2OG binding [119]. These compounds act as nonreactive analogs of 2OG, and their functionalization enables inhibition, either by increasing potency towards a particular 2OG oxygenase or by blocking binding to another oxygenase. Most of the molecules targeting the active site have been found to be the generic inhibitors for FeII-2OG dependent dioxygenase family. Welford *et al* have extensively studied the inhibition of this family of enzymes using 2OG analogs. They have found N-oxalyl glycine (NOG), N-oxalyl-4s-alanine, N-oxalyl-4r-alanine, 2-thiono derivative of NOG, 2-hydroxyglutamate and 2-mercaptoglutamate be a generic inhibitors for AlkB family [119]. These compounds are essentially analogs of 2OG. Crystallographic studies have shown that these molecules bind to the active site of AlkB. Several structural analogs of NOG have also been screened for potent AlkB inhibitors. N-oxalyl-L-cysteine derivatives 1 and 3-hydroxypyridine carboxamides have been identified as potent inhibitors of AlkB family [120]. There

have not been any studies relating to the *in vivo* efficiency of 2OG analogs as inhibitors of AlkB family. Inhibition of AlkB and its human homologues using DNA aptamers were also studied. Highly efficient aptamer for AlkB was characterized which binds to AlkB with nanomolar affinity [121, 122] . Inhibition of AlkBH2 using aptamer was also studied [121, 122] . The aptamers are highly potent in targeting this sub-family of enzymes as they bind selectively in a non-competitive manner to both DNA substrate and co-substrate 2OG[121, 122]. However, no such aptamer has been identified for AlkBH3 inhibition which is clinically more crucial drug target than AlkBH2. Also, the *in vivo* significance of aptamer-based drug candidate needs to be established. The *in vivo* evaluation of aptamer-based inhibitors for AlkB has not been done.

Glutamine deficiency also leads to inhibition of AlkBH family of enzymes by depleting the levels of 2OG in tumors which are Myc and K-Ras driven [123] . The levels of 2OG are maintained by TCA cycle in these cells. 2OG is an essential co-substrate for AlkBH enzymes, depletion of which leads to the inactive enzyme. This implies that small molecule inhibitors of glutamine metabolism such as DON (6-Diazo-5-oxo-L-norleucine), CB-839, and BPTES (Bis-2-(5-phenylacetamide-1,3,4-thiadiazol-2-yl)ethyl sulfide) would be potential inhibitors of AlkB family of enzymes [123].

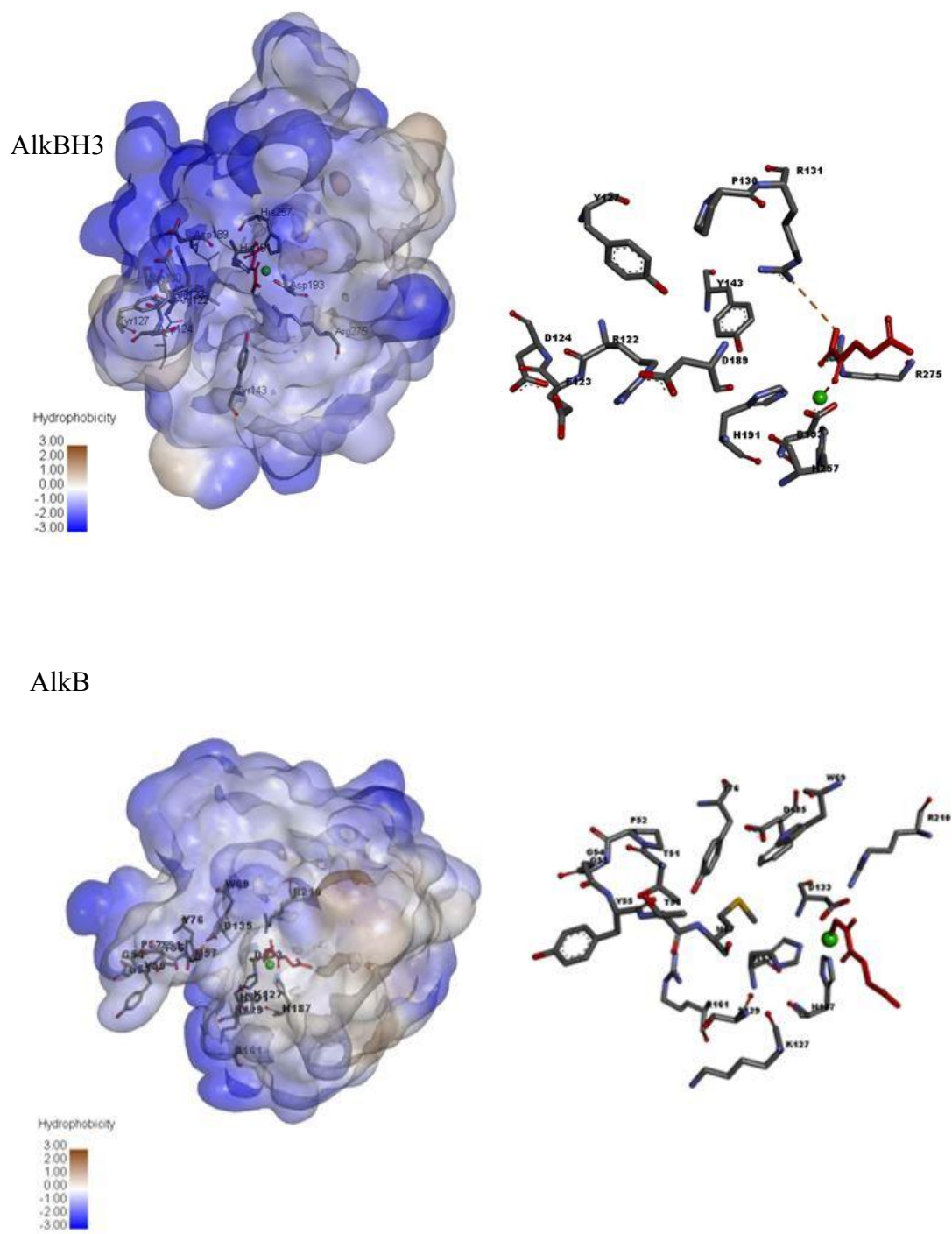


Figure 2: Hydrophobicity analysis of AlkBH3 structure (2IUW) and AlkB structure (3I2O) shows that the DNA binding pocket of AlkBH3 is comparatively rich in polar amino acids compared to AlkB.

Copper ion has also been identified as an inhibitor of AlkB and its human homologues AlkBH2 and AlkBH3 under Wilson's disease conditions [124]. The normal cellular concentration of copper does not affect the activity of these enzymes, but under Wilson's disease condition the cellular concentration of copper goes up and accumulation of Cu(II) ions inhibit AlkBH2 and AlkBH3 activity [124].

Oncometabolites are another important group of AlkBH3 inhibitors. Molecule 2-hydroxyglutarate (2HG) and its two stereoisomers (D- and L-2HG) have been characterized as inhibitors of AlkB family of enzymes AlkBH2 and AlkBH3 [125, 126]. These molecules are generated in tumor cells due to a mutation in TCA cycle enzyme iso-citrate dehydrogenase 1 and 2 (IDH1 and IDH2). Tumor-derived mutant forms of IDH catalyze the NAD-dependent dehydrogenation of 2OG to D-2-hydroxyglutarate (D-2HG), in renal cell carcinomas and in tissues under hypoxic conditions. These compounds act as competitive inhibitors of 2OG [125, 126].

A flavonoid Quercetin, which is an iron chelator, has also been studied as an inhibitor of FeII/2OG dependent dioxygenases. It has been found that Quercetin depletes the cellular iron levels below 1 μ M thereby inhibiting enzymes such as PHDs and AlkB by non-specific iron chelation [127, 128].

Tanaka and co-workers have screened a library of pyrazole derivatives for AlkBH3 inhibition and found HUHS015 to be a potent AlkBH3 inhibitor [106, 129, 130]. The study has been focused on the pre-clinical aspect of AlkBH3 inhibition in prostate cancer cell lines and xenograft mouse model without molecular characterization. The important aspects of drug targeting such as bioavailability, toxicity, dosage have been characterized. However, the key biochemical mechanism

remains to be determined. Also, subfamily selectivity, which is a major concern while designing inhibitors for AlkBH family has not been studied. Ueda *et al* screened another chemical library and identified compound **71** as an inhibitor of AlkBH3 which was more potent than HUHS015 [129]. The study has shown the characterization of the compound *in vivo* and extended their pre-clinical data on mice with prostate cancer. They have tested the AlkBH3 inhibition by compound **71** *in vitro* as well as *in vivo* conditions. However, the *in vitro* characterization of the compound such as the mechanism of inhibition, binding affinity, selectivity and determination of the binding pocket has not been done [129].

Another AlkBH3 inhibitors studied recently is rhein [131]. Li *et al* have studied the biochemical mechanism of inhibition by rhein followed by *in vivo* effect. But, this study has not been extended to the pre-clinical level. Another limiting factor to Rhein is that it does not target AlkBH3 selectively. Rhein has been shown to inhibit activities of bacterial AlkB and Human another AlkB human Homologue FTO[132]. Since Rhein is not a selective inhibitor, it cannot be a potential lead molecule to target cancer cells dependent on AlkBH3 expression.

Recently, Das *et al* have developed a new technique involving zwitterionic peptide-based tags to differentiate between proteins of a subfamily [133]. Using the technique they have identified selective inhibitors to AlkBH3, AlkBH5, and FTO [133]. They have shown compound **8** to be a selective inhibitor of AlkBH3. They have also proposed the binding site of ligand to be the DNA binding pocket of AlkBH3. Compound **8** has been proposed to be interacting with residues essential for DNA binding [133], however, crystallography studies need to be performed to

substantiate the results. Also, the *in vivo* effect of compound **8** remains unknown, which is required for characterization of this compound as a lead molecule [133].

Table 2: Inhibitors of AlkB and AlkBH3 reported in the literature

Inhibitor Name	Target	Reference
Analogs of 2OG (N-oxalyl-4s-alanine, N-oxalyl-4r-alanine, 2-thiono derivative of NOG, 2-hydroxyglutamate and 2- mercaptoglutamate)	AlkB	Welford et al, [119]
Analogs of 2OG (N-oxalyl-L-cysteine derivatives- 1and3-hydroxypyridine arboxamides)	AlkB	Woon et al, [120]
Glutamine metabolism inhibitors (Glutaminase inhibitors- DON, CB-839, BPTES)	AlkBH3	Tran et al, [123]
DNA aptamers (5' TGC CTA GCG TTT CAT TGT CCC TTC TTA TTA GGT GAT AAT A 3')	AlkB, AlkBH2	Krylova et al, [122]
Copper ion (Cu ²⁺)	AlkB AlkBH2 AlkBH3	Bian et al, [124]
Oncometabolite (D- and L-2Hydroxyglutamate)	AlkB AlkBH2 AlkBH3	Chen et al, [125]
Iron chelator (Quercetine)	AlkB	Triantafyllou et al, [127]
Pyrazol derivative HUHS015	AlkBH3	Ueda et al, [77]
Rhein	AlkB, AlkBH2 AlkBH3	Li et al, [131]
Sulphonamide analog (compound 8)	AlkBH3	Das et al, [133]

1.8 Indenone derivatives as AlkBH3 inhibitor

Indenone is a biologically important structural motif present in several natural products. [134]. Indenone derivatives have garnered a wide attention in medicinal

chemistry as indenone analogs have been used for a variety of applications. For example, euplectin is a lichen derived indenone derivative which has cytotoxic properties against murine P-815 mastocytoma cell line[135]. The indenone core is also found in resveratrol-derived natural products such as plauciflorol-F which are known to inhibit cancer proliferation[136]. The indenone core is also present in the neo-lignin isolated from the fruit of *Virola sebifera* and 3-arylindenone has been found to have anti-tumor activity[137]. From the synthetic chemistry point of view, indenone is a neutral molecule which is well suited to derivatization. Several indenone analogs have been synthesized and their biological activity has been evaluated. Indenone derivatives have been studied as agonist for PARP activation in type II diabetes [138]. Indenone analogs were found to be moderate inhibitors of estrogen receptors. Structural analogs of indenone have also been used as a fluorescent binding agent to estrogen receptors[139, 140]. Several 2-arylidene-1-ones have been screened for inhibition of estrogen receptor- β and estrogen receptor- α [141]. Indenone analogs have been used as a novel scaffold for targeting Androgen receptors in breast cancer[142]. Indenone derivatives have shown tubulin inhibition without any cytotoxicity in breast cancer cell line MCF-7[143]. Indenone analogs have also been explored as anti-mitotic molecules for targeting tubulin. The molecule can be used as an anti-cancer drug[144]. Derivatives with indenone core have also been evaluated for inhibition of tyrosine kinase activity of Fibroblast Growth factor Receptor (FGFR) and loss of FGFR regulation has been associated with several vascular diseases[145]. Indenone derivatives have been studied as inhibitors of cyclooxygenase-2 (COX-2) as well. Structural analogs of nimesulide and flosulid having indenone skeleton were studied as selective inhibitors of COX-

2[146]. Indenone derivatives have also been used as fermentation activators, estrogen binding receptors, and precursors for gibberellins[147].

In the present study, one indenone derivatives were evaluated as the inhibitor for Fe(II)-2OG-dependent dioxygenase and one compound **5c** was identified as a selective inhibitor for human AlkBH3 and another compound **3o** was identified as a selective inhibitor for AlkB. The biochemical parameters for these small molecules interacting with AlkBH3 and AlkB have also been characterized.

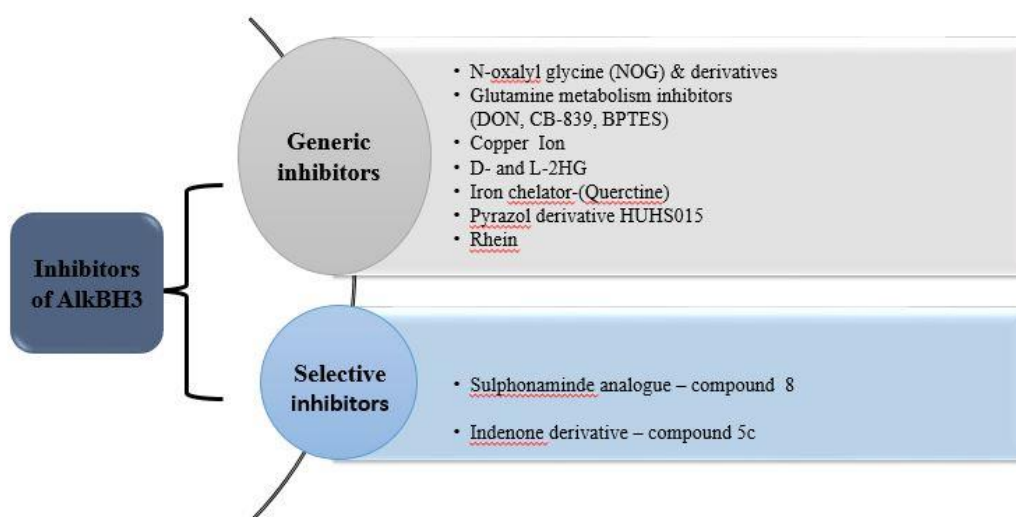


Figure 3: Summary of AlkBH3 inhibitors

1.9 Significance and specific objectives

AlkB and its human homologs AlkBH2 and AlkBH3 are essential for maintaining the genome integrity by removing methyl adducts from DNA which are potentially mutagenic. A thorough understanding of the substrate preference and mechanism of DNA repair is essential for determining the suitable strategy to inhibit these enzymes. AlkB and its human homolog AlkBH3 have been known to prefer N3meC and N1meA adducts on single stranded DNA as substrate; however, it is also well

established that single stranded regions of the DNA remain coated with ssDNA binding protein SSB. Thus, it is important to understand how presence of SSB affects the activity of AlkB. Since the studies for selective inhibition of AlkB family of enzymes have not been able to achieve the sub-family selectivity, it is essential to study the designing and mechanism of small molecule inhibitor for AlkB, which could then provide a scaffold and act as guiding principle for designing small molecule inhibitors for AlkBH1-8. The role of AlkBH3 in promotion of cell proliferation and metastasis of cancer has been widely studied. Since AlkBH3 overexpression has direct implication on cancer cell survival, selective inhibition of these enzymes will prove to be an effective as combinatorial therapy along with chemotherapeutic agents. It could be speculated that inhibition of AlkBH3 repair pathway will lead to accumulation of DNA damage. DNA damage can be tolerated by cell to certain extent beyond which it will lead to stalling of replication fork causing cell to undergo apoptosis. Genome instability is one of the major driving-force of cancer. The activity of repair pathways is coordinated by damage signaling network which is lost in case of cancerous cells thus, uncontrolled DNA repair promotes genome instability and cancer progression [148]. DNA repair inhibitors can be implemented for reducing the amount of cytotoxic alkylating agents used in cancer chemotherapy such as mechlorethamine, chlorambucil, cyclophosphamide, busulfan, dacarbazine (DTIC) [149-151]. Also, cancer cells usually have high metabolic rate, which leads to generation of endogenous alkylating agents such as SAM. These damages are repaired by direct repair pathway. Inhibition of AlkBH3 may cause extensive DNA damage in cells endogenously, ultimately causing prolonged cell cycle arrest. [152]. The synthesis of inhibitors of AlkB family is

important for targeting cancer cells which are heavily dependent on AlkBH3 for genome maintenance. Cancer cells often have several DNA repair pathways inactivated and they rely on a few DNA repair enzymes. Targeting these enzymes may lead to loss of genomic integrity and cell death due to synthetic lethality. AlkBH3 inhibitors in combination with other chemotherapeutic drugs may also be synthetic lethal in cancers such as lung adenocarcinoma, prostate and pancreatic cancer which are dependent on the AlkBH3 overexpression.

1.9.1 Specific objectives

- Functional characterization of *E. coli* DNA dealkylation repair protein AlkB
- Interaction of AlkB with SSB
- Screening and evaluation of indenone derivatives as AlkB inhibitors
- Screening and evaluation of Indenone derivatives as human AlkBH3 inhibitors.

1.10 References

1. Hecht, S.S. and D. Hoffmann, *Tobacco-specific nitrosamines, an important group of carcinogens in tobacco and tobacco smoke*. *Carcinogenesis*, 1988. **9**(6): p. 875-884.
2. Singer, B. and D. Grunberger, *Molecular biology of mutagens and carcinogens*. 2012: Springer Science & Business Media.
3. Schulz, W.G., R.A. Nieman, and E.B.J.P.o.t.N.A.o.S. Skibo, *Evidence for DNA phosphate backbone alkylation and cleavage by pyrrolo [1, 2-a] benzimidazoles: small molecules capable of causing base-pair-specific phosphodiester bond hydrolysis*. 1995. **92**(25): p. 11854-11858.
4. Friedberg, E.C., et al., *DNA repair and mutagenesis*. 2005: American Society for Microbiology Press.
5. Kelly, J.D., et al., *Relationship between DNA methylation and mutational patterns induced by a sequence selective minor groove methylating agent*. 1999. **274**(26): p. 18327-18334.
6. Delaney, J.C. and J.M.J.P.o.t.N.A.o.S. Essigmann, *Mutagenesis, genotoxicity, and repair of 1-methyladenine, 3-alkylcytosines, 1-methylguanine, and 3-methylthymine in alkB Escherichia coli*. 2004. **101**(39): p. 14051-14056.
7. Monti, P., et al., *Mutagenicity of N3-methyladenine: a multi-translesion polymerase affair*. 2010. **683**(1): p. 50-56.

8. Pegg, A.E., M.E. Dolan, and R.C. Moschel, *Structure, function, and inhibition of O6-alkylguanine-DNA alkyltransferase*, in *Progress in nucleic acid research and molecular biology*. 1995, Elsevier. p. 167-223.
9. Rajski, S.R. and R.M. Williams, *DNA cross-linking agents as antitumor drugs*. Chemical reviews, 1998. **98**(8): p. 2723-2796.
10. Beranek, D.T., *Distribution of methyl and ethyl adducts following alkylation with monofunctional alkylating agents*. Mutation Research/Fundamental and Molecular Mechanisms of Mutagenesis, 1990. **231**(1): p. 11-30.
11. Koivisto, P., et al., *Demethylation of 3-methylthymine in DNA by bacterial and human DNA dioxygenases*. 2004. **279**(39): p. 40470-40474.
12. Li, D., et al., *Repair of DNA alkylation damage by the Escherichia coli adaptive response protein AlkB as studied by ESI-TOF mass spectrometry*. 2010. **2010**.
13. Jia, G., et al., *N6-methyladenosine in nuclear RNA is a major substrate of the obesity-associated FTO*. 2011. **7**(12): p. 885.
14. Wu, T.P., et al., *DNA methylation on N 6-adenine in mammalian embryonic stem cells*. 2016. **532**(7599): p. 329.
15. Zheng, G., et al., *ALKBH5 is a mammalian RNA demethylase that impacts RNA metabolism and mouse fertility*. 2013. **49**(1): p. 18-29.
16. Falnes, P.Ø., et al., *Substrate specificities of bacterial and human AlkB proteins*. Nucleic acids research, 2004. **32**(11): p. 3456-3461.
17. Jia, G., et al., *Oxidative demethylation of 3-methylthymine and 3-methyluracil in single-stranded DNA and RNA by mouse and human FTO*. 2008. **582**(23-24): p. 3313-3319.

18. Li, D., et al., *Removal of N-alkyl modifications from N 2-alkylguanine and N 4-alkylcytosine in DNA by the adaptive response protein AlkB*. 2013. **26**(8): p. 1182-1187.
19. Posnick, L.M. and L.D.J.J.o.b. Samson, *Influence of S-Adenosylmethionine Pool Size on Spontaneous Mutation, Dam Methylation, and Cell Growth of Escherichia coli*. 1999. **181**(21): p. 6756-6762.
20. Barrows, L.R. and P.N.J.C. Magee, *Nonenzymatic methylation of DNA by S-adenosylmethionine in vitro*. 1982. **3**(3): p. 349-351.
21. Rydberg, B. and T. Lindahl, *Nonenzymatic methylation of DNA by the intracellular methyl group donor S-adenosyl-L-methionine is a potentially mutagenic reaction*. The EMBO journal, 1982. **1**(2): p. 211-216.
22. Näslund, M., D. Segerbäck, and A.J.M.R.L. Kolman, *S-Adenosylmethionine, an endogenous alkylating agent*. 1983. **119**(3-4): p. 229-232.
23. El Ghissassi, F., et al., *Formation of 1, N6-ethenoadenine and 3, N4-ethenocytosine by lipid peroxidation products and nucleic acid bases*. Chemical research in toxicology, 1995. **8**(2): p. 278-283.
24. Rošić, S., et al., *Evolutionary analysis indicates that DNA alkylation damage is a byproduct of cytosine DNA methyltransferase activity*. 2018. **50**(3): p. 452.
25. Scott, J.D. and R.M.J.C.R. Williams, *Chemistry and biology of the tetrahydroisoquinoline antitumor antibiotics*. 2002. **102**(5): p. 1669-1730.
26. Hayashi, T., et al., *Inhibition of nucleic acid biosynthesis in procaryotic and eucaryotic cells by cyanocycline A*. 1983. **36**(9): p. 1228-1235.

27. Beranek, D.T.J.M.R.F. and M.M.o. Mutagenesis, *Distribution of methyl and ethyl adducts following alkylation with monofunctional alkylating agents*. 1990. **231**(1): p. 11-30.
28. Trewick, S.C., et al., *Oxidative demethylation by Escherichia coli AlkB directly reverts DNA base damage*. 2002. **419**(6903): p. 174.
29. Lindahl, T., et al., *Regulation and expression of the adaptive response to alkylating agents*. Annual review of biochemistry, 1988. **57**(1): p. 133-157.
30. Falnes, P.Ø., R.F. Johansen, and E.J.N. Seeberg, *AlkB-mediated oxidative demethylation reverses DNA damage in Escherichia coli*. 2002. **419**(6903): p. 178.
31. Falnes, P., A. Klungland, and I. Alseth, *Repair of methyl lesions in DNA and RNA by oxidative demethylation*. Neuroscience, 2007. **145**(4): p. 1222-1232.
32. Trewick, S.C., et al., *Oxidative demethylation by Escherichia coli AlkB directly reverts DNA base damage*. Nature, 2002. **419**(6903): p. 174.
33. Delaney, J.C. and J.M. Essigmann, *Mutagenesis, genotoxicity, and repair of 1-methyladenine, 3-alkylcytosines, 1-methylguanine, and 3-methylthymine in alkB Escherichia coli*. Proceedings of the National Academy of Sciences, 2004. **101**(39): p. 14051-14056.
34. Yu, B., et al., *Crystal structures of catalytic complexes of the oxidative DNA/RNA repair enzyme AlkB*. 2006. **439**(7078): p. 879.
35. Yang, C.-G., et al., *Crystal structures of DNA/RNA repair enzymes AlkB and ABH2 bound to dsDNA*. Nature, 2008. **452**(7190): p. 961.

36. Holland, P.J. and T. Hollis, *Structural and mutational analysis of Escherichia coli AlkB provides insight into substrate specificity and DNA damage searching*. PLoS One, 2010. **5**(1): p. e8680.
37. Holland, P.J. and T.J.P.O. Hollis, *Structural and mutational analysis of Escherichia coli AlkB provides insight into substrate specificity and DNA damage searching*. 2010. **5**(1): p. e8680.
38. Yang, C.G., K. Garcia, and C.J.C. He, *Damage detection and base flipping in direct DNA alkylation repair*. 2009. **10**(3): p. 417-423.
39. Ng, S.S., et al., *Crystal structures of histone demethylase JMJD2A reveal basis for substrate specificity*. Nature, 2007. **448**(7149): p. 87.
40. Clifton, I.J., et al., *Structural studies on 2-oxoglutarate oxygenases and related double-stranded β -helix fold proteins*. Journal of inorganic biochemistry, 2006. **100**(4): p. 644-669.
41. Johansson, C., et al., *The roles of Jumonji-type oxygenases in human disease*. Epigenomics, 2014. **6**(1): p. 89-120.
42. Zheng, G., Y. Fu, and C. He, *Nucleic acid oxidation in DNA damage repair and epigenetics*. Chemical reviews, 2014. **114**(8): p. 4602-4620.
43. Ougland, R., et al., *Non-homologous functions of the AlkB homologs*. Journal of molecular cell biology, 2015. **7**(6): p. 494-504.
44. Wei, Y.-F., et al., *Molecular cloning and functional analysis of a human cDNA encoding an Escherichia coli AlkB homolog, a protein involved in DNA alkylation damage repair*. Nucleic acids research, 1996. **24**(5): p. 931-937.

45. Silvestrov, P., et al., *Homology modeling, molecular dynamics, and site-directed mutagenesis study of AlkB human homolog 1 (ALKBH1)*. Journal of Molecular Graphics and Modelling, 2014. **54**: p. 123-130.
46. Ougland, R., et al., *ALKBH1 is a histone H2A dioxygenase involved in neural differentiation*. Stem cells, 2012. **30**(12): p. 2672-2682.
47. Westbye, M.P., et al., *Human AlkB homolog 1 is a mitochondrial protein that demethylates 3-methylcytosine in DNA and RNA*. Journal of Biological Chemistry, 2008. **283**(36): p. 25046-25056.
48. Kawarada, L., et al., *ALKBH1 is an RNA dioxygenase responsible for cytoplasmic and mitochondrial tRNA modifications*. Nucleic acids research, 2017. **45**(12): p. 7401-7415.
49. Haag, S., et al., *NSUN3 and ABH1 modify the wobble position of mt-tRNAMet to expand codon recognition in mitochondrial translation*. The EMBO journal, 2016. **35**(19): p. 2104-2119.
50. Ougland, R., et al., *Role of ALKBH1 in the core transcriptional network of embryonic stem cells*. Cellular Physiology and Biochemistry, 2016. **38**(1): p. 173-184.
51. Pan, Z., et al., *Impaired placental trophoblast lineage differentiation in Alkbh1^{-/-} mice*. Developmental dynamics, 2008. **237**(2): p. 316-327.
52. Zhou, C., et al., *DNA N 6-methyladenine demethylase ALKBH1 enhances osteogenic differentiation of human MSCs*. Bone research, 2016. **4**: p. boneres201633.
53. Wu, T.P., et al., *DNA methylation on N 6-adenine in mammalian embryonic stem cells*. Nature, 2016. **532**(7599): p. 329.

54. Müller, T.A., K. Meek, and R.P. Hausinger, *Human AlkB homologue 1 (ABH1) exhibits DNA lyase activity at abasic sites*. DNA repair, 2010. **9**(1): p. 58-65.
55. Korvald, H., et al., *The Schizosaccharomyces pombe AlkB homolog Abh1 exhibits AP lyase activity but no demethylase activity*. DNA repair, 2012. **11**(5): p. 453-462.
56. Müller, T.A., et al., *Biochemical characterization of AP lyase and m6A demethylase activities of human AlkB homologue 1 (ALKBH1)*. Biochemistry, 2017. **56**(13): p. 1899-1910.
57. Müller, T.A., M.M. Andrzejak, and R.P. Hausinger, *A covalent protein–DNA 5'-product adduct is generated following AP lyase activity of human ALKBH1 (AlkB homologue 1)*. Biochemical Journal, 2013. **452**(3): p. 509-518.
58. Müller, T.A., et al., *ALKBH1 is dispensable for abasic site cleavage during base excision repair and class switch recombination*. PloS one, 2013. **8**(6): p. e67403.
59. Aas, P.A., et al., *Human and bacterial oxidative demethylases repair alkylation damage in both RNA and DNA*. Nature, 2003. **421**(6925): p. 859-863.
60. Duncan, T., et al., *Reversal of DNA alkylation damage by two human dioxygenases*. Proceedings of the National Academy of Sciences, 2002. **99**(26): p. 16660-16665.

61. Chen, B., et al., *Mechanistic insight into the recognition of single-stranded and double-stranded DNA substrates by ABH2 and ABH3*. *Molecular BioSystems*, 2010. **6**(11): p. 2143-2149.
62. Yi, C., et al., *Duplex interrogation by a direct DNA repair protein in search of base damage*. *Nature structural & molecular biology*, 2012. **19**(7): p. 671.
63. Fu, D., et al., *The interaction between ALKBH2 DNA repair enzyme and PCNA is direct, mediated by the hydrophobic pocket of PCNA and perturbed in naturally-occurring ALKBH2 variants*. *DNA repair*, 2015. **35**: p. 13-18.
64. Tsujikawa, K., et al., *Expression and sub-cellular localization of human ABH family molecules*. *Journal of cellular and molecular medicine*, 2007. **11**(5): p. 1105-1116.
65. Müller, R., et al., *Targeting proliferating cell nuclear antigen and its protein interactions induces apoptosis in multiple myeloma cells*. *PloS one*, 2013. **8**(7): p. e70430.
66. Gilljam, K.M., et al., *Identification of a novel, widespread, and functionally important PCNA-binding motif*. *The Journal of cell biology*, 2009. **186**(5): p. 645-654.
67. Nay, S.L., et al., *Alkbh2 protects against lethality and mutation in primary mouse embryonic fibroblasts*. *DNA repair*, 2012. **11**(5): p. 502-510.
68. Lee, D.-H., et al., *Repair of methylation damage in DNA and RNA by mammalian AlkB homologues*. *Journal of Biological Chemistry*, 2005. **280**(47): p. 39448-39459.

69. Ringvoll, J., et al., *Repair deficient mice reveal mABH2 as the primary oxidative demethylase for repairing 1meA and 3meC lesions in DNA*. The EMBO journal, 2006. **25**(10): p. 2189-2198.
70. Johannessen, T.-C.A., et al., *The DNA repair protein ALKBH2 mediates temozolomide resistance in human glioblastoma cells*. Neuro-oncology, 2012. **15**(3): p. 269-278.
71. Calvo, J.A., et al., *DNA repair is indispensable for survival after acute inflammation*. The Journal of clinical investigation, 2012. **122**(7): p. 2680-2689.
72. Cetica, V., et al., *Pediatric brain tumors: mutations of two dioxygenases (hABH2 and hABH3) that directly repair alkylation damage*. Journal of neuro-oncology, 2009. **94**(2): p. 195-201.
73. Gao, W., et al., *Frequent down-regulation of hABH2 in gastric cancer and its involvement in growth of cancer cells*. Journal of gastroenterology and hepatology, 2011. **26**(3): p. 577-584.
74. Fujii, T., et al., *ALKBH 2, a novel A lk B homologue, contributes to human bladder cancer progression by regulating MUC 1 expression*. Cancer science, 2013. **104**(3): p. 321-327.
75. Ougland, R., et al., *AlkB restores the biological function of mRNA and tRNA inactivated by chemical methylation*. Molecular cell, 2004. **16**(1): p. 107-116.
76. Dango, S., et al., *DNA unwinding by ASCC3 helicase is coupled to ALKBH3-dependent DNA alkylation repair and cancer cell proliferation*. Molecular cell, 2011. **44**(3): p. 373-384.

77. Ueda, Y., et al., *AlkB homolog 3-mediated tRNA demethylation promotes protein synthesis in cancer cells*. Scientific reports, 2017. **7**: p. 42271.
78. Bjørnstad, L.G., et al., *Spectroscopic and magnetic studies of wild-type and mutant forms of the Fe (II)-and 2-oxoglutarate-dependent decarboxylase ALKBH4*. Biochemical Journal, 2011. **434**(3): p. 391-398.
79. Bjørnstad, L.G., et al., *Human ALKBH4 interacts with proteins associated with transcription*. PLoS One, 2012. **7**(11): p. e49045.
80. Nilsen, A., et al., *ALKBH4 depletion in mice leads to spermatogenic defects*. PloS one, 2014. **9**(8): p. e105113.
81. Zheng, G., et al., *ALKBH5 is a mammalian RNA demethylase that impacts RNA metabolism and mouse fertility*. Molecular cell, 2013. **49**(1): p. 18-29.
82. Aik, W., et al., *Structure of human RNA N 6-methyladenine demethylase ALKBH5 provides insights into its mechanisms of nucleic acid recognition and demethylation*. Nucleic acids research, 2014. **42**(7): p. 4741-4754.
83. Thalhammer, A., et al., *Human AlkB homologue 5 is a nuclear 2-oxoglutarate dependent oxygenase and a direct target of hypoxia-inducible factor 1 α (HIF-1 α)*. PloS one, 2011. **6**(1): p. e16210.
84. Tsujikawa, K., et al., *Expression and sub-cellular localization of human ABH family molecules*. 2007. **11**(5): p. 1105-1116.
85. Fu, D., et al., *Human ALKBH7 is required for alkylation and oxidation-induced programmed necrosis*. 2013.
86. Wang, G., et al., *The Atomic-Resolution Structure of Human Alkb Homolog 7 (ALKBH7), a Key Protein for Programmed Necrosis and Fat Metabolism*. 2014: p. jbc. M114. 590505.

87. Wallach, D., et al., *Programmed necrosis in inflammation: toward identification of the effector molecules*. 2016. **352**(6281): p. aaf2154.
88. Solberg, A., et al., *Deletion of mouse Alkbh7 leads to obesity*. 2013. **5**(3): p. 194-203.
89. Fu, D., et al., *Human AlkB homolog ABH8 Is a tRNA methyltransferase required for wobble uridine modification and DNA damage survival*. *Molecular and cellular biology*, 2010. **30**(10): p. 2449-2459.
90. Songe-Møller, L., et al., *Mammalian ALKBH8 possesses tRNA methyltransferase activity required for the biogenesis of multiple wobble uridine modifications implicated in translational decoding*. *Molecular and cellular biology*, 2010. **30**(7): p. 1814-1827.
91. Leihne, V., et al., *Roles of Trm9-and ALKBH8-like proteins in the formation of modified wobble uridines in Arabidopsis tRNA*. *Nucleic acids research*, 2011. **39**(17): p. 7688-7701.
92. Zdżalik, D., et al., *Protozoan ALKBH8 oxygenases display both DNA repair and tRNA modification activities*. *PloS one*, 2014. **9**(6): p. e98729.
93. Begley, U., et al., *Trm9-catalyzed tRNA modifications link translation to the DNA damage response*. *Molecular cell*, 2007. **28**(5): p. 860-870.
94. Gerken, T., et al., *The obesity-associated FTO gene encodes a 2-oxoglutarate-dependent nucleic acid demethylase*. *Science*, 2007. **318**(5855): p. 1469-1472.
95. Jia, G., et al., *N6-methyladenosine in nuclear RNA is a major substrate of the obesity-associated FTO*. *Nature chemical biology*, 2011. **7**(12): p. 885.

96. Wu, Q., et al., *The obesity-associated Fto gene is a transcriptional coactivator*. *Biochemical and biophysical research communications*, 2010. **401**(3): p. 390-395.
97. Dina, C., et al., *Variation in FTO contributes to childhood obesity and severe adult obesity*. *Nature genetics*, 2007. **39**(6): p. 724.
98. Frayling, T.M., et al., *A common variant in the FTO gene is associated with body mass index and predisposes to childhood and adult obesity*. *Science*, 2007.
99. Scott, L.J., et al., *A genome-wide association study of type 2 diabetes in Finns detects multiple susceptibility variants*. *science*, 2007.
100. Scuteri, A., et al., *Genome-wide association scan shows genetic variants in the FTO gene are associated with obesity-related traits*. *PLoS genetics*, 2007. **3**(7): p. e115.
101. Camps, M. and B.F.J.M.c. Eichman, *Unraveling a connection between DNA demethylation repair and cancer*. 2011. **44**(3): p. 343-344.
102. Liefke, R., et al., *The oxidative demethylase ALKBH3 marks hyperactive gene promoters in human cancer cells*. *Genome medicine*, 2015. **7**(1): p. 66.
103. Konishi, N., et al., *High expression of a new marker PCA-1 in human prostate carcinoma*. 2005. **11**(14): p. 5090-5097.
104. Shimada, K., et al., *Prostate cancer antigen-1 contributes to cell survival and invasion through discoidin receptor 1 in human prostate cancer*. 2008. **99**(1): p. 39-45.
105. Koike, K., et al., *anti-tumor effect of AlkB homolog 3 knockdown in hormone-independent prostate cancer cells*. 2012. **12**(7): p. 847-856.

106. Nakao, S., et al., *Design and synthesis of prostate cancer antigen-1 (PCA-1/ALKBH3) inhibitors as anti-prostate cancer drugs*. *Bioorganic & medicinal chemistry letters*, 2014. **24**(4): p. 1071-1074.
107. Yamato, I., et al., *PCA-1/ALKBH3 contributes to pancreatic cancer by supporting apoptotic resistance and angiogenesis*. 2012: p. canres. 0328.2012.
108. Shimada, K., et al., *ALKBH3 contributes to survival and angiogenesis of human urothelial carcinoma cells through NADPH oxidase and tweak/Fn14/VEGF signals*. *Clinical Cancer Research*, 2012: p. clincanres. 0955.2012.
109. Tasaki, M., et al., *ALKBH3, a human AlkB homologue, contributes to cell survival in human non-small-cell lung cancer*. *British journal of cancer*, 2011. **104**(4): p. 700.
110. Kogaki, T., et al., *TP53 gene status is a critical determinant of phenotypes induced by ALKBH3 knockdown in non-small cell lung cancers*. *Biochemical and biophysical research communications*, 2017. **488**(2): p. 285-290.
111. Hotta, K., et al., *Clinical significance and therapeutic potential of prostate cancer antigen-1/ALKBH3 in human renal cell carcinoma*. *Oncology reports*, 2015. **34**(2): p. 648-654.
112. Stefansson, O.A., et al., *CpG promoter methylation of the ALKBH3 alkylation repair gene in breast cancer*. *BMC cancer*, 2017. **17**(1): p. 469.
113. Choi, S.-y., J.H. Jang, and K.R. Kim, *Analysis of differentially expressed genes in human rectal carcinoma using suppression subtractive hybridization*. *Clinical and experimental medicine*, 2011. **11**(4): p. 219-226.

114. Neta, G., et al., *Common genetic variants related to genomic integrity and risk of papillary thyroid cancer*. *Carcinogenesis*, 2011. **32**(8): p. 1231-1237.
115. Wang, Q., et al., *Association of AlkB homolog 3 expression with tumor recurrence and unfavorable prognosis in hepatocellular carcinoma*. *Journal of gastroenterology and hepatology*, 2018.
116. Zhu, C. and C. Yi, *Switching Demethylation Activities between AlkB Family RNA/DNA Demethylases through Exchange of Active-Site Residues*. *Angewandte Chemie International Edition*, 2014. **53**(14): p. 3659-3662.
117. Monsen, V.T., et al., *Divergent β -hairpins determine double-strand versus single-strand substrate recognition of human AlkB-homologues 2 and 3*. *Nucleic acids research*, 2010. **38**(19): p. 6447-6455.
118. Sundheim, O., et al., *Human ABH3 structure and key residues for oxidative demethylation to reverse DNA/RNA damage*. *The EMBO journal*, 2006. **25**(14): p. 3389-3397.
119. Welford, R.W., et al., *The selectivity and inhibition of AlkB*. 2003. **278**(12): p. 10157-10161.
120. Woon, E.C., et al., *Dynamic combinatorial mass spectrometry leads to inhibitors of a 2-oxoglutarate-dependent nucleic acid demethylase*. 2012. **55**(5): p. 2173-2184.
121. McKeague, M., *Aptamers for DNA Damage and Repair*. *International journal of molecular sciences*, 2017. **18**(10): p. 2212.
122. Krylova, S.M., et al., *Mechanistic studies on the application of DNA aptamers as inhibitors of 2-oxoglutarate-dependent oxygenases*. *Journal of medicinal chemistry*, 2012. **55**(7): p. 3546-3552.

123. Tran, T.Q., et al., *Glutamine deficiency induces DNA alkylation damage and sensitizes cancer cells to alkylating agents through inhibition of ALKBH enzymes*. PLoS biology, 2017. **15**(11): p. e2002810.
124. Bian, K., et al., *Copper Inhibits the AlkB Family DNA Repair Enzymes under Wilson's Disease Condition*. Chemical research in toxicology, 2017. **30**(10): p. 1794-1796.
125. Chen, F., et al., *Oncometabolites d-and l-2-hydroxyglutarate inhibit the AlkB family DNA repair enzymes under physiological conditions*. Chemical research in toxicology, 2017. **30**(4): p. 1102-1110.
126. Wang, P., et al., *Oncometabolite D-2-hydroxyglutarate inhibits ALKBH DNA repair enzymes and sensitizes IDH mutant cells to alkylating agents*. Cell reports, 2015. **13**(11): p. 2353-2361.
127. Triantafyllou, A., et al., *The flavonoid quercetin induces hypoxia-inducible factor-1 α (HIF-1 α) and inhibits cell proliferation by depleting intracellular iron*. Free radical research, 2007. **41**(3): p. 342-356.
128. Welford, R.W., et al., *The selectivity and inhibition of AlkB*. Journal of Biological Chemistry, 2003. **278**(12): p. 10157-10161.
129. Ueda, M., et al., *Novel Metabolically Stable PCA-1/ALKBH3 Inhibitor Has Potent Antiproliferative Effects on DU145 Cells In Vivo*. Anticancer research, 2018. **38**(1): p. 211-218.
130. Mabuchi, M., et al., *Improving the bioavailability and anticancer effect of the PCA-1/ALKBH3 inhibitor HUHS015 using sodium salt*. In Vivo, 2015. **29**(1): p. 39-43.

131. Li, Q., et al., *Rhein inhibits AlkB repair enzymes and sensitizes cells to methylated DNA damage*. Journal of Biological Chemistry, 2016: p. jbc.M115.711895.
132. Shivange, G., et al., *RecA stimulates AlkB-mediated direct repair of DNA adducts*. Nucleic acids research, 2016. **44**(18): p. 8754-8763.
133. Das, M., et al., *Multi-Protein Dynamic Combinatorial Chemistry: A Novel Strategy that Leads to Simultaneous Discovery of Subfamily-Selective Inhibitors for Nucleic Acid Demethylases FTO and ALKBH3*. Chemistry—An Asian Journal, 2018.
134. Mal, D. and S.R. De, *Total synthesis of euplectin, a natural product with a chromone fused indenone*. Organic letters, 2009. **11**(19): p. 4398-4401.
135. Ernst-Russell, M.A., et al., *Euplectin and coneuplectin, new naphthopyrones from the lichen Flavoparmelia euplecta*. Journal of natural products, 2000. **63**(1): p. 129-131.
136. Jeffrey, J.L. and R. Sarpong, *Concise synthesis of Pauciflorol F using a Larock annulation*. Organic letters, 2009. **11**(23): p. 5450-5453.
137. Harrowven, D.C., N.A. Newman, and C.A. Knight, *On the identity of a neolignan from the fruits of Virola sebifera*. Tetrahedron letters, 1998. **39**(37): p. 6757-6760.
138. Ahn, J.H., et al., *Indenone derivatives: a novel template for peroxisome proliferator-activated receptor γ (PPAR γ) agonists*. Journal of medicinal chemistry, 2006. **49**(15): p. 4781-4784.
139. Anstead, G.M., S.R. Wilson, and J.A. Katzenellenbogen, *2-Arylindenones and 2-arylindenones: Molecular structures and considerations in the binding*

- orientation of unsymmetrical nonsteroidal ligands to the estrogen receptor.*
Journal of medicinal chemistry, 1989. **32**(9): p. 2163-2171.
140. Anstead, G.M., et al., *2, 3-Diarylindenes and 2, 3-diarylindenones: synthesis, molecular structure, photochemistry, estrogen receptor binding affinity, and comparisons with related triarylethylenes.* Journal of medicinal chemistry, 1988. **31**(7): p. 1316-1326.
141. McDevitt, R.E., et al., *Estrogen receptor ligands: design and synthesis of new 2-arylindene-1-ones.* Bioorganic & medicinal chemistry letters, 2005. **15**(12): p. 3137-3142.
142. Schmieder, P.K., et al., *Quantitative structure-activity relationship models for prediction of estrogen receptor binding affinity of structurally diverse chemicals.* Environmental toxicology and chemistry, 2003. **22**(8): p. 1844-1854.
143. McNulty, J., et al., *Antimitotic activity of structurally simplified biaryl analogs of the anticancer agents colchicine and combretastatin A4.* Bioorganic & medicinal chemistry letters, 2015. **25**(1): p. 117-121.
144. Singh, R. and H. Kaur, *Advances in synthetic approaches for the preparation of combretastatin-based anti-cancer agents.* Synthesis, 2009. **2009**(15): p. 2471-2491.
145. Barvian, M., et al., *1-Oxo-3-aryl-1H-indene-2-carboxylic acid derivatives as selective inhibitors of fibroblast growth factor receptor-1 tyrosine kinase.* Bioorganic & Medicinal Chemistry Letters, 1997. **7**(22): p. 2903-2908.

146. Park, C.H., et al., *Investigations of new lead structures for the design of novel cyclooxygenase-2 inhibitors*. European journal of medicinal chemistry, 2002. **37**(6): p. 461-468.
147. Babu, K.R. and F.A. Khan, *A domino reaction of tetrahalo-7, 7-dimethoxybicyclo [2.2. 1] heptenyl alcohols leading to indenones and a de novo synthesis of ninhydrin derivatives*. Organic & biomolecular chemistry, 2015. **13**(1): p. 299-308.
148. Shen, Z., *Genomic instability and cancer: an introduction*. Journal of Molecular Cell Biology, 2011. **3**(1): p. 1-3.
149. Thalhammer, A., et al., *The potential of 2-oxoglutarate oxygenases acting on nucleic acids as therapeutic targets*. Drug Discovery Today: Therapeutic Strategies, 2012. **9**(2–3): p. e91-e100.
150. Welford, R.W.D., et al., *The Selectivity and Inhibition of AlkB*. Journal of Biological Chemistry, 2003. **278**(12): p. 10157-10161.
151. Rose, N.R., et al., *Inhibition of 2-oxoglutarate dependent oxygenases*. Chemical Society Reviews, 2011. **40**(8): p. 4364-4397.
152. Barrows, L.R. and P.N. Magee, *Nonenzymatic methylation of DNA by S-adenosylmethionine in vitro*. Carcinogenesis, 1982. **3**(3): p. 349-351.
153. Drabløs, F., et al., *Alkylation damage in DNA and RNA—repair mechanisms and medical significance*. DNA repair, 2004. **3**(11): p. 1389-1407.
154. Shen, L., et al., *Mechanism and function of oxidative reversal of DNA and RNA methylation*. Annual review of biochemistry, 2014. **83**: p. 585-614.

155. Raghunathan, S., et al., *Structure of the DNA binding domain of E. coli SSB bound to ssDNA*. Nature Structural and Molecular Biology, 2000. **7**(8): p. 648.
156. Savvides, S.N., et al., *The C-terminal domain of full-length E. coli SSB is disordered even when bound to DNA*. Protein Science, 2004. **13**(7): p. 1942-1947.
157. Costes, A., et al., *The C-terminal domain of the bacterial SSB protein acts as a DNA maintenance hub at active chromosome replication forks*. PLoS genetics, 2010. **6**(12): p. e1001238.
158. Lohman, T.M. and L.B. Overman, *Two binding modes in Escherichia coli single strand binding protein-single stranded DNA complexes. Modulation by NaCl concentration*. Journal of Biological Chemistry, 1985. **260**(6): p. 3594-3603.
159. Roy, R., et al., *SSB protein diffusion on single-stranded DNA stimulates RecA filament formation*. Nature, 2009. **461**(7267): p. 1092.
160. Meyer, R.R. and P.S. Laine, *The single-stranded DNA-binding protein of Escherichia coli*. Microbiological reviews, 1990. **54**(4): p. 342-380.
161. Shereda, R.D., et al., *SSB as an organizer/mobilizer of genome maintenance complexes*. Critical reviews in biochemistry and molecular biology, 2008. **43**(5): p. 289-318.
162. Han, E.S., et al., *RecJ exonuclease: substrates, products and interaction with SSB*. Nucleic acids research, 2006. **34**(4): p. 1084-1091.
163. Handa, P., N. Acharya, and U. Varshney, *Chimeras between single stranded DNA binding proteins from Escherichia coli and Mycobacterium*

- tuberculosis* reveal that their C-terminal domains interact with uracil DNA glycosylases. *Journal of Biological Chemistry*, 2001.
164. Umezu, K. and R.D. Kolodner, *Protein interactions in genetic recombination in Escherichia coli. Interactions involving RecO and RecR overcome the inhibition of RecA by single-stranded DNA-binding protein.* *Journal of Biological Chemistry*, 1994. **269**(47): p. 30005-30013.
165. Shivange, G., N. Kodipelli, and R. Anindya, *A nonradioactive restriction enzyme-mediated assay to detect DNA repair by Fe (II)/2-oxoglutarate-dependent dioxygenase.* *Analytical biochemistry*, 2014. **465**: p. 35-37.
166. Shivange, G., et al., *A role for Saccharomyces cerevisiae Tpa1 protein in direct alkylation repair.* *Journal of Biological Chemistry*, 2014: p. jbc.M114.590216.
167. Roy, T.W. and A. Bhagwat, *Kinetic studies of Escherichia coli AlkB using a new fluorescence-based assay for DNA demethylation.* *Nucleic acids research*, 2007. **35**(21): p. e147-e147.
168. Falnes, P.Ø., *Repair of 3-methylthymine and 1-methylguanine lesions by bacterial and human AlkB proteins.* *Nucleic acids research*, 2004. **32**(21): p. 6260-6267.
169. Delaney, J.C., et al., *AlkB reverses etheno DNA lesions caused by lipid oxidation in vitro and in vivo.* *Nature Structural and Molecular Biology*, 2005. **12**(10): p. 855.
170. Falnes, P.Ø., R.F. Johansen, and E. Seeberg, *AlkB-mediated oxidative demethylation reverses DNA damage in Escherichia coli.* *Nature*, 2002. **419**(6903): p. 178.

171. Mishina, Y., C.H.J. Lee, and C. He, *Interaction of human and bacterial AlkB proteins with DNA as probed through chemical cross-linking studies*. Nucleic acids research, 2004. **32**(4): p. 1548-1554.
172. Yu, B., et al., *Crystal structures of catalytic complexes of the oxidative DNA/RNA repair enzyme AlkB*. Nature, 2006. **439**(7078): p. 879.
173. Mishina, Y., C.-G. Yang, and C. He, *Direct repair of the exocyclic DNA adduct 1, N6-ethenoadenine by the DNA repair AlkB proteins*. Journal of the American Chemical Society, 2005. **127**(42): p. 14594-14595.
174. Reyes-Lamothe, R., D.J. Sherratt, and M.C. Leake, *Stoichiometry and architecture of active DNA replication machinery in Escherichia coli*. Science, 2010. **328**(5977): p. 498-501.
175. Antony, E., et al., *Multiple C-terminal tails within a single E. coli SSB homotetramer coordinate DNA replication and repair*. Journal of molecular biology, 2013. **425**(23): p. 4802-4819.
176. Lohman, T.M. and M.E. Ferrari, *Escherichia coli single-stranded DNA-binding protein: multiple DNA-binding modes and cooperativities*. Annual review of biochemistry, 1994. **63**(1): p. 527-570.
177. Purnapatre, K. and U. Varshney, *Cloning, over-expression and biochemical characterization of the single-stranded DNA binding protein from Mycobacterium tuberculosis*. European journal of biochemistry, 1999. **264**(2): p. 591-598.
178. Couture, J.-F., et al., *Specificity and mechanism of JMJD2A, a trimethyllysine-specific histone demethylase*. Nature Structural and Molecular Biology, 2007. **14**(8): p. 689.

179. Kozlov, A.G., et al., *Intrinsically disordered C-terminal tails of E. coli single-stranded DNA binding protein regulate cooperative binding to single-stranded DNA*. Journal of molecular biology, 2015. **427**(4): p. 763-774.
180. Furukohri, A., et al., *Interaction between Escherichia coli DNA polymerase IV and single-stranded DNA-binding protein is required for DNA synthesis on SSB-coated DNA*. Nucleic acids research, 2012. **40**(13): p. 6039-6048.
181. Arad, G., et al., *Single-stranded DNA-binding protein recruits DNA polymerase V to primer termini on RecA-coated DNA*. Journal of Biological Chemistry, 2008. **283**(13): p. 8274-8282.
182. Chen, S.H., R.T. Byrne-Nash, and M.M. Cox, *Escherichia coli RadD Protein Functionally Interacts with the Single-stranded DNA-binding Protein*. Journal of Biological Chemistry, 2016: p. jbc. M116. 736223.
183. Genschel, J., U. Curth, and C. Urbanke, *Interaction of E. coli single-stranded DNA binding protein (SSB) with exonuclease I. The carboxy-terminus of SSB is the recognition site for the nuclease*. Biological chemistry, 2000. **381**(3): p. 183-192.
184. Lu, D., et al., *Mechanism of Exonuclease I stimulation by the single-stranded DNA-binding protein*. Nucleic acids research, 2011. **39**(15): p. 6536-6545.
185. Shereda, R.D., D.A. Bernstein, and J.L. Keck, *A central role for SSB in E. coli RecQ DNA helicase function*. Journal of Biological Chemistry, 2007.
186. James, P., J. Halladay, and E.A. Craig, *Genomic libraries and a host strain designed for highly efficient two-hybrid selection in yeast*. Genetics, 1996. **144**(4): p. 1425-1436.

187. Marceau, A.H., et al., *Structure of the SSB–DNA polymerase III interface and its role in DNA replication*. The EMBO journal, 2011. **30**(20): p. 4236-4247.
188. Kozlov, A.G. and T.M. Lohman, *Calorimetric studies of E. coli SSB protein-single-stranded DNA interactions. Effects of monovalent salts on binding enthalpy*. Journal of molecular biology, 1998. **278**(5): p. 999-1014.
189. Bleijlevens, B., et al., *Dynamic states of the DNA repair enzyme AlkB regulate product release*. EMBO reports, 2008. **9**(9): p. 872-877.
190. Kelly, S.M., T.J. Jess, and N.C. Price, *How to study proteins by circular dichroism*. Biochimica et Biophysica Acta (BBA)-Proteins and Proteomics, 2005. **1751**(2): p. 119-139.
191. Kelly, S.M. and N.C. Price, *The use of circular dichroism in the investigation of protein structure and function*. Current protein and peptide science, 2000. **1**(4): p. 349-384.
192. Mishina, Y. and C. He, *Oxidative dealkylation DNA repair mediated by the mononuclear non-heme iron AlkB proteins*. Journal of inorganic biochemistry, 2006. **100**(4): p. 670-678.
193. Fedeles, B.I., et al., *The AlkB family of Fe (II)/ α -ketoglutarate dependent dioxygenases: repairing nucleic acid alkylation damage and beyond*. Journal of Biological Chemistry, 2015: p. jbc. R115. 656462.
194. Kurowski, M.A., et al., *Phylogenomic identification of five new human homologs of the DNA repair enzyme AlkB*. BMC genomics, 2003. **4**(1): p. 48.

195. Yu, B. and J.F.J.P.o.t.N.A.o.S. Hunt, *Enzymological and structural studies of the mechanism of promiscuous substrate recognition by the oxidative DNA repair enzyme AlkB*. 2009. **106**(34): p. 14315-14320.
196. Lindahl, T., et al., *Regulation and expression of the adaptive response to alkylating agents*. 1988. **57**(1): p. 133-157.
197. Falnes, P.Ø., et al., *Substrate specificities of bacterial and human AlkB proteins*. 2004. **32**(11): p. 3456-3461.
198. Koike, K., et al., *anti-tumor effect of AlkB homolog 3 knockdown in hormone-independent prostate cancer cells*. *Current cancer drug targets*, 2012. **12**(7): p. 847-856.
199. Yamato, I., et al., *PCA-1/ALKBH3 contributes to pancreatic cancer by supporting apoptotic resistance and angiogenesis*. *Cancer research*, 2012: p. canres. 0328.2012.
200. Shivange, G., et al., *A role for Saccharomyces cerevisiae Tpa1 protein in direct alkylation repair*. 2014: p. jbc. M114. 590216.
201. Sundheim, O., et al., *Human ABH3 structure and key residues for oxidative demethylation to reverse DNA/RNA damage*. 2006. **25**(14): p. 3389-3397.

Chapter 2: Functional characterization of *E. coli* DNA repair protein AlkB

2.1 Introduction

DNA is constantly damaged by many endogenous and exogenous alkylating agents and alkylated DNA adducts are formed [1]. N1meA and N3meC are two methylation adducts which are specifically generated by S_N2 type methylating agent MMS and prevent proper Watson-Crick base-pairing. *E. coli* DNA repair enzyme AlkB, a Fe(II)-2OG-dependent dioxygenase, is involved in the repair of N1meA and N3meC [2]. AlkB repairs the damaged DNA by catalyzing hydroxylation of methyl group present on the ring nitrogen atoms and subsequently the oxidized methyl group is released as formaldehyde, thus restoring the undamaged nucleotides in the DNA [3]. AlkB has been known to preferentially repair methyl adducts found in ssDNA [4]. However, it is well known that bacterial ssDNA regions are stabilized by protein binding, such as, single-stranded DNA-binding protein SSB. *E. coli* SSB is a tetrameric protein and each monomer has three domains: the characteristic oligonucleotide/oligosaccharide binding (OB) domain [5] that binds ssDNA and C-terminal domain acidic domain (CTD) [6], characterized as binding domain for several proteins involved in DNA metabolism [7] and an intrinsically disordered linker (IDL) domain. For the *E. coli* SSB, two major DNA-binding states were reported [9], (SSB)₆₅, where the tetramer binds to 65 nucleotides at high salt concentration (NaCl concentration >200 mM), and (SSB)₃₅, where the SSB binds to 35 nucleotides at lower salt concentration (NaCl concentration <20 mM). Single

molecule experiments have demonstrated that SSB binding to ssDNA is not static, rather, it diffuses randomly back and forth along ssDNA [9] and the DNA ends undergo spontaneous unwrapping. SSB plays direct role in the DNA replication and recombination [10]. During recombination, SSB helps in heteroduplex formation by binding to the displaced strand and preventing strand annealing [11]. SSB is also involved in DNA repair pathways including base excision repair and recombination repair [12-14].

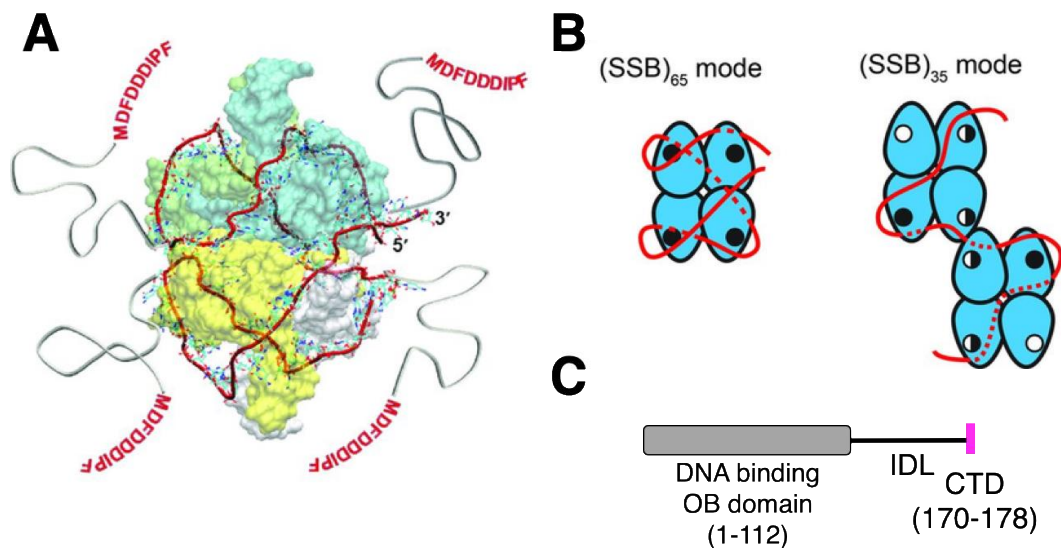


Figure 4. Structure and binding modes of *E. coli* SSB (A) Structural model of 65 nucleotides of ssDNA (red ribbon), wrapped around the EcSSB tetramer in the (SSB)₆₅ mode. (B) The proposed ssDNA binding pathways of the (SSB)₆₅ and (SSB)₃₅ modes of SSB (C) Domain organization of SSB, depicting the DNA binding domain (OB), IDL and the C-terminal acidic domain (CTD).

2.2 Materials and methods

2.2.1 Cloning

AlkB gene was cloned into pTYB3 vector using NcoI and XhoI restriction enzyme sites. Oligonucleotides used for cloning were shown in **Table 3**. SSB was also cloned into pTYB3 vector using NcoI and XhoI site. SSB-1-115 was cloned using internal deletion method from pTYB3-SSB clone.

Table 3: Cloning strategy for generation of clones described in 2.2.1.

Clone	Clone No.	Oligo Sequence (5' – 3')	Restriction sites
pTYB3-SSB	251	pTYB3_SSB_SalI_F AAT AGT CGA CAT GGC CAG CAG AGG CGT AAA CAA GG pTYB3_SSB_EcoRI_R TTA TGA ATT CGA ACG GAA TGT CAT CAT CAA AGT CC	EcoRI Xho1
pTYB3-SSB-del CTD	252	Tagless SSB delta CTD_F GAA TTC CTC GAA GGC TCT TCC TGC TTT GCC Tagless SSB delta CTD_R ACC ACC CAG CAT CTG CAT GGT GCC GCC AAC	Internal deletion
pTYB3-AlkB	253	pTYB3_AlkB_NcoI_F ATT ACC ATG GAA ATG TTG GAT CTG TTT GCC GAT GCT G pTYB3_AlkB_SalI_R TTT TGT CGA CTT CTT TTT TAC CTG CCT GAC GG	Nco1 Xho1

2.2.2 Purification of recombinant proteins

AlkB, SSB and SSB-1-115 were expressed as chitin-fusion protein and purification was carried out using chitin agarose, as suggested by NEB protocol. pTYB3-AlkB, pTYB3-SSB and pTYB3-SSB-1-115 plasmids were transformed into the *E. coli* strain BL21- CodonPlus(DE3)-RIL (Stratagene). BL21+pTYB3-AlkB or BL21+pTYB3-SSB or BL-21+pTYB3-SSB-1-115 transformed colonies were

inoculated into 100ml LB-broth with 100 µg/ml ampicillin and grown on incubatory shaker at 37°C at 200 rpm. The grown culture was 20 fold diluted into 2L fresh TB-broth with 100 µg/ml ampicillin. Incubation was carried out at 37°C at 200 rpm for 3 hrs. The culture was then induced with 1mM IPTG and kept for 5 hrs at 30°C at 200 rpm. Cells were harvested after centrifugation at 8000 rpm for 15 minutes at 4°C. The cell pellet was re-suspended in 20ml of 50mM Tris-HCl buffer (pH 8.5) containing 300mM sodium chloride, 0.1% Triton-X, 1mM Imidazole and sonicated for 30 minutes. The sample was then centrifuged at 14,000 rpm for 20 minutes at 4°C to remove insoluble debris. The soluble fraction was mixed with 2ml of chitin resin pre-equilibrated with the same buffer and allowed to rotate in rotary shaker for 4h to allow the protein to bind to the resin. The sample was then centrifuged at 1000 g for 5 minutes at 4°C and the beads were washed six times with 150 ml wash buffer (50 mM Tris,pH8.5, 350 mM NaCl, 0.1% Triton-X and 5 mM Imidazole). After washing beads were centrifuged as at 1000g for 4 minutes at 4°C. Bound protein was eluted with elution buffer (10 mM Tris, pH 6.5, 100 mM NaCl, 400 mM Imidazole). The beads were incubated with 6.5 pH buffer for 5 hours and the protein gets cleaved under low pH conditions.

For tag-less protein production, Proteins were further purified by Superose-12 (GE Healthcare) gel filtration column and analyzed using an AKTA Prime FPLC system (GE Healthcare). The purity of the proteins was analyzed by 12% SDS-PAGE followed by Coomassie Brilliant Blue staining and concentrations were determined by Bradford assays (Bio-Rad).

2.2.3 N3meC containing oligonucleotide substrate

70-mer oligo nucleotide substrate consisting of 69 thymine and single N3meC at 35th position, 15th position or at 1st position was chemically synthesized (Active™-Imperial Life sciences). Shorter oligonucleotides (10-mer) containing N3meC at 5th position were also synthesized.

2.2.4 Preparation of Methylated DNA substrate

M13mp18 ssDNA was purchased from NEB and MMS treated to generate methyl adducts and purified following our previously published protocol [15]. Methylation adducts were generated by treating the oligonucleotide with MMS (Sigma, 129925). 40 µg ssDNA oligonucleotides was incubated with 5% (v/v) (0.59 M) MMS, 200 mM K₂HPO₄ in 500µl of total reaction at room temperature overnight (14-15hrs). Excess MMS was removed by dialysis against TE buffer (10 mM Tris-HCl, pH 8.0, 1 mM EDTA) using Spectra/Por dialysis membrane (MWCO: 1000). Then the damaged substrate was precipitated by adding 0.3 M sodium acetate pH 5.2 and one volume of ice-cold Iso-propanol. The precipitated ssDNA was washed with 80% ethanol and finally dissolved in molecular grade water [15].

2.2.5 Preparation of Acetoacetanillide

10x stock of Acetoacetanilide (Sigma-538329; Mol wt-177.2) was prepared by dissolving it in DMSO to a final concentration of 0.5mM [16].

2.2.6 Preparation of ammonium acetate

A 5M solution of ammonium acetate (Sigma A-1542; Mol. Wt. 77.08) was prepared by dissolving it in water. This 5M solution was used as 2.5X stock [16].

2.2.7 10X demethylation assay buffer

10X assay buffer was made using the composition: 200mM HEPES pH7.5, 2mM 2-oxoglutarate, 20mM L. ascorbate and 200µM Fe(NH₄)₂SO₄. 200mM stock of L.

ascorbate prepared in water, 20mM stock of 2-oxoglutarate prepared in water and 1mM stock $\text{Fe}(\text{NH}_4)_2\text{SO}_4$ prepared in water were used for buffer preparation. All the stocks were prepared fresh. All the components were added in the same order as mentioned above. The buffer was prepared in a 50ml tube which was kept on ice all the time. The prepared solution shows a tinge of pink colour when prepared correctly. The buffer was then aliquoted into smaller tubes and stored at -86°C [16].

2.2.8 Demethylation assay by direct detection of formaldehyde

AlkB mediated demethylation was analyzed by repair of different lengths of N3meC present in ssDNA[16]. In this assay this released formaldehyde is detected to estimate the AlkB activity. The assay was performed in 96 well plates with the total reaction volume of 50 μL . 0.2 μM of AlkB was incubated with methylated nucleotide containing substrate such as M13 ssDNA containing N3meC or 70-mer oligo nucleotide substrate consisting of 69 thymine and single N3meC at 35th position, 15th position or at 1st position in demethylation buffer (20 mM HEPES, pH 8.0, 200 μM 2OG, 2 mM L-Ascorbate, 20 μM $\text{Fe}(\text{NH}_4)_2(\text{SO}_4)_2$, 100 $\mu\text{g}/\text{ml}$ bovine serum albumin), at 37°C for 1 hour. Next, to quantify the formaldehyde released 40 μL ammonium acetate (5M) and 10 μl acetoacetanilide (0.5M) was added to reaction. Formaldehyde reacts with ammonia and acetoacetanilide to form a fluorescent dihydropyridine product which has excitation maximum at 365 nm and emission maximum at 465nm. The resulting fluorescent product was analyzed using spectral scanning in the wavelength range 421-521 nm with excitation wavelength of 365 nm using Synergy (Biotek Instrument) multimode reader. The RFU value at 465 nm was then converted to formaldehyde using formaldehyde standard curve.

2.2.9 Preparation of formaldehyde standard curve

Formaldehyde standard curve was prepared using a range of concentration from 0.1 μ M to 2 μ M. 40 μ l Ammonium acetate and 10 μ l acetoacetanillide were added to reaction mixture containing desired formaldehyde concentration in demethylation assay buffer. Spectral scan in the range 421nm to 521 nm was recorded. The RFU values at 465 nm were plotted with formaldehyde concentration to get a standard curve using linear regression method in graph pad prism 5.0 [16].

2.2.10 Demethylation assay by FDH-coupled indirect detection of formaldehyde

Formaldehyde Dehydrogenase enzyme from *Pseudomonas* species (Sigma F1879) was dissolved in buffer containing 100mM HEPES pH8.0, 4mM EDTA, 6mM DTT and 50% glycerol. The enzyme was dissolved to a final concentration of 0.01Units/ μ l. 10X stock of NAD⁺ was prepared by dissolving it in H₂O to a final concentration of 10mM. Assay buffer was same as demethylation assay buffer used in the direct repair assay. A 100 μ L reaction was set up by adding DNA substrate 1 μ M, AlkB 0.2 μ M, SSB/ SSB delta CTD 4 μ M, 1mM NAD⁺ and 0.01U FDH in assay buffer containing (20 mM HEPES, pH 8.0, 200 μ M 2OG, 2 mM L-Ascorbate, 20 μ M Fe(NH₄)₂(SO₄)₂). The reaction was set up in 96 well plate and monitored for abs at 340nm for 1hr. A control reaction was set up wherein DNA substrate was not added. The control reaction was used for baseline correction [16, 17].

2.2.11 Enzyme Kinetic analysis

Enzyme kinetics analysis was performed by using 0.2 μ M AlkB and a range of oligonucleotide substrate concentration ranging from 0.2 μ M to 6.3 μ M. 70 mer oligonucleotides with internally located methylated nucleotide at 35th position or

15th position or 70 mer oligonucleotide with terminally located methylated nucleotide were used as substrate for enzyme kinetic analysis. AlkB (0.2 μM) was mixed with the eight different concentration of SSB-bound or free 70-mer internal N3meC containing oligonucleotide (ranging from 0.2 to 6.3 μM). The amount of formaldehyde released at each time point was quantified as described before [16]. The initial velocity was calculated by the analysis of the slope of these time course reactions. The velocity data were then fit to the Michaelis-Menten equation and Lineweaver-Burk plot to calculate V_{max} (maximal velocity), K_{M} (Michaelis constant) using GraphPad Prism 7.0 (GraphPad Software, Inc., San Diego, CA) [16].

2.3 Results and discussion

So far, all the *in vitro* studies of AlkB activity have been carried out either in the presence of very short oligonucleotide or completely protein-free ssDNA [4, 8-25] but never in the presence of SSB-bound single-stranded DNA. It was estimated that *E. coli* had 1000-2000 tetrameric SSB molecules per cell which are sufficient for stoichiometric binding of SSB molecules to all ssDNA formed predominantly during replication and repair [10, 26]. It was hypothesized that AlkB has to repair the SSB-coated ssDNA *in vivo*. The objective was to determine whether SSB, being an ssDNA binding protein, hinders or promotes AlkB function.

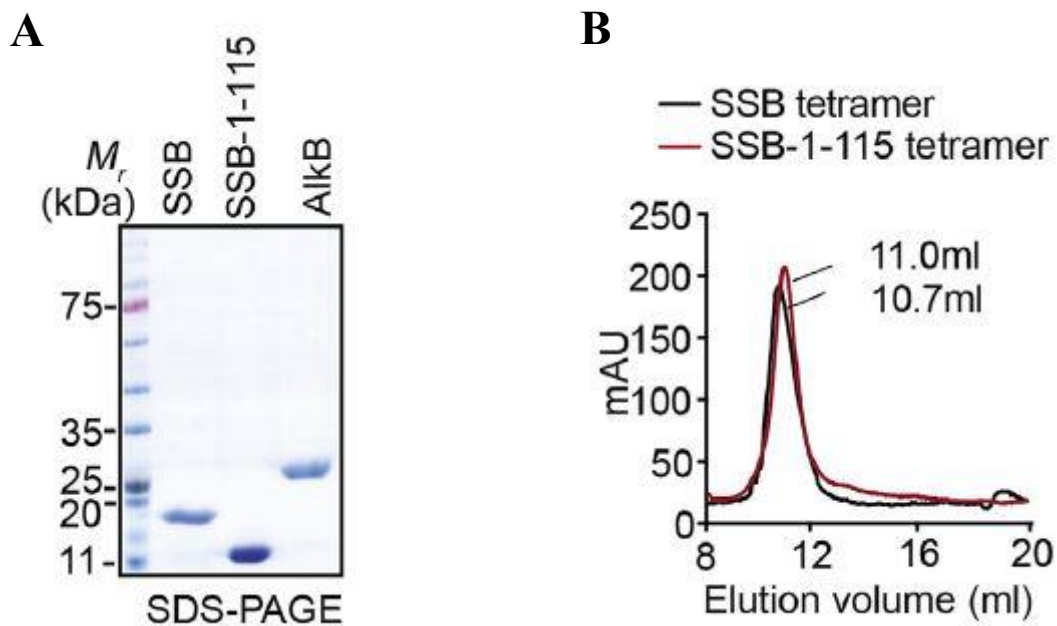


Figure 5: (A) SDS-PAGE analysis of purified tagless *E. coli* AlkB, SSB and SSB-1-115. (B) Size exclusion chromatography (SEC) analysis of purified SSB and SSB-1-115 (100mg). SEC was performed using Superose-12. Comparison of elution volume of SSB and SSB-1-115 with molecular weight standard indicates both the protein to be tetramer. SSB tetramer eluted (10.7 ml) ahead of SSB-1-115 tetramer (11 ml).

2.3.1. SSB facilitated repair of longer ssDNA by AlkB

To study that AlkB mediated repair activity was examined in presence of SSB-bound ssDNA containing methylated nucleotide as substrate. It was observed that SSB indeed stimulated AlkB activity. SSB facilitated AlkB-mediated repair of longer ssDNA. Although repair of methyl adducts on ssDNA substrate by AlkB was reported previously, none of the earlier studies had examined SSB-bound ssDNA as the substrate of AlkB.

To investigate this question, AlkB, SSB and truncated SSB containing only the OB domain (SSB-1-115) without any affinity tag (Fig.5A) were overexpressed and purified. Size exclusion chromatography analysis revealed that both SSB and SSB-1-115 were able to form tetramer (Fig.5B) in agreement with the previous report [27]. It was demonstrated before that unstructured C-terminal domain of SSB are located at the periphery of the tetramer and are not involved in the interaction with DNA [5]. It was also found that both SSB and SSB-1-115 could bind ssDNA. The SSB tetramer binds ssDNA in a variety of binding modes depending on solution conditions, especially salt concentration. At low monovalent salt concentrations (<20mM NaCl), an SSB tetramer binds to approximately 35 nucleotides of ssDNA, known as (SSB)₃₅ mode. However, at higher salt concentrations (>0.2M NaCl), an SSB tetramer binds to approximately 65 nucleotides of ssDNA, known as (SSB)₆₅ mode [28]. Because increasing ionic strength might affect possible AlkB-SSB interaction, the role of SSB in AlkB-mediated repair was studied at low ionic strength (10mM NaCl) throughout the study. As the substrate for in vitro repair variety of damaged DNA were used including MMS-damaged M13 ssDNA containing multiple methyl-adducts or chemically-synthesized DNA substrate of 10-mer oligo-dT containing single N3meC at position 5 and 70-mer oligo-dT consisting of a single N3meC located either at the 35th position or 15th position. In AlkB-catalyzed oxidative demethylation, oxidized methyl groups are released as formaldehyde which was measured by adding acetoacetanilide and ammonia directly to the repair reaction to generate a fluorescent compound with peak emission of 465 nm, as described previously [16]. Concentration of released formaldehyde was determined from the formaldehyde standard curve [29].

In first set of experiment, 1mg of MMS-damaged M13 ssDNA containing numerous randomly located methyl adducts was used as the AlkB substrate. As expected, AlkB (0.2 μ M) was able to remove the methyl adducts and formaldehyde release was detected (Fig.6). Next 4 μ M purified SSB was incubated with methylated M13 DNA (1 μ g) to form ssDNA-SSB complex and this complex was used as substrate for AlkB reaction. As shown in Fig. 6, significantly higher formaldehyde release was observed, suggesting that the repair activity was diminished when free M13 ssDNA was used as substrate. To rule out any stimulation due to molecular crowding effect, equivalent amount of BSA was added instead of SSB in the reaction mixture. As expected, BSA did not alter the amount of formaldehyde release (Fig.6). It was hypothesized that if the stimulation of AlkB activity was dependent on SSB-DNA interaction, then the repair would be unaffected if SSB lacking C-terminal disordered region was used. Indeed, when the repair reaction was carried out in the presence of SSB-1-115, enhanced formaldehyde released was observed (Fig. 6), suggesting that binding of ssDNA to SSB itself might promote the AlkB activity. The released formaldehyde was quantified using formaldehyde standard curve as shown in fig.6. Binding of large M13 ssDNA to full length or truncated SSB could prevent secondary structure formation and promote AlkB-mediated repair. Previous in vitro DNA binding experiments determined that only oligonucleotides longer than 20 nucleotide could efficiently bind to *E. coli* SSB [30]. So it was hypothesized that shorter (<20 bases) methylated ssDNA would not be able to bind SSB and, therefore, DNA would be completely accessible to AlkB. Hence, if free SSB protein is able to stimulate AlkB activity in allosteric manner, there might be an enhanced repair. Therefore, shorter oligonucleotides (10- mer) containing single N3meC (2

mM) were used as substrate of AlkB in the presence or absence of SSB (4 μ M). As shown in Fig. 7, AlkB was able to oxidatively demethylate N3meC present in 10-mer oligonucleotide and produce formaldehyde. Notably, the amount of formaldehyde released was very small compared to methylated M13 substrate. This could be due the large size of M13 ssDNA which is 6400 base long and methylated by MMS treatment and ought to have large number methylated DNA adducts.

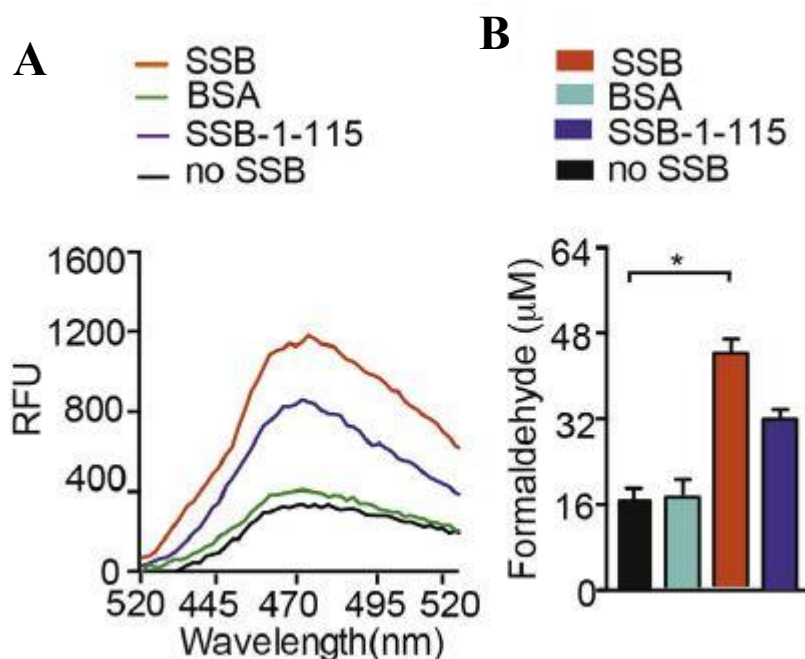


Figure 6: (A) Comparison of DNA repair by AlkB (0.2 μ M) in the presence of SSB (4 μ M). BSA (2 μ M) was used as control. Methylated M13 ssDNA (1 μ g) was used as substrate. Emission spectra depict the product of reaction between acetoacetanilide and formaldehyde, formed due to repair of methyl adducts. Formaldehyde production due to oxidative demethylation of methylated M13 ssDNA. (B) Formaldehyde release was quantified by formaldehyde standard curve. Error bar

depicts the standard error. The P value was calculated by two-tailed Student's t-test (* indicates $P < .05$).

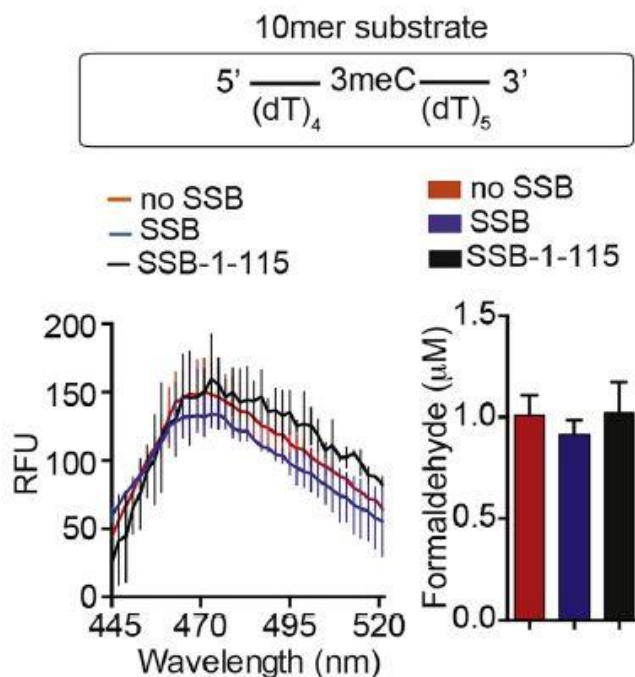


Figure 7: Comparison of DNA repair using 10-mer single N3meC containing oligonucleotide (2µM) as substrate. Error bar depicts the standard error.

The 10-mer and 70-mer substrate used here have single damage lesion and yield very low level of formaldehyde during repair. However, no stimulation of AlkB activity was observed in the presence of SSB. SSB-1-115 also had no effect on AlkB mediated repair of 10-mer N3meC containing oligonucleotide (Fig.7). This data suggested that when the length of ssDNA was too short for SSB binding, AlkB activity could not be allosterically activated by SSB.

Next, longer oligonucleotides were used as the substrate that can bind SSB. 70-mer oligonucleotide with single N3meC at 35th position (2µM) was used as substrate of AlkB (0.2µM) in the presence or absence of SSB (4µM). As shown in Fig. 8, AlkB was able to oxidatively demethylate N3meC present in 70-mer oligonucleotide and

produce formaldehyde, albeit with lower efficiency compared to 10-mer oligonucleotide. However, when SSB was added stimulation of AlkB activity was observed. Truncated SSB lacking C terminal unstructured region (SSB-1-115) also resulted stimulation on AlkB mediated repair of 70-mer N3meC containing oligonucleotide (Fig. 8). These results were in agreement with the previous experimental results obtained with M13 ssDNA and indicated that both DNA wrapping by SSB and AlkB-SSB interaction promote AlkB activity.

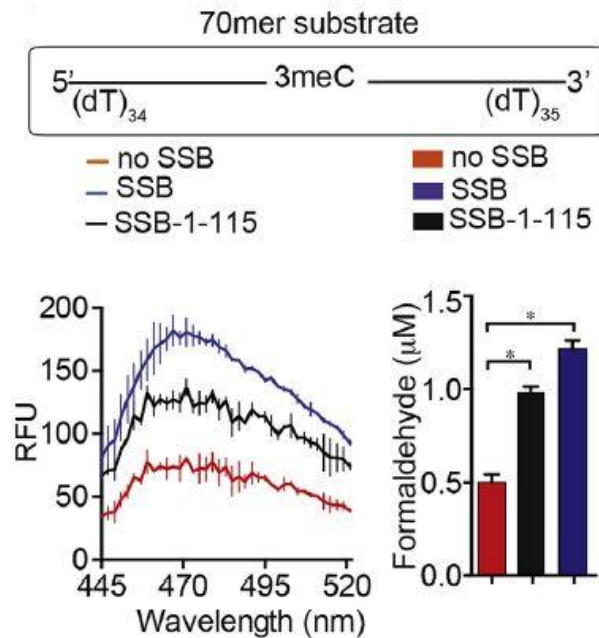


Figure 8: Comparison of DNA repair using 70-mer single N3meC containing oligonucleotide (2µM) was used as substrate. Error bar depicts the standard error.

The P value was calculated by two-tailed Student's t-test (* indicates $P < .05$).

2.3.2. FDH coupled indirect assay to confirm SSB promotes AlkB activity

To further confirm that AlkB was probably inefficient in repairing large ssDNA and the role of SSB could perhaps be to promote AlkB activity to the normal level

alternate indirect assay method was used. Formaldehyde dehydrogenase (FDH) oxidizes formaldehyde to formate using NAD⁺ as the electron acceptor whose reduction to NADH can be measured by absorbance at 340 nm and previously used to monitor formaldehyde release including JmjC histone demethylase [31] and AlkB [17]. The reactions were initiated by adding oligonucleotide containing single N3meC and absorbance at 340 nm at different time points revealed production of formaldehyde. As shown in Fig. 9, comparable increase of absorbance at 340 nm was observed when N3meC containing shorter oligonucleotide (10-mer) were used, indicating that the presence of SSB had no influence on the amount of formaldehyde produced in the AlkB-catalyzed demethylation reaction. The fact that similar amount of formaldehyde was generated in the demethylation of 10-mer DNA strongly suggests that the reaction had occurred.

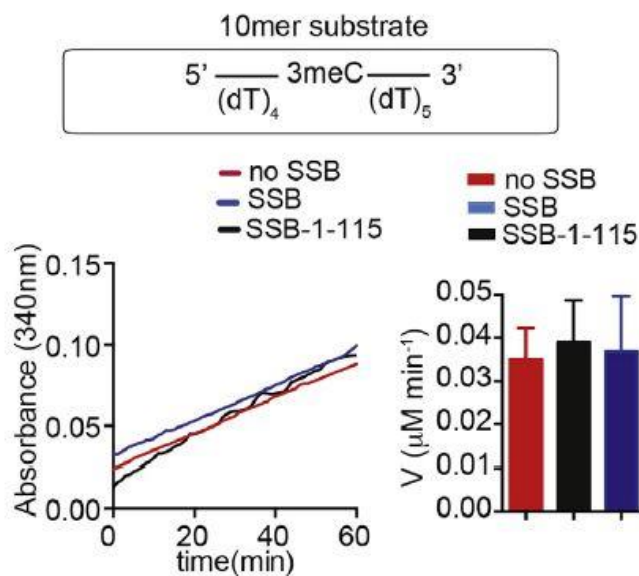


Figure 9: Demethylation reaction using 10-mer single N3meC containing oligonucleotide (2μM) and AlkB (0.2μM) in the presence or absence of tetrameric

SSB (4 μ M) 4 mM, AlkB-mediated repair reaction for formaldehyde production and its detection by formaldehyde dehydrogenase (FDH)-coupled assay. Error bar depicts the standard error.

Next, the repair reaction with 70-mer oligonucleotide (2 μ M) with single N3meC at 35th position was studied. As before, *E. coli* AlkB (0.2 μ M) was added in the presence and absence of SSB (4 μ M) and formaldehyde release was detected. Stimulation of AlkB activity was observed in the presence of full length SSB (Fig. 10). Stimulation was also observed with truncated SSB lacking C-terminal unstructured region (SSB-1-115), suggesting that SSB-binding and protein-protein interaction both are responsible for stimulation of AlkB activity. These findings from the indirect FDH-coupled repair assay were in accord with the observations from the direct repair assay.

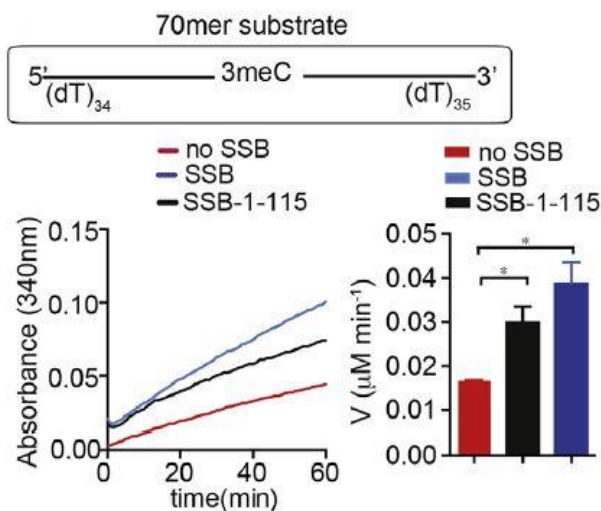


Figure 10: 70-mer single N3meC containing oligonucleotide (2 μ M) was used as substrate. Error bar depicts the standard error. The P value was calculated by two-tailed Student's t-test (* indicates $P < .05$).

2.3.3. AlkB enzyme kinetics in presence of SSB

To further explore the mechanism of stimulation of AlkB mediated DNA repair by SSB, the kinetics of AlkB catalyzed reaction using 70-mer oligo-dT with single N3meC containing oligonucleotides was studied. For all of the experiments, complexes of SSB under low-salt conditions without Mg^{2+} cation which could retain AlkB interaction were used. Under those conditions, the binding mode of *E. coli* SSB was such that two monomers of the SSB tetramer were in contact with ssDNA and two SSB tetramers together could bind a 70-mer ssDNA. *E. coli* SSB is also known to translocate spontaneously and rapidly along the ssDNA via partial unwrapping of one end segment of ssDNA followed by re-wrapping of the other end in its place. So it was hypothesized that if the terminal nucleotide contained the methyl adducts, it might be mostly accessible to AlkB for repair compared to the damage nucleotide which is located internally. Therefore, while SSB-wrapping and AlkB-SSB interaction might be required to promote the repair of an internally located methyl adduct, it might be redundant for terminally located methyl adduct repair. First, 70-mer oligo-dT with single N3meC at the 5'-end was examined for repair in presence or absence of AlkB (Fig. 11). It was observed that, AlkB was able to repair 70-mer terminal N3meC containing oligonucleotide with a K_M values 2.4 μM . When tetrameric SSB was added to the reaction mixture, the K_M remained almost unchanged (2.7 μM), suggesting SSB had little effect on AlkB activity (Fig.11). Similar K_M was also calculated by us using a 40-mer N3-me oligo-dC substrate [29], and others with 19-mer oligo containing a single N3meC [17]. These results indicated that N3meC positioned at the 5'-termini of SSB-bound DNA is as accessible to AlkB as it is in the short oligonucleotide. Next, 70-mer oligo-dT with

single N3meC located internally, either at the 15th position or at the 35th position was studied for repair. AlkB was able to repair 70-mer oligonucleotide with internal N3meC (35th), but with a high K_M (6.7 μM) (Fig. 12). Interestingly, when SSB was added to the reaction mixture, the K_M decreased significantly (2 μM), suggesting strong stimulation of AlkB activity by SSB. Repair 70-mer internal N3meC (15th) was also observed but as expected with a high K_M (8.2 μM) (Fig. 13). As before, when SSB was added to the reaction mixture, the K_M reduced (1.8 μM). The K_M of 15th position N3meC oligonucleotide was higher than that of 35th position oligonucleotide. It was assumed that 35th nucleotide is located at the interface between the two SSB tetramers and could be exposed; whereas, the methylation site at the 15th position could be wrapped by SSB.

Table 4: Comparison of kinetic constants of AlkB

S. No.	Substrate	K_M (μM)	K_{cat} (min^{-1})	Reference
1.	30mer ssDNA 5'CGTCGAATTN3meCTA GAGCCCC3'	3.4	2.2	[17]
2.	40mer oligodC (N3meC)40	2.72	1.89	[29]
3.	T(N3meC)T	24	21	[32]
4.	70mer oligodT with N3meC at position1	2.4	3.071	
5.	70mer oligodT with N3meC at position1 + SSB	2.7	3.050	
6.	70mer oligodT with N3meC at position15	8.2	2.42	
7.	70mer oligodT with N3meC at position15 + SSB	1.8	2.67	
8.	70mer oligodT with N3meC at position35	6.7	2.37	
9.	70mer oligodT with N3meC at position35 + SSB	2.0	2.7	

The kinetic experiment implied that AlkB-mediated repair of internally located damage of 70-mer DNA is indeed augmented by SSB as a result of increased

affinity for substrate binding. These results unveiled an important role of SSB in AlkB mediated repair of large ssDNA.

The presence of SSB lowered the K_M of AlkB catalyzed reaction and was crucial for efficient repair of longer substrate but may be dispensable for the small oligonucleotide substrate. When the length of the single-stranded DNA increased, the catalytic efficiency of AlkB decreased. Since longer stretch of ssDNA would always remain bound by SSB, AlkB can readily repairs such SSB-bound DNA. SSB-AlkB interaction may further promote AlkB-mediated repair. The binding affinity of SSB to ssDNA decreased drastically with decreasing length of the oligonucleotide. However, removal of methyl adducts by AlkB from very short patch of single-stranded region was rather efficient and therefore would be SSB independent. It was speculated that AlkB-mediated repair of methyl adduct would probably be executed without affecting any cellular process, such as replication and recombination, where the long stretches of ssDNA remains predominantly SSB-bound. Thus, based on the data, it was found that wrapping of ssDNA by SSB could alter the ssDNA structure and melt the secondary structure that is more suitable to AlkB-mediated repair resulting in reduction of the K_M and alleviated repair.

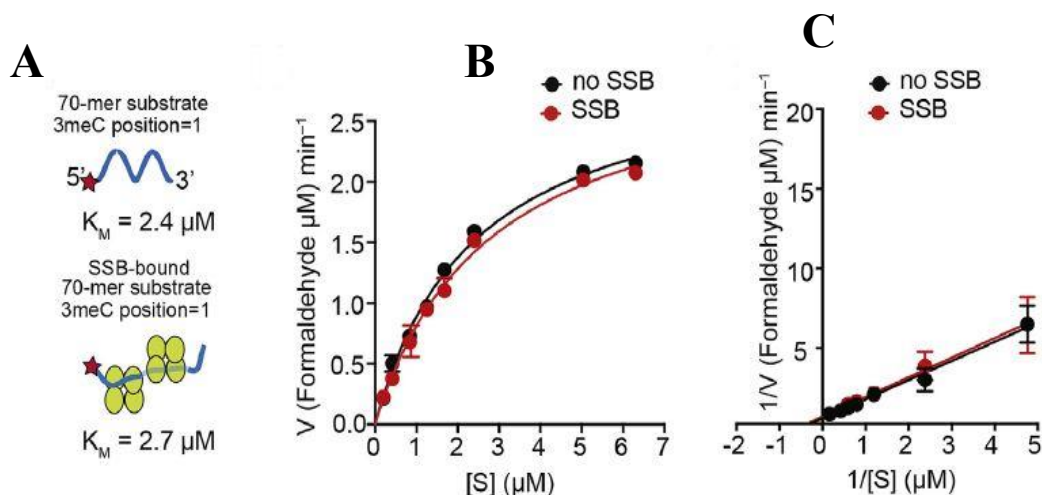


Figure 11: Kinetics of repair of SSB-bound 3meC containing 70-mer oligonucleotide substrate. (A) 70-mer oligonucleotide containing single N3meC at the 5'-end as substrate for AlkB reaction. (B) Michaelis-Menten analysis of steady-state kinetics for AlkB-mediated repair of free and SSB-bound 70-mer terminal N3meC containing oligonucleotide. AlkB (0.2 μM) was mixed with various concentration of free oligonucleotide and SSB-bound oligonucleotide as substrate. (C) Lineweaver-Burk transformation of the steady-state kinetics data.

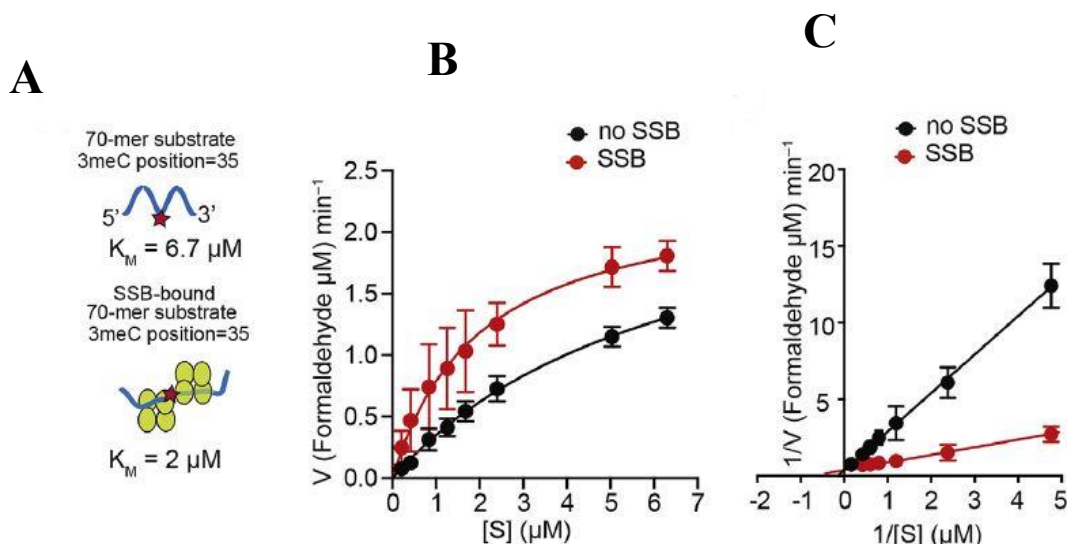


Figure 12: Kinetics of repair of SSB-bound 3meC containing 70-mer oligonucleotide substrate with N3meC at 35th position. (A) 70-mer oligonucleotide containing single

N3meC at the 35th position. (B) Michaelis-Menten analysis of steady-state kinetics for AlkB-mediated repair of free and SSB-bound 70-mer internal N3meC oligo-dT (35th position). (C) Lineweaver-Burk transformation of the steady-state kinetics data. Graphs represent averages of six experiments. Error bar depicts the standard error.

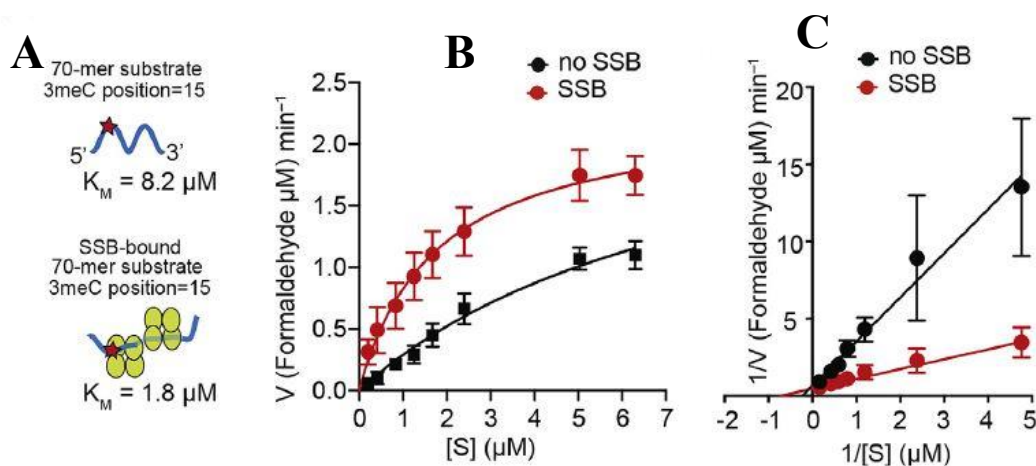


Figure 13: Kinetics of repair of SSB-bound 3meC containing 70-mer oligonucleotide substrate with N3meC at 15th position. (A) 70-mer oligonucleotide containing single N3meC at the 15th position. (B) Michaelis-Menten analysis of steady-state kinetics for AlkB-mediated repair of free and SSB-bound 70-mer internal N3meC oligo-dT (15th position). (C) Lineweaver-Burk transformation of the steady-state kinetics data. Reactions were quantified by detecting formaldehyde released using formaldehyde standard plot. Curves represent nonlinear regressions to the Michaelis-Menten equation obtained using GraphPad Prism 7.0 software. Error bar depicts the standard error.

In summary, it was found that AlkB inefficiently repaired longer single stranded DNA; however, it readily repaired SSB-bound methylated ssDNA of equal length.

Considering the critical role of SSB as a platform for recruitment of DNA repair and recombination proteins, it was demonstrated that SSB plays crucial role in promoting oxidative demethylation repair.

2.4. References

1. Drabløs, F., et al., *Alkylation damage in DNA and RNA—repair mechanisms and medical significance*. DNA repair, 2004. **3**(11): p. 1389-1407.
2. Aas, P.A., et al., *Human and bacterial oxidative demethylases repair alkylation damage in both RNA and DNA*. Nature, 2003. **421**(6925): p. 859-863.
3. Shen, L., et al., *Mechanism and function of oxidative reversal of DNA and RNA methylation*. Annual review of biochemistry, 2014. **83**: p. 585-614.
4. Falnes, P.Ø., et al., *Substrate specificities of bacterial and human AlkB proteins*. Nucleic acids research, 2004. **32**(11): p. 3456-3461.
5. Raghunathan, S., et al., *Structure of the DNA binding domain of E. coli SSB bound to ssDNA*. Nature Structural and Molecular Biology, 2000. **7**(8): p. 648-652.
6. Savvides, S.N., et al., *The C-terminal domain of full-length E. coli SSB is disordered even when bound to DNA*. Protein Science, 2004. **13**(7): p. 1942-1947.
7. Costes, A., et al., *The C-terminal domain of the bacterial SSB protein acts as a DNA maintenance hub at active chromosome replication forks*. PLoS genetics, 2010. **6**(12): p. e1001238.
8. Lohman, T.M. and L.B. Overman, *Two binding modes in Escherichia coli single strand binding protein-single stranded DNA complexes. Modulation by NaCl concentration*. Journal of Biological Chemistry, 1985. **260**(6): p. 3594-3603.

9. Roy, R., et al., *SSB protein diffusion on single-stranded DNA stimulates RecA filament formation*. Nature, 2009. **461**(7267): p. 1092-1097.
10. Meyer, R.R. and P.S. Laine, *The single-stranded DNA-binding protein of Escherichia coli*. Microbiological reviews, 1990. **54**(4): p. 342-380.
11. Shereda, R.D., et al., *SSB as an organizer/mobilizer of genome maintenance complexes*. Critical reviews in biochemistry and molecular biology, 2008. **43**(5): p. 289-318.
12. Han, E.S., et al., *RecJ exonuclease: substrates, products and interaction with SSB*. Nucleic acids research, 2006. **34**(4): p. 1084-1091.
13. Handa, P., N. Acharya, and U. Varshney, *Chimeras between single stranded DNA binding proteins from Escherichia coli and Mycobacterium tuberculosis reveal that their C-terminal domains interact with uracil DNA glycosylases*. Journal of Biological Chemistry, 2001, p. 16992-16997.
14. Umezū, K. and R.D. Kolodner, *Protein interactions in genetic recombination in Escherichia coli. Interactions involving RecO and RecR overcome the inhibition of RecA by single-stranded DNA-binding protein*. Journal of Biological Chemistry, 1994. **269**(47): p. 30005-30013.
15. Shivange, G., N. Kodipelli, and R. Anindya, *A nonradioactive restriction enzyme-mediated assay to detect DNA repair by Fe (II)/2-oxoglutarate-dependent dioxygenase*. Analytical biochemistry, 2014. **465**: p. 35-37.
16. Shivange, G., et al., *A role for Saccharomyces cerevisiae Tpa1 protein in direct alkylation repair*. Journal of Biological Chemistry, 2014: p. 35939-35952.

17. Roy, T.W. and A. Bhagwat, *Kinetic studies of Escherichia coli AlkB using a new fluorescence-based assay for DNA demethylation*. Nucleic acids research, 2007. **35**(21): p. e147-e147.
18. Falnes, P.Ø., *Repair of 3-methylthymine and 1-methylguanine lesions by bacterial and human AlkB proteins*. Nucleic acids research, 2004. **32**(21): p. 6260-6267.
19. Delaney, J.C., et al., *AlkB reverses etheno DNA lesions caused by lipid oxidation in vitro and in vivo*. Nature Structural and Molecular Biology, 2005. **12**(10): p. 855-860.
20. Falnes, P.Ø., R.F. Johansen, and E. Seeberg, *AlkB-mediated oxidative demethylation reverses DNA damage in Escherichia coli*. Nature, 2002. **419**(6903): p. 178-182.
21. Holland, P.J. and T. Hollis, *Structural and mutational analysis of Escherichia coli AlkB provides insight into substrate specificity and DNA damage searching*. PLoS One, 2010. **5**(1): p. e8680.
22. Mishina, Y., C.H.J. Lee, and C. He, *Interaction of human and bacterial AlkB proteins with DNA as probed through chemical cross-linking studies*. Nucleic acids research, 2004. **32**(4): p. 1548-1554.
23. Welford, R.W., et al., *The selectivity and inhibition of AlkB*. Journal of Biological Chemistry, 2003. **278**(12): p. 10157-10161.
24. Yu, B., et al., *Crystal structures of catalytic complexes of the oxidative DNA/RNA repair enzyme AlkB*. Nature, 2006. **439**(7078): p. 879-884.

25. Mishina, Y., C.-G. Yang, and C. He, *Direct repair of the exocyclic DNA adduct 1, N6-ethenoadenine by the DNA repair AlkB proteins*. Journal of the American Chemical Society, 2005. **127**(42): p. 14594-14595.
26. Reyes-Lamothe, R., D.J. Sherratt, and M.C. Leake, *Stoichiometry and architecture of active DNA replication machinery in Escherichia coli*. Science, 2010. **328**(5977): p. 498-501.
27. Antony, E., et al., *Multiple C-terminal tails within a single E. coli SSB homotetramer coordinate DNA replication and repair*. Journal of molecular biology, 2013. **425**(23): p. 4802-4819.
28. Lohman, T.M. and M.E. Ferrari, *Escherichia coli single-stranded DNA-binding protein: multiple DNA-binding modes and cooperativities*. Annual review of biochemistry, 1994. **63**(1): p. 527-570.
29. Shivange, G., et al., *RecA stimulates AlkB-mediated direct repair of DNA adducts*. Nucleic acids research, 2016. **44**(18): p. 8754-8763.
30. Purnapatre, K. and U. Varshney, *Cloning, over-expression and biochemical characterization of the single-stranded DNA binding protein from Mycobacterium tuberculosis*. European journal of biochemistry, 1999. **264**(2): p. 591-598.
31. Couture, J.-F., et al., *Specificity and mechanism of JMJD2A, a trimethyllysine-specific histone demethylase*. Nature Structural and Molecular Biology, 2007. **14**(8): p. 689-695.
32. Yu, B. and J.F.J.P.o.t.N.A.o.S. Hunt, *Enzymological and structural studies of the mechanism of promiscuous substrate recognition by the oxidative DNA repair enzyme AlkB*. 2009. (106)34: p.14315-1420

Chapter 3: Interaction of AlkB with SSB

3.1. Introduction

E coli SSB is a tetrameric protein consisting of four identical subunits. Each SSB monomer consists of 178 amino acid residues and has three domains: N-terminal OB-domain (Oligonucleotide/oligosaccharide Binding) [1] that binds ssDNA (residues 1–115), intrinsically disordered linker (IDL) region (residues 116–169) and [2] C-terminal acidic domain (residues 170–178) that binds several proteins involved in DNA metabolism [3]. The IDL of SSB is not observable in crystal structures, suggesting that these C-terminal tails are intrinsically disordered. Indeed, the IDL displayed low sequence complexity and enriched with a large number of proline, glycine, and glutamine residues, resulting in highly disordered/unstructured characteristics. Computational analysis revealed that the IDL is essential for highly cooperative binding of SSB to ssDNA [4]. Beside this, no other functional importance of IDL is known. C-terminal acidic domain of SSB act as protein interaction platform and bind various replication and repair proteins including base excision repair pathway enzyme uracil DNA glycosylase [5], translesion DNA polymerases [6, 7], RecJ [8], recombination mediator RecO [9], repair protein RadD [10], Exonuclease- 1 [11, 12] and RecQ helicase [13]. As many DNA repair proteins are known to interact with SSB, the objective in this chapter is to characterize the direct interaction of DNA dealkylation repair protein AlkB with SSB. AlkB has been known to repair various alkyl adducts, including N1meA and N3meC, present in DNA by oxidative demethylation. Previous studies have shown that AlkB preferentially removes alkyl-adducts from ssDNA. Although the molecular

mechanism of AlkB-mediated catalysis is well-understood, it was not clear whether SSB is involved in direct interaction with AlkB. In this chapter, the analysis of SSB-AlkB interaction has been done to address whether SSB can bind to AlkB. For this several truncated SSB construct were generated and the SSB-AlkB interaction was studied by yeast-two-hybrid and pull-down analysis. Surprisingly, it was found that that binding of SSB to AlkB involves the IDL of SSB. The C-terminal acidic domain of SSB, which is widely involved in protein-protein interaction, is dispensable for this interaction.

3.2. Materials and method:

3.2.1. Cloning

For His tag expression AlkB gene was sub-cloned from pBluscript-AlkB clone No. 151 into pET28a-1 vector using BamH1 and Sal1 sites. For GST fusion expression, SSB gene was cloned in pGEX-6p1 vector using BamH1 and Xho1 sites. SSB-1-115 was cloned into pGEX-6p1 vector using BamHI and XhoI sites. SSB-116-178 was cloned into pGEX-6p1 vector using NcoI-EcoRI and XhoI sites. SSB-116-169 was cloned into pGEX-6p1 vector using NcoI-EcoRI and XhoI sites. SSB-116-151 was cloned into pGEX-6p1 vector using NcoI-EcoRI and XhoI sites. For Yeast two hybrid assay, AlkB gene was cloned into pACT2 vector using NcoI and SalI sites. SSB was cloned into pGBKT7 vector using NcoI and XhoI sites. SSB-1-116-178 and SSB-1-115 were cloned into pGBKT7 vector using NcoI and SalI site and NoI and XhoI site respectively. SSB-1-169 was cloned in pGBKT7 vector using NcoI and XhoI sites. SSB-152-169 was cloned by internal deletion method.

Table 5: Cloning strategy for genes cloned in section 3.2.1.

Clone	Clone No.	Oligo Sequence (5' – 3')	Cloning sites
pGBKT7-SSB- 1-169	248	SSB-NcoI-Sen AAA ACC ATG GAG ATG GCC AGC AGA GGC GTA AAC SSBΔC8-Xho-Anti GCC GCT CGA GTC ACA TCG GCG GCT CGT TAG ACG	NcoI XhoI
pGBKT7-SSB- 1-151	249	SSB-NcoI-Sen AAA ACC ATG GAG ATG GCC AGC AGA GGC GTA AAC SSBΔ26-XhoI-Anti AGA TCT CGA GCT ACG CGC CGC CGC TGA ACT G	NcoI XhoI
pGBKT7-SSB- 152-169	250	pGBKT7_EagI_Sen CTC GAC CTG CAG CGG ACG CAT AAC TAG CAT SSB del 152-169_reverse GCC GCC GCT GAA CTG ATT GCC ACC CTG CGG	Internal deletion
pGEX-6p1- SSB-16-151	216	SSB _{CTD} -NcoI-EcoRI-sen AAA ACC ATG GAA TTC CGT CAG GGT GGT GGC GCT CCG GC SSBΔ26-XhoI-anti AGA TCT CGA GCT ACG CGC CGC CGC TGA ACT G	EcoRI XhoI
pACT2-AlkB	198	AlkB-NCOI-sen	NcoI

		AAA ACC ATG GAG ATG TTG GAT CTG TTT GCC GAT GC AlkB-SalI-Anti TTT TGT CGA CTT ATT CTT TTT TAC CTG CCT GAC GG	SalI
pGBKT7-SSB	220	SSB-NcoI-sen AAA ACC ATG GAG ATG GCC AGC AGA GGC GTA AAC SSB-XhoI-anti GCC GCT CGA GTC AGA ACG GAA TGT CAT CAT CAA AGT CC	NcoI XhoI
pET-28-a-AlkB	196	Subcloned from pBluescript-AlkB (clone No. 151)	BamHI SalI
pTYB3-AlkB	253	pTYB3_AlkB_NcoI_F ATT AC CAT GGA AAT GTT GGA TCT GTT TGC CGA TGC TG pTYB3_AlkB_SalI_R TTT TG TCG ACT TCT TTT TTA CCT GCC TGA CGG	NcoI XhoI

3.2.2. *In vitro* GST pull-down assay

For GST pull-down experiments, full-length SSB and different truncated mutants of SSB were expressed as GST fusion proteins and AlkB was expressed as His-tag protein. For ssDNA-dependent interaction, 10 μ M of 70-mer oligonucleotide was added along with His-tagged AlkB and GST-SSB. Protein complexes were then pulled down and analyzed by western blot with an anti-His antibody

3.2.2.1. Purification of recombinant His-AlkB protein

The recombinant His AlkB soluble protein was purified by Ni-NTA affinity chromatography. For this, the pET28a-AlkB plasmid was transformed in BL-21(DE3)pLysS cells. Few BL21+pET28a-AlkB transformed colonies were inoculated into 100ml LB-broth with 100 µg/ml ampicillin and grown on an incubator shaker at 37°C at 200 rpm. The grown culture was 20-fold diluted into 2L fresh TB-broth with 100 µg/ml ampicillin. Incubation was carried out at 37°C at 200 rpm for 3 hrs. The culture was then induced with 1mM IPTG and kept for 5 hrs at 30°C at 200 rpm. Cells were harvested after centrifugation at 8000 rpm for 15 minutes at 4°C. The cell pellet was resuspended in 20ml of 50mM Tris-HCl buffer (pH 8.0) containing 300mM sodium chloride, 0.1% Triton-X, 1mM Imidazole and sonicated for 30 minutes. The sample was then centrifuged at 14,000 rpm for 20 minutes at 4°C to remove insoluble debris. The soluble fraction was mixed with 2ml of Ni-NTA resin pre-equilibrated with the same buffer and allowed to rotate in a rotary shaker for 4h to allow the protein to bind to the resin. The sample was then centrifuged at 1000 g for 5 minutes at 4°C and the washing is carried out in 3 steps with 75 ml wash buffer (50 mM Tris, pH8.0, 350 mM NaCl, 0.1% Triton-X and 5mM Imidazole). Centrifugation was carried out at 1000g for 4 minutes at 4°C. Bound protein was eluted with elution buffer (10 mM Tris,pH 8.0, 100 mM NaCl, 400 mM Imidazole). 1.5ml of elute1, 1ml of elute 2 and 1ml of eluting 3 were collected. All eluates were checked in 12% SDS-PAGE.

3.2.2.2. Preparation of glutathione sepharose bead-bound GST-SSB

The 750ml culture of BL-21(DE3)pLysS cells transformed with pGEX-SSB or truncated constructs of SSB: pGEX-SSB(116-178), pGEX-SSB(116-169), pGEX-SSB(116-151), pGEX-SSB(1-115) was grown. Cell extract was prepared by

sonication at 25% amplitude and pulse a 10sec for 20min. The soluble fraction was collected by centrifugation at 14000rpm/20min/4°C and mixed with 500µl glutathione-Sepharose bead slurry (GE-healthcare). The glutathione-Sepharose beads were allowed to interact and get saturate with GST-SSB or mutant SSB for 4h at 4°C on gentle rotation of 10rpm. Non-specific and loosely bound protein contaminants were removed by washing the medium with 10mM Tris-HCl pH 7.4, 500mM NaCl and 0.1% TritonX. Finally, the GST-SSB bound beads were resuspended in 10mM Tris-HCl pH 7.4, 100mM NaCl and 5% glycerol. Using the same procedure, as a control, GST protein-bound glutathione beads were prepared by growing BL-21(DE3)pLysS cells transformed with pGEX-6p1. The quality and quantity of bound GST-SSB were checked by taking 20µl of protein-bound slurry in 20µl of H₂O and mixed with 20µl loading dye. The entire mixture was boiled at 95°C for 10min and 10µl was analyzed in 10% SDS-PAGE.

3.2.2.3. Interaction of glutathione bead-bound GST-SSB and His-AlkB

50µl of Glutathione-Sepharose medium, saturated with GST-SSB or truncated SSB constructs or GST alone, was then incubated with 175µg of His-AlkB in 500ul interaction reaction containing 10mM Tris-HCl pH7.4, 100mM NaCl and 5% glycerol at room temperature for 2h. The beads were then separated by centrifugation 500g/5min. Non-specific and loosely bound His-AlkB was removed by washing three times with 1ml of phosphate buffer saline (PBS) using centrifugation 500g/5min.

3.2.2.4. SDS-PAGE

Sample preparation: Washed beads were then resuspended in 40 μ l PBS and mixed with 40 μ l of 3X loading dye. 30 μ l of unbound and wash fractions were mixed with 15 μ l of 3X loading dye. All samples were boiled at 95°C for 10min.

Electrophoresis: 5 μ l of pulled fraction and 15 μ l of unbound/wash sample is separated by 10% SDS-PAGE. Staining and destaining of the gel were carried out as per the protocol described in section 2.2.2.6. As the sizes of GST protein (25.4kDa) and His-AlkB (27.6kDa) are close to differentiate background His-AlkB western blotting was employed.

3.2.2.5. Western blotting

Presence of His-AlkB was confirmed by western blotting using Anti-His antibody (GE healthcare). First, SDS-PAGE electrophoresis was done with 1.5 μ l of input His-AlkB (0.3 μ g) and 7 μ l of pulled fractions loaded along with protein ladder in 10% SDS-PAGE run at 140V/70min. After electrophoresis, the separated protein bands were transferred to nitrocellulose membrane (Hybond-C Amersham) by using BIO-RAD wet transfer system. Transfer cassette was assembled with the gel sandwiched between sheets of filter paper pre-soaked in cold transfer buffer (25mM Tris, 192mM Glycine and 20% methanol). The electrophoresis tank was filled with transfer buffer and the transfer was run at constant 20 mA for 100min. After transfer, the membrane was stained with Ponceau.

Ponceau-S Staining: Ponceau-S staining is a reversible staining process which, after analysis, can be easily removed by any salt solution. This step helps in checking the transfer success and locating the blot area to be developed by comparing with the protein ladder. After completion of the transfer, the transfer cassette was disassembled and the membrane was rinsed with Milli-Q water. The blot was then

immersed into Ponceau-S (Sigma 141194) solution (0.1% solution prepared in 5% acetic acid) for 1 to 2min with gentle shaking followed by washing to remove background stain. Ponceau stain was removed from blot by washing with PBS after imaging. Anti-His antibody (GE-Healthcare Amersham, 27-4710-01) was used as primary antibody and was used at 1:5000 dilution. The blot was incubated with the primary antibody for 1h at room temperature on gentle shaking. It was then washed with PBS thrice with 10ml of PBS and 10mins incubation. HRP-linked secondary antibody (Amersham ECL mouse IgG, NA931) was used as secondary antibody. The secondary antibody was diluted to 1:10000. The blot was immersed and incubated in secondary antibody solution for 1h at room temperature on gentle shaking. The membrane was then washed three ECL Western blotting detection reagents (Amersham, RPN2106) were used to detect the His-AlkB. An equal volume of detection solution 1 was mixed with detection solution 2 in a final volume of 500 μ l, was spread on the blot. Luminescence was detected by using SynGENE Gel Doc system. The images were captured in a continuous manner at different exposures times for total 30min.

3.2.3. Isothermal titration calorimetry (ITC)

3.2.3.1. Purification of tagless AlkB

the pTYB3-AlkB plasmid was transformed in BL-21 BL-21(DE3)pLysS cells. The protein was purified by affinity purification by fusing with the intein-chitin domain. The detailed protocol for chitin resin based protein purification has been same as discusses in section 2.2.1. The protein was then dialyzed in a buffer containing 20mM Tris pH8.0, 100mM NaCl and 1 mM β -Mercaptoethanol.

3.2.3.2. The Peptide (ligand) for ITC

Synthetic peptide corresponding to amino acid residues 152–169 of SSB (AQSRPQQSAPAAPSNEP) were obtained from GM Research Foundation Pvt. Ltd. The peptide was dissolved in buffer containing 20mM Tris pH8.0, 100mM NaCl and 1 mM β -Mercaptoethanol.

3.2.3.3. ITC experiment

All the ITC experiments were carried out in Microcal ITC 200 instrument at 25 °C while stirring at 750 rpm in 20 mM Tris–HCl, pH 8.0 containing 100 mM NaCl and 1 mM β -Mercaptoethanol. The tag-less AlkB (50 μ M) protein was filled in the cell (280 μ L). The syringe was loaded with peptide 250 mM in the same buffer as that of protein. The titrant peptides were injected in the cell in 20 successive injections of 2 μ L each at an interval of 180 s. The collected data was processed using origin 7.0 software.

3.2.4. CD-spectroscopy

3.2.4.1. Preparation of protein

Purified Tagless AlkB and SSB were used for CD experiment. pTYB3-AlkB and pTYB3-SSB plasmids were transformed into BL-21(DE3)pLysS cells. The proteins were purified using standard chitin resin based purification protocol as discussed in section 2.2.1. The purified protein was split into two batches which were dialyzed in two different buffers. One batch of the proteins was dialyzed in a low salt buffer containing 20 mM Tris–HCl, pH 7.4 and 0.1 M NaCl. Another batch was dialyzed in a High salt buffer containing 20 mM Tris–HCl, pH 7.4, 0.1 M NaCl. SSB peptide SSB-152–169 (0.25 mM) was dissolved in buffer containing 20 mM Tris–HCl, pH 8.0, and 50 mM NaCl.

3.2.4.2. CD-experiment

The CD experiments were conducted on a JASCO J-1500 instrument. A quartz cell of 1 mm path length was used for all the experiments. To examine the effect of NaCl on the AlkB and SSB conformation, CD spectra was recorded with SSB (20 μ M) and AlkB (20 μ M). Spectra were obtained at room temperature. Before measuring the spectra of proteins, a baseline was recorded for each of the proteins using the protein dialysis buffer or the dilution buffer. CD spectra of SSB-152–169 peptide (0.25 mM) was measured in buffer containing 20 mM Tris–HCl, pH 8.0, 50 mM NaCl. The CD spectra were recorded in the far-UV wavelength range of 190-260nm. Before, measuring CD spectra, the CD machine was infused with nitrogen gas for 10minutes. The baseline was loaded before running the sample spectra. The spectra were recorded as an average of five spectral scans with bandwidth 1 nm, step 1 nm and 0.5 sec/point. The data pitch was kept 0.5 nm and scanning speed was 50 nm/sec. The recorded data were analyzed using spectra manager software.

3.2.5. Yeast two-hybrid analysis of AlkB and SSB interaction

3.2.5.1. Yeast strain:

The yeast two-hybrid reporter strain, PJ69-4A (MATa, trp1-901, leu2-3, 112ura3-52 his3-200 gal4 Δ , Yeast strain: gal80 Δ , LYS2:: GAL1-HIS3, GAL2-ADE2, met2:: GAL7-lacz) [14] was used for the yeast-two-hybrid study.

The yeast strain possess three marker genes ADE2, HIS3 and lacZ reporter genes that are expressed only when a functional Gal4 protein is reconstituted by an interaction between the activation domain and the DNA binding domain fusion proteins. GAL4 Activation domain was fused with AlkB (pACT2-AlkB), and the binding domain was fused with SSB, (pGBKT7-SSB), for yeast two hybrid assay.

Different truncated constructs of SSB SSB-1-115, SSB-16-178, SSB-116-169, SSB116-151 and SSB-152-169 were also created as pGBKT7 fusion construct. The pACT2-AlkB (activation domain) plasmid was cotransformed with pGBKT7-SSB, pGBKT7-SSB-116-177, pGBKT7-SSB-1-115 (binding domain) , pGBKT7-SSB-1-169, pGBKT7-SSB-1-151, and pGBKT7-SSB-152-169 plasmid into yeast strain pJ69-4A to generate strain J69RA1 (pACT2-AlkB + pGBKT7-SSB), J69RA2 (pACT2-AlkB + pGBKT7-SSB-116-177), J69RA3 (pACT2-AlkB + pGBKT7-SSB-1-115), J69RA4 (pACT2-AlkB + pGBKT7-SSB-1-169), J69RA5 (pACT2- AlkB + pGBKT7-SSB-1-151), J69RA6 (pACT2- AlkB + pGBKT7-SSB-152-169) and J69RA7 (pACT2- AlkB + pGBKT7-SSB-170-178).

3.2.5.2. Media preparation

As PJ69-4A strain is deficient in adenine biosynthesis, it was maintained on YPAD medium (2% Tryptone, 2% Dextrose, 1% Yeast Extract, and 0.1mg/ml adenine sulfate). On YPAD media, lacking adenine, the PJ69-4A colonies appeared red in color. The pACT2 vector contains LEU2 marker and pGBKT7 is with TRP1 marker. For selecting co-transformed PJ69-4A strains, the synthetically defined (SD) media lacking Leucine and Tryptophan was used. It was prepared by mixing 2.67% of DOB growth medium (Drop Out Base, Himedia, G082), 0.64mg/ml CSM w/o LEU TRP (Complete Supplement Mixture, Himedia, G115) and 1.5% agar. The media was sterilized by autoclaving at 115°C for 20min.

3.2.5.3. Yeast transformation

Single colony was inoculated in 5 ml of YPAD broth (Yeast extract-1%, Peptone-2%, Glucose-2% and Adenine sulfate-0.1mg/ml). The culture was incubated at 30°C /200 rpm/overnight. Overnight grown pre-inoculum was then 50-fold diluted (500µl

into 25ml YPD-broth) and further incubated at 30°C /200rpm/4h (should allow 2 divisions). After the incubation cells were pelleted by centrifugation at 3000g/5min at room temperature (all the spin conditions were carried out at room temperature). The pelleted cells were washed with 10 ml of autoclaved water and harvested by centrifugation at 3000g/5min. The pellet was then resuspended in 500µl of 100mM LiOAc (Sigma, Cat.no.L6883) and split into five aliquots of 100µl each into a 2ml tubes. The cells were then pelleted at top speed for 20sec and the supernatant was discarded. To the pelleted cells a, transformation mixture was added in the following sequence: 2µl (100ng) of plasmid DNA, 36µl of 1M LiOAc, 25µl of heat denatured salmon sperm DNA (Sigma, Cat.no.D1626), 240µl of 50% PEG (Sigma, Cat.no.P4338). Carrier DNA was converted to single stranded DNA by heating at 95°C for 5min and immediately chilling on ice. After addition of all the reagents the transformation mixture was vortexed vigorously for a minute and then incubated in 30°C incubator for 30min. Heat treatment was given at 42°C for 25min in water-bath (Lauda, Version RA). Following the heat shock, cells were pelleted by centrifugation at 8000 rpm for 1 min and resuspended in 300µl of autoclaved water. The cells were finally plated on SD w/o LEU-TRP agar plate incubated at 30°C for 2-3 days till the isolated colonies appeared. The grown isolated colonies were re-streaked on selective media and grown for further screening by PCR based gene amplification.

3.2.5.4. Yeast two-hybrid analysis

The pACT2-AlkB plasmid was co-transformed with pGBKT7-SSB constructs plasmids into yeast strain pJ69-4A to generate strain J69RA (pACT2-AlkB + pGBKT7-SSB). The transformants were plated onto synthetically defined (SD)

growth medium w/o LEU-TRP (Himedia) plates and incubated at 30°C for 2–3 days. As a control, pACT2 vector was co-transformed to pGBKT7 and pGBKT7-AlkB. Similarly, pACT2-AlkB was transformed to pGBKT7 vector. The transformants were screened for interaction by using *HIS3* reporter and *lacZ* reporter system.

3.2.5.5. HIS3 selection for interaction positive cells

Single colonies, from all the transformants grown on SD w/o Leu-Trp, were resuspended into 100µl of autoclaved water and 10µl spotting was performed onto SD w/o Leu-Trp-His plates. The plates were incubated at 30°C for 3-5 days and examined for the growth. A similar pattern of spots was carried on SD w/o Leu-Trp and used as control plate.

3.2.5.6. Colony lift filter assay using lacZ reporter

The β-galactosidase (β-gal) activity was measured according to the Yeast Protocols Handbook (Clontech). All the transformants were spotted on SD w/o Leu-Trp media and grown for three days at 30°C. Two autoclaved filter papers (Whatman No. 5) was taken and cut in the size of the Petri plate. One filter paper was presoaked in 5 ml Z buffer (60mM Na₂HPO₄, 40mM NaH₂PO₄, 10mM KCl, 1mM MgSO₄, 40mM β-mercaptoethanol) containing 8mg/ml X-gal. A stock of Z-buffer containing 60mM Na₂HPO₄, 40mM NaH₂PO₄, 10mM KCl, 1mM MgSO₄ without β-mercaptoethanol and X-gal was autoclaved and stored at 4°C. β-mercaptoethanol and X-gal were freshly added whenever required. Other filter paper was used to lift the cells by placing on the surface of grown media plate. To help colonies to cling to the filter, the side of the forceps was gently rubbed on the filter. Filter carrying transferred cells was carefully lifted and dipped in liquid nitrogen for 1min and then

thawed at room temperature. This step makes cells porous and helps in β -galactosidase and X-gal interaction. After thawing, the filter disc was placed on the pre-soaked filter containing X-gal, facing cells upward, and incubated at 30°C till the blue colour developed. The appearance of blue color was monitored for 30min to 10hr and documented by scanning the filter paper under the scanner.

3.3. Result and discussion

3.3.1. Characterization of the direct interaction of AlkB with SSB by Yeast-two-hybrid assay

In order to characterize AlkB-SSB interaction, several deletion constructs were generated as shown in Fig. 14. First, the DNA binding (OB) domain (SSB-1-115) was separated from the disordered C-terminal domain (SSB-116-177). It has been reported that C-terminal 26-residues of SSB was important for the characterization of SSB- χ protein interaction [15]. Hence, SSB-1-151 lacking C-terminal 26 residues were created. However, a later crystal structure of the χ -SSB interaction site revealed the C-terminal 8 residues of SSB was the true interaction domain [153]. Therefore SSB-116-169 which would retain the entire structurally disordered region except for the terminal 8 acidic amino acid-rich segment and SSB-116-151 which would lack C-terminal 26 amino acid were also generated. In order to further confirm if SSB actually interacted with via the C-terminal 8 amino acids or the remaining 18 residues, SSB-170-178 and SSB-152-169 respectively were also created.

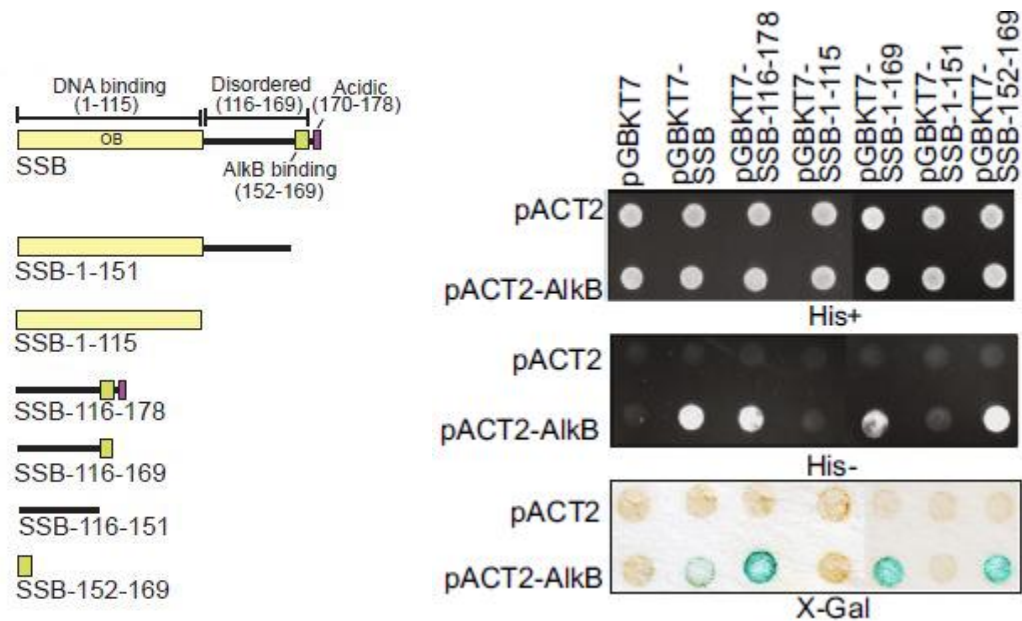


Figure 14: (A) Schematic representation of various SSB deletion constructs which were generated for Yeast-two-hybrid study. (B) SSB-AlkB interaction analysis by yeast two-hybrid system. Positive interactions are indicated by growth on media lacking histidine and expression of β -galactosidase

To assess whether AlkB can directly interact with SSB without the involvement of any intermediate proteins, yeast two-hybrid analysis was performed. *E. coli* SSB and *alkB* genes were cloned into vectors pGBKT7 (TRP1 marker) and pACT2 (LEU2 marker) rendering SSB fusion with DNA binding domain and AlkB fusion with transcription activation domains of the Gal4 transcription factor. The direct interactions of fusion partners were investigated by expression of all the reporter genes (HIS3, and lacZ). PJ69-4A cells carrying plasmid pair pACT2-AlkB/pGBKT7-SSB grew on media lacking leucine, tryptophan, and histidine and showed a blue color on media supplemented with X-gal, suggesting direct AlkB-SSB interaction as shown in fig.14. This result indicated that AlkB and SSB directly

interact with each other in the cellular context. To identify if the N-terminal DNA binding OB domain or the C-terminal domain of SSB interacts with AlkB, SSB-116-178 and SSB-1-115 constructs were studied. As shown in Fig. 14, only pACT2-AlkB/pGBKT7-SSB-116-178 grew well on media lacking histidine and showed a blue colour on media containing X-gal, suggesting AlkB interaction domain is located within the 116-178 amino acid residues of SSB and not within the N-terminal OB domain. Within this C-terminal half of SSB, there are two domains, (1) IDL (residues 116-169) and (2) acidic region (residues 170-178). If the acidic domain is involved in binding AlkB, then a truncated form of SSB without these residues will not be able to interact with SSB. PJ69-4A cells expressing AlkB and SSB-1-169 which lacks the last 9 amino acids grew on media lacking histidine, suggesting that the acidic region is not involved in binding. However, SSB-1-151 which lacks the last 27 amino acids failed to grow on media lacking histidine, suggesting that the region involved in binding must be located between the amino acid 152 and 169. To confirm this interaction domain more precisely, the growth of pACT2-AlkB/SSB-152-169 was examined on media lacking histidine. It was observed that SSB-152-169 supported the growth, suggesting that the 18 amino acid residues, corresponding to amino acid residues 152-169 and located in the IDR, could be involved in the interaction.

3.3.2. Verification of SSB-AlkB interaction *in vitro*

To independently verify the SSB-AlkB direct interaction *in vitro*, the GST-pull down assay was performed. In this experiment, AlkB protein was expressed with His-tag and SSB protein was produced as a GST-fusion, which could be pulled down using glutathione-sepharose beads. The *in vitro* pull-down results show that

His-tagged AlkB protein was bound to GST-SSB (Fig. 15A, lane 2), but not to GST alone. These results suggest that AlkB and SSB made direct contact *in vitro*. Having established *in vitro* interaction of SSB with AlkB, the next objective was to know which part of the unstructured C-terminal region of SSB is involved in the interaction. The entire C-terminal domain (SSB-116-177), or the same domain lacking C-terminal 8 amino acids (SSB-116-169) or 26 amino acids (SSB-116-151) was expressed as GST-fusion protein. SSB construct containing only DNA binding OB domain (SSB-1-115) was also generated. To study *in vitro* interaction, purified His-tagged AlkB was mixed with GST-SSB-116-169, GST-SSB-116-151, and GST-SSB-115 and pull-down experiments were performed as before. Western blot analysis revealed that AlkB could indeed bind to GST-SSB-116-177 and GST-SSB-116-169 but not with GST-SSB-116-151 and SSB-1-115 as shown in Fig.17B. Based on this *in vitro* interaction result together with the yeast two-hybrid data, the residues 152-169 of SSB were mapped as the AlkB-interacting region.

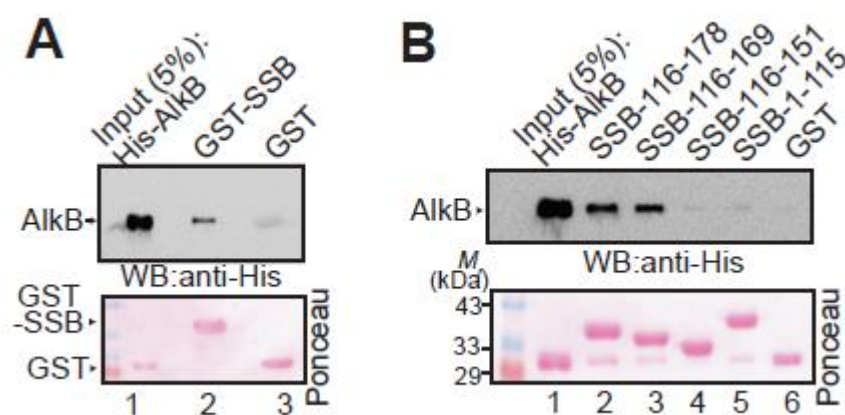


Figure 15: (A) GST pull down experiment of SSB AlkB interaction. (B) GST-SSB fusion proteins used for mapping the AlkB-interacting regions on SSB. Top: inputs

and pull downs were separated by SDS-PAGE and analyzed by western blot with anti-His antibody. Bottom: ponceau-S staining.

3.3.3 Examination of the strength of AlkB-SSB interaction

The strength of SSB-AlkB interaction was also examined by performing a pull-down experiment in the presence of increasing concentration of NaCl. As shown in Fig. 16 the association of AlkB with SSB was not salt-stable and NaCl interrupted the binding. However, when ssDNA was included in the interaction mixture, SSB-AlkB interaction was more stable. 10 μ M of 70-mer single stranded oligonucleotide DNA was added to His-tagged AlkB. SSB-AlkB interaction remained intact at 0.5M NaCl suggesting that ssDNA may render the complex more resistant to high salt washes.

The effect of NaCl on the confirmation of AlkB and SSB was also examined by using CD spectroscopy. As shown in Fig. 17, the CD spectra of SSB remained almost unchanged in the presence 1.0 M NaCl. This result is in agreement with an earlier report suggesting that tetrameric SSB is resistant to NaCl-dependent conformational changes [17]. The confirmation of AlkB protein was also analyzed using CD spectroscopy. *E.coli* AlkB CD spectrum was reported to have a characteristic negative peak at 214 nm [18]. This negative peak was also observed at 100 mM NaCl. However, at a higher salt concentration (1.0 M NaCl) this negative peak was absent indicating some conformational changes in the AlkB structure. Taken together, these results suggest that SSB-AlkB interaction is facilitated by the presence of ssDNA in low ionic strength condition.

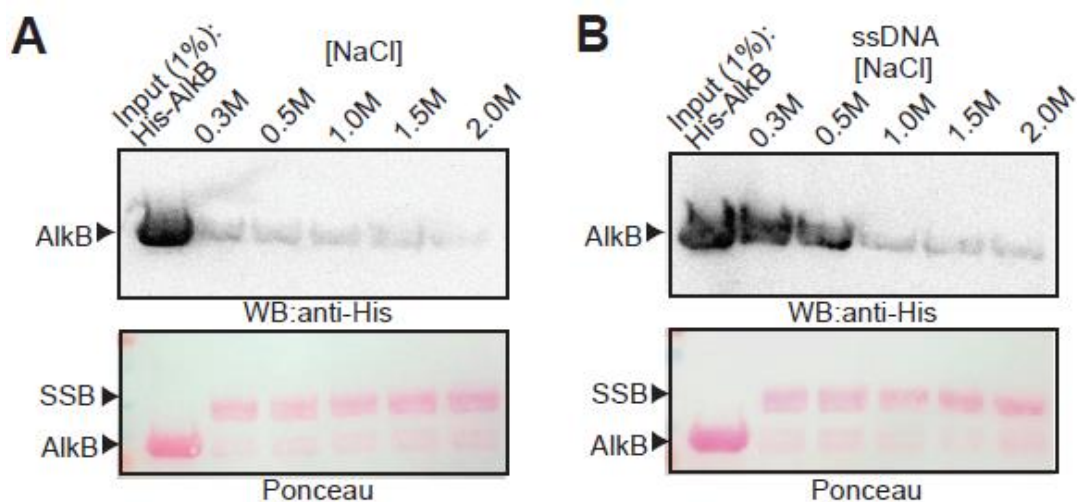


Figure 16: (A) GST pull-down experiments with His-tag AlkB and GST-tagged SSB proteins in presence of varying NaCl concentration to determine the effect of salt concentration on AlkB-SSB interaction. (B) Effect of presence of ssDNA on SSB-AlkB interaction studied by adding 10 μ M of 70-mer ssDNA to the GST-pull down assay.

To further, characterize the strength of the interaction between residues 152-169 of SSB and AlkB, ITC was used. First, the intrinsically disordered nature of the peptide was confirmed by CD analysis. The peptide corresponding to residues 152-169 peptide exhibited a negative minimum close to 200 nm and a relatively low ellipticity above 210 nm (Fig. 18), a typical observation for disordered proteins [154, 155]. Subsequently, ITC experiment was performed with this SSB peptide (residues 152-169) and AlkB. The best fit obtained with a two-site binding model, suggesting a high-affinity site ($K_d = 0.15\mu$ M) and a very low-affinity site ($K_d = 0.45$ mM). As shown in Fig.19 the result from ITC experiment demonstrated that AlkB binds to an SSB-152-169 peptide, albeit weakly.

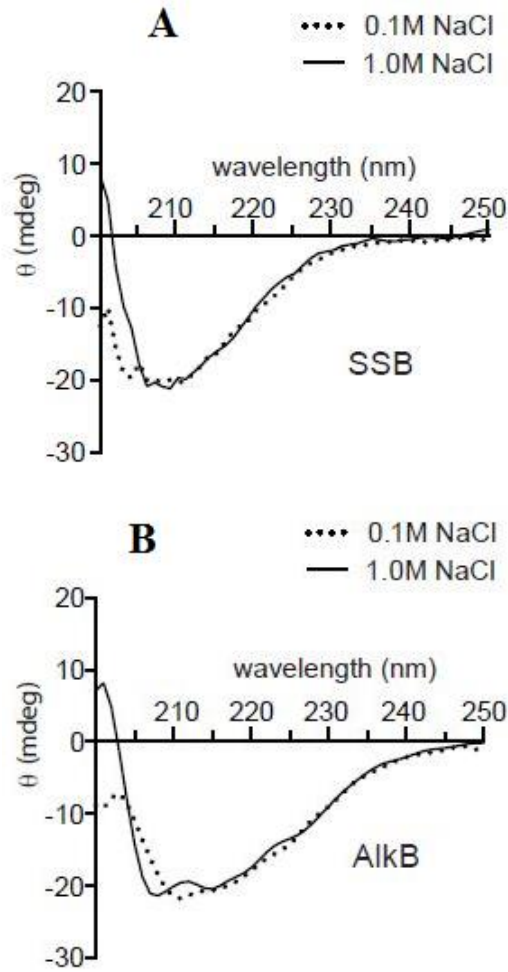


Figure 17: Circular dichroism (CD) analysis of (A) SSB and (B) AlkB in the presence of low (0.1 M) and high (1.0 M) concentration of NaCl.

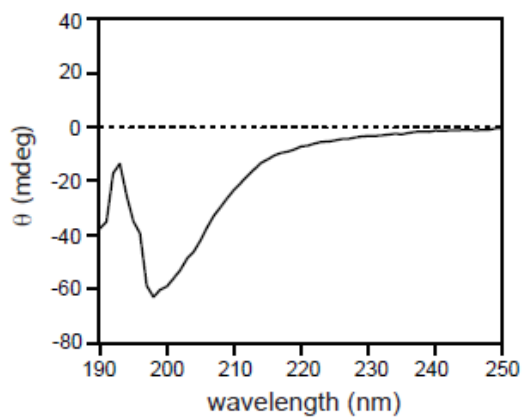


Figure 18: Conformational analysis of SSB peptide 152-169 using CD.

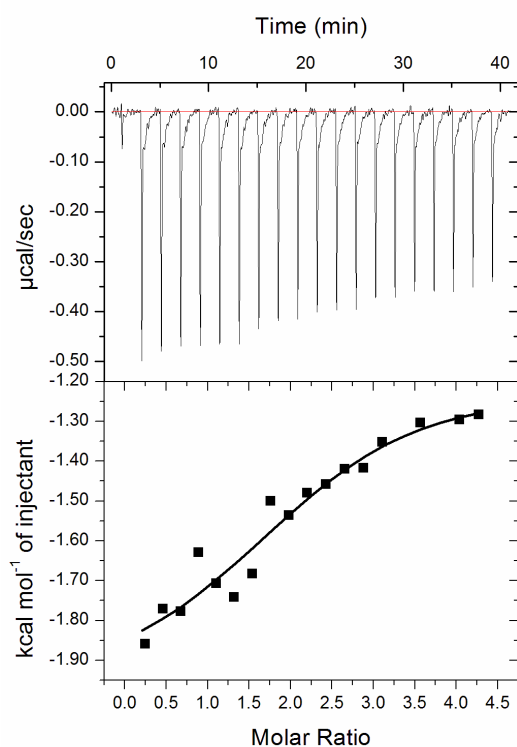


Figure 19: Binding of SSB peptide 152– 169 to recombinant AlkB was carried out using ITC. The top panel represents the raw data from the titration as a series of peaks corresponding to the heat change ($\mu\text{cal/s}$) with each injection. The bottom panel is heat change on ligand addition (kcal/mole) against the peptide:AlkB molar ratio.

In summary, this chapter identified a new binding site and a new binding partner for *E.coli* SSB protein. It was shown that an 18 amino acids (152-169) region of SSB located within IDR is involved in the AlkB interaction. The role of the C-terminal acidic domain of SSB as a platform for the recruitment of DNA repair and recombination proteins is well established. Considering the site of AlkB-SSB interaction being at IDR of SSB, It has been speculating that the C-terminal acidic domain of SSB would remain free for other protein-protein interaction.

Identification of IDR of SSB as protein interaction site opens up the possibility that many other proteins might also interact with SSB via this site.

3.4. References

1. Raghunathan, S., et al., *Structure of the DNA binding domain of E. coli SSB bound to ssDNA*. Nature Structural and Molecular Biology, 2000. **7**(8): p. 648-652.
2. Savvides, S.N., et al., *The C-terminal domain of full-length E. coli SSB is disordered even when bound to DNA*. Protein Science, 2004. **13**(7): p. 1942-1947.
3. Costes, A., et al., *The C-terminal domain of the bacterial SSB protein acts as a DNA maintenance hub at active chromosome replication forks*. PLoS genetics, 2010. **6**(12): p. e1001238.
4. Kozlov, A.G., et al., *Intrinsically disordered C-terminal tails of E. coli single-stranded DNA binding protein regulate cooperative binding to single-stranded DNA*. Journal of molecular biology, 2015. **427**(4): p. 763-774.
5. Handa, P., N. Acharya, and U. Varshney, *Chimeras between single stranded DNA binding proteins from Escherichia coli and Mycobacterium tuberculosis reveal that their C-terminal domains interact with uracil DNA glycosylases*. Journal of Biological Chemistry, 2001, p. 16992-16997.
6. Furukohri, A., et al., *Interaction between Escherichia coli DNA polymerase IV and single-stranded DNA-binding protein is required for DNA synthesis on SSB-coated DNA*. Nucleic acids research, 2012. **40**(13): p. 6039-6048.
7. Arad, G., et al., *Single-stranded DNA-binding protein recruits DNA polymerase V to primer termini on RecA-coated DNA*. Journal of Biological Chemistry, 2008. **283**(13): p. 8274-8282.

8. Han, E.S., et al., *RecJ exonuclease: substrates, products and interaction with SSB*. Nucleic acids research, 2006. **34**(4): p. 1084-1091.
9. Umezu, K. and R.D. Kolodner, *Protein interactions in genetic recombination in Escherichia coli. Interactions involving RecO and RecR overcome the inhibition of RecA by single-stranded DNA-binding protein*. Journal of Biological Chemistry, 1994. **269**(47): p. 30005-30013.
10. Chen, S.H., R.T. Byrne-Nash, and M.M. Cox, *Escherichia coli RadD Protein Functionally Interacts with the Single-stranded DNA-binding Protein*. Journal of Biological Chemistry, 2016: p. 20779-20786.
11. Genschel, J., U. Curth, and C. Urbanke, *Interaction of E. coli single-stranded DNA binding protein (SSB) with exonuclease I. The carboxy-terminus of SSB is the recognition site for the nuclease*. Biological chemistry, 2000. **381**(3): p. 183-192.
12. Lu, D., et al., *Mechanism of Exonuclease I stimulation by the single-stranded DNA-binding protein*. Nucleic acids research, 2011. **39**(15): p. 6536-6545.
13. Shereda, R.D., D.A. Bernstein, and J.L. Keck, *A central role for SSB in E. coli RecQ DNA helicase function*. Journal of Biological Chemistry, 2007, 19247-19258.
14. James, P., J. Halladay, and E.A. Craig, *Genomic libraries and a host strain designed for highly efficient two-hybrid selection in yeast*. Genetics, 1996. **144**(4): p. 1425-1436.
15. Shereda, R.D., et al., *SSB as an organizer/mobilizer of genome maintenance complexes*. Critical reviews in biochemistry and molecular biology, 2008. **43**(5): p. 289-318.

16. Marceau, A.H., et al., *Structure of the SSB–DNA polymerase III interface and its role in DNA replication*. The EMBO journal, 2011. **30**(20): p. 4236-4247.
17. Kozlov, A.G. and T.M. Lohman, *Calorimetric studies of E. coli SSB protein-single-stranded DNA interactions. Effects of monovalent salts on binding enthalpy*. Journal of molecular biology, 1998. **278**(5): p. 999-1014.
18. Bleijlevens, B., et al., *Dynamic states of the DNA repair enzyme AlkB regulate product release*. EMBO reports, 2008. **9**(9): p. 872-877.
19. Kelly, S.M., T.J. Jess, and N.C. Price, *How to study proteins by circular dichroism*. Biochimica et Biophysica Acta (BBA)-Proteins and Proteomics, 2005. **1751**(2): p. 119-139.
20. Kelly, S.M. and N.C. Price, *The use of circular dichroism in the investigation of protein structure and function*. Current protein and peptide science, 2000. **1**(4): p. 349-384.

Chapter 4: Screening and evaluation of indenone derivatives as AlkB inhibitors

4.1 Introduction

Alkylating agents induce DNA alkylation damages that can affect genomic stability, cellular viability and lead to diseases such as cancer and aging. DNA alkylation can lead to the modification of Nitrogen and Oxygen atom of the DNA base and result in the formation of N-alkylation or O-alkylation lesions, respectively. N-alkylated DNA adducts are repaired by Fe(II)/2OG-dependent dioxygenases. These enzymes activate oxygen for incorporation into an alkyl group and also involve an iron (Fe^{2+}) as co-factor and the co-substrate 2-oxoglutarate (2OG) ultimately releasing the alkyl group as formaldehyde and restoring the damaged DNA [1]. *Escherichia coli* AlkB is one of the most well characterized member of the family of Fe(II)/2OG-dependent dioxygenases [2]. AlkB homologs have been found to be present in almost all organisms including human [3]. *E. coli* AlkB acts preferably on ssDNA and RNA and its primary substrates are N1meA and N3meC [4, 5]. Extensive efforts have been made for selectively inhibiting DNA repair activity of AlkB family of dioxygenase [6-8]. Since there are several crystal structures of full-length AlkB available with various substrates and the enzyme structure and catalytic mechanism has been thoroughly studied, selective inhibitor of AlkB can be useful in further understanding the reaction mechanism. The objective of the chapter was to screen a library of indenone analogs for finding an inhibitor of AlkB. Since indenone skeleton is found in a wide range of bioactive compounds and natural products as discussed in section 1.8. indenone analogs were screened for inhibiting AlkB

demethylation activity. The library of indenone analogs was synthesized by Prof. FA Khan's lab, Dept. of Chemistry, IIT Hyderabad.

4.2. Materials and method

4.2.1 Cloning

AlkB was cloned into pTYB3 plasmid as described in section 2.2.1.

4.2.2. Purification of recombinant AlkB

Tagless AlkB protein was expressed in BL-21(DE3)plysS cells by transformation of the pTYB3-AlkB plasmid. The purification protocol followed was same as discussed in section 2.2.2. The purified protein was then dialyzed in a buffer containing 20mM Tris pH8.0 and 300mM NaCl.

4.2.3. Preparation of methylated DNA substrate

Desalted oligonucleotide 40mer polydT with single C was purchased from Imperial Lifescience. Methylation adducts were generated by treating the oligonucleotide with MMS (Sigma, 129925). 40 μ g ssDNA oligonucleotides was incubated with 5% (v/v) (0.59 M) MMS, 200 mM K₂HPO₄ in 500 μ l of total reaction at room temperature overnight for 14-15 hours. MMS was then removed by dialysis against TE buffer (10 mM Tris-HCl, pH 8.0, 1 mM EDTA) using Spectra/Por dialysis membrane (MWCO: 1000) for around 10 hours, with three changes of dialysis buffer. The dialysis was done at 4°C in ice-cold buffer. Then the damaged substrate was precipitated by adding 0.3 M sodium acetate pH 5.2 and 1 volume of ice-cold Iso-propanol. The precipitated ssDNA was washed with ice cold 80% ethanol and finally dissolved in molecular grade water. [9]

4.2.4. Screening of Indenone analogs for AlkB inhibition

In vitro screening of compounds for AlkB inhibition was carried out with purified tag-less AlkB protein. 0.2 μ M of AlkB was incubated with 50 μ M of different compounds dissolved in DMSO at 37°C for 1h in reaction buffer (20mM Tris-HCl pH 8.0, 0.2mM 2OG, 20 μ M Fe(NH₄)₂(SO₄)₂, 2mM L-Ascorbate). 1 μ M of the substrate (single-stranded 40 mer oligonucleotide DNA containing single N3-meC) was then added to the AlkB reaction mix and incubated for 1 hour. The released formaldehyde was directly quantified by direct repair assay where the reaction of released formaldehyde with acetoacetanillide in presence of ammonia leads to the formation of an enamine-type fluorescent intermediate (Amax 365nm, Emax 465nm) [9]. 50 μ l demethylation repair reaction product was mixed with 40 μ l of 5M ammonium acetate and 10 μ l of 0.5M acetoacetanillide (final volume 100 μ l). After 15min, fluorescence spectra were measured in the wavelength range of 421 to 521 nm, with excitation wavelength 365nm. The RFU values at excitation maxima (465nm) were used to quantify released formaldehyde using standard curve. The assay was performed using a 96-well microplate and Synergy (Biotek Instrument) multimode reader.

4.2.5. Determination of IC50

Different concentrations of indenone compounds ranging from 0.5 μ M to 1000 μ M were dissolved in DMSO and added to AlkB demethylation reaction mix. 1.5 μ l of 6.5 μ M AlkB was incubated in 5 μ l reaction buffer (20mM Tris-HCl pH 8.0, 0.2mM 2OG, 20 μ M Fe(NH₄)₂(SO₄)₂, 2mM L-Ascorbate) and incubated at 37°C for 60 min. The reaction was initiated by adding 5 μ l of the 10 μ M substrate followed by further incubation of 1hr at 37°C. The total reaction volume was 50 μ L. The formaldehyde

generation was determined as described before by using fluorescence-based method for direct detection of formaldehyde. The initial velocity V_0 was measured for each reaction and plotted against compound concentrations in order to determine the IC50 values using GraphPadPrism software.

4.2.6. CD-spectroscopy

Protein AlkB was dialyzed in a buffer containing 10mM Tris-HCl pH7.4 and 50mM NaCl for CD spectroscopy. The ligand (compound **3o**) was also diluted in the AlkB dialysis buffer to reduce the final DMSO concentration to 0.1% for the purpose of CD spectroscopy. 1:1 ratio of AlkB and the compound **3o** was used for the CD spectroscopy. 12 μ M of AlkB and 12 μ M of compound **3o** were mixed in assay buffer comprising 10mM Tris-HCl, pH 7.4 and 50mM NaCl and incubated for 1 hour at room temperature. CD spectra were recorded for both far UV CD in the wavelength range of 190nm to 160nm and near UV CD in the wavelength range of 240-360nm using a 1mm path length quartz cell. CD spectra were also recorded for the protein AlkB and compound **3o** individually. Since the compounds were dissolved in DMSO, it was added in all the three samples ie. AlkB or compound **3o** or AlkB + compound **3o** to the final concentration of 0.1%. CD spectroscopy was done using JASCO J-1500 instrument. The CD machine was infused with nitrogen gas for 10 minutes. A baseline was recorded for each of the samples which were the dilution buffer for that sample. The baseline was loaded before running the sample spectra. The spectra were recorded as an average of five spectral scans with bandwidth 1nm, step 1nm and 0.5sec/point. The data pitch was kept 0.5nm and scanning speed was 50nm/sec. The recorded data were analyzed using spectra manager software.

4.2.7. Isothermal titration calorimetry (ITC)

ITC experiments were done using ITC Microcal-200. 10 μ M of AlkB was added to the ITC cell in buffer containing 50mM Tris-HCl pH8.0, 100mM NaCl and 10mM β -mercaptoethanol. Compound **3o** or **3a** or **3j** at 100 μ M was added to the syringe. The ligand was injected into the cell with 20 consecutive injections of 2 μ l each with 2 min intervals between successive injections. The syringe was being rotated at 600 rpm. The heat pulse obtained for each titration was fitted using MicroCal Origin 7.0 software. The one-site binding model was used to calculate the corresponding dissociation constant.

4.2.8. Enzyme kinetics

Purified recombinant AlkB (0.2 μ M) was mixed with the eight different concentration of 40-mer internal N3me-oligo-dC (ranging from 0.12-3.8 μ M) in reaction buffer (20mM Tris-HCl pH 8.0, 0.2mM 2OG, 20 μ M Fe(NH₄)₂(SO₄)₂, 2mM L-Ascorbate). Reactions were also performed in presence of 50, 100, 250 and 500 μ M of compound **3o**. The enzyme was mixed with compounds for 1h and the reaction started by adding the substrate. The amount of formaldehyde released at different time point was quantified using direct repair assay. The initial velocities after addition of the compounds were calculated by the analysis of the slopes of time course reactions. The initial velocity data were then fit to the Michaelis-Menten equation to calculate V_{max} (maximal velocity), K_M (Michaelis constant) using GraphPad Prism 7.0 (GraphPad Software, Inc., San Diego, CA). Transformation of Michaelis-Menten to Lineweaver-Burk plot was also carried out by GraphPad Prism 7.0.

4.2.9. Molecular Docking

Protein structure 3i49 was used for AlkB docking. Autodock-4.0 was used for docking **3o** to and AlkB. 3D structure of the ligands was prepared using the MarvinSketch software. The geometry optimization and energy minimization of ligands were carried out using an MM94 force field. The protein structure was prepared by adding Hydrogen atoms followed by removal of all the water molecules, using Autodock-4.0. Kollman charges were added to protein prior to docking using Autodock tools. The compound **3o** was docked to AlkB blindly using standard rigid docking protocol. The grid box dimensions were 30 X 30 X 30 with grid box center at (14.268, 13.335, -7.861) and spacing of 0.3Å. Analysis of the docked structures and evaluation of binding energy was done using analysis tool of Autodock suite. Visualization of the docked structure of protein-ligand and comparison of the docked positions of different ligands was done using Discovery studio visualizer.

4.2.10. Cell survival Assay

A single colony of wild-type *E.coli* or AlkB mutant strain HK-82 was inoculated in 5ml autoclaved LB broth at 200rpm for 14-16hours to obtain the primary culture. 10 ml of fresh LB broth was then inoculated with 1% primary culture. The culture was allowed to grow at 37°C, 200rpm till it reached early log phase. The optical density of the culture was measured at 600nm using a spectrophotometer. Fresh LB medium was used as a blank. The culture was grown till the OD reached ~ 0.2. The culture was then transferred to 96-well plates, with 200uL of culture in each well. MMS was added to each well to the final concentration of 0.01%. Compound **3o** was also added to the culture in 96 well plates to the final concentration of 50uM.

The 96-well plate was incubated at 37°C, 200rpm for 5hours. Optical density at 600nm was recorded every hour using the multimode reader. The experiment was repeated 5 times independently and the mean value was considered.

4.2.11. Effect of compound 3o on MMS sensitivity

A single colony of wild-type *E.coli* was inoculated in 5ml autoclaved LB broth at 200rpm for 14-16hours to obtain the primary culture. 10 ml of fresh LB broth was then inoculated with 1% primary culture. The culture was allowed to grow at 37°C, 200rpm till it reached early log phase. The optical density of the culture was measured at 600nm using a spectrophotometer. Fresh LB medium was used as a blank. The culture was grown till the OD reached ~ 0.2. The culture was then transferred to 96-well plates, with 200µL of culture in each well. MMS was added to each well to the final concentration of 0.01%. Different compounds (**3a-3q**) were added to the culture in 96 well plates to the final concentration of 50 µM. The 96-well plate was incubated at 37°C, 200 rpm for 5 h. Optical density at 600nm was recorded every one hour using the multimode reader. The experiment was repeated 5 times independently and the mean value was considered. Relative survival percentage was calculated by using OD of the No treatment well as 100 % survival. The experiment was repeated 5 times independently and the mean value was considered.

4.3. Result and discussion

4.3.1. Evaluation indenone compounds as an inhibitor of DNA demethylation repair protein AlkB

The library of seventeen 2-Chloro-3-Amino indenone compounds (Fig.20) was screened for their inhibitory effect on the activity of *E.coli* AlkB. Recombinant

AlkB was used for this study using direct repair assay where formaldehyde released over time was monitored. The screening assay was set up with 1 μ M of MMS-damaged 40-mer oligonucleotide (T20 3meC T19) consisting of single N3meC as a substrate for 0.2 μ M AlkB and 50 μ M of each of the indenone compounds were added in the DNA repair reaction with final volume 50 μ L. Fig. 21 represents the results of the screening. It was found that most of the compounds showed no inhibitory effects, however, a few compounds affected AlkB activity significantly. A compound was considered to have an inhibitory effect on the AlkB activity when the formaldehyde release was measured less than 20% of the control AlkB activity wherein only DMSO was added to the AlkB repair reaction Compound **3o** was found to be a primary hit for AlkB inhibition from the initial screening of 17

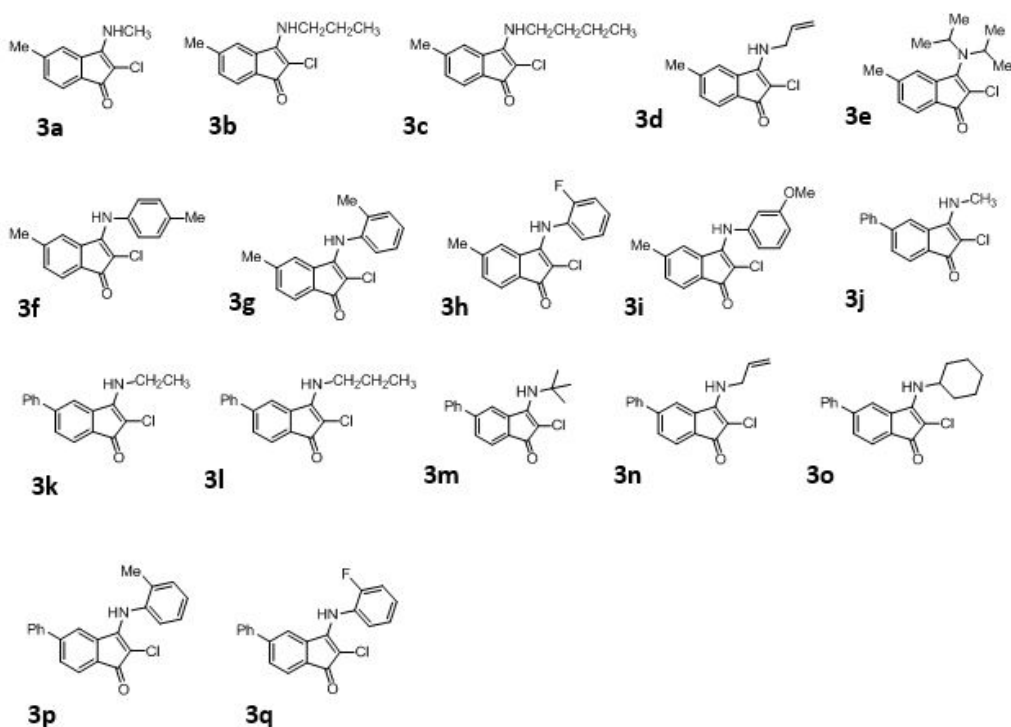


Figure 20: Library of 17 Indenone analogs screened for inhibition of AlkB demethylation activity.

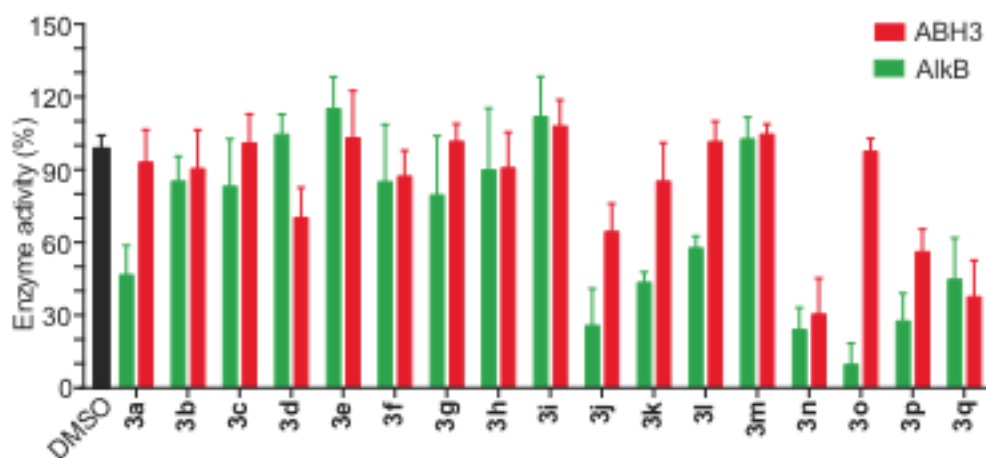
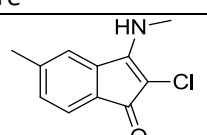
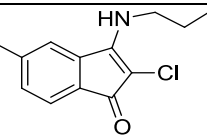
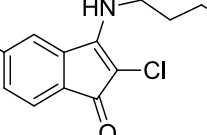
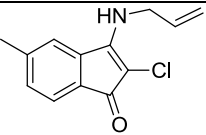
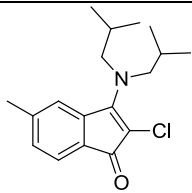
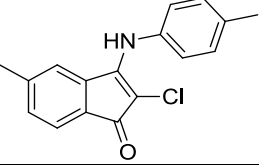
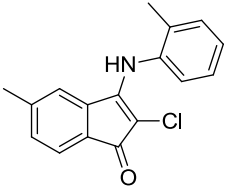
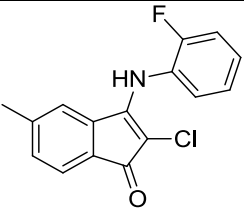
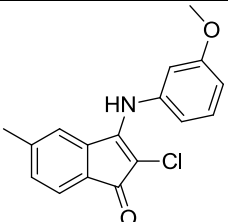
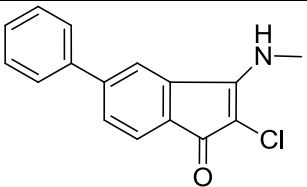
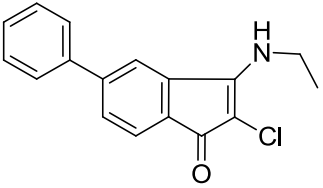
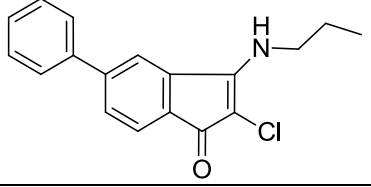
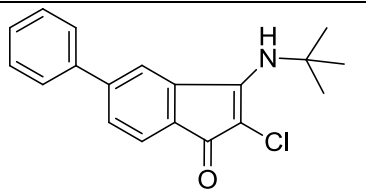
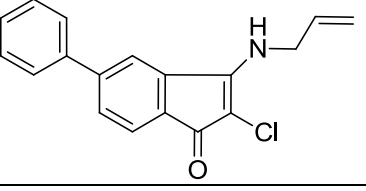
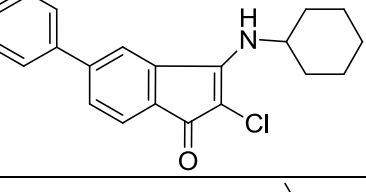
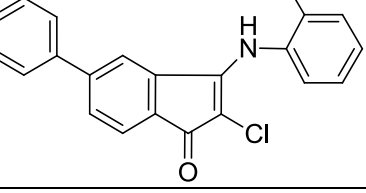
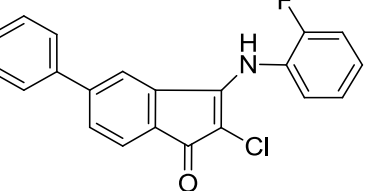


Figure 21: Screening for inhibition of AlkB activity with 17 indenone compounds, arranged in the descending order of activity. Effect of these compounds on AlkBH3 activity is also shown for comparison. Error bars depict the standard error.

Table 6: Library of indenone compounds screened for AlkB inhibition

Structure	Molecular weight	Compound No.
	207.65	3a
	235.70	3b
	249.73	3c
	233.69	3d

	305.84	3e
	283.75	3f
	283.75	3g
	287.71	3h
	299.75	3i
	269.72	3j
	283.75	3k
	297.77	3l

	311.80	3m
	295.76	3n
	334.84	3o
	345.82	3p
	349.78	3q

compounds. Compound **3o** was also evaluated for inhibition of AlkBH3 activity to determine its specificity. As shown in Fig. 21 AlkB inhibition was found to be specific as the activity of Human AlkBH3 was not altered by compound **3o**.

4.3.2. Conformational and binding analysis of AlkB and **3o**.

The ability of the compound **3o** to form a complex with AlkB was evaluated by Isothermal titration calorimetry (ITC). To rule out the possibility that the observed energy changes could be non-specific and are not due to AlkB and compound **3o** interaction, control ITC experiments were performed with compounds **3a** and **3j**

which are structurally similar to **3o**. The raw ITC data and the one-site model fit are shown in Fig.22(A). It was found that the inhibitory activity of compound **3o** is due to direct interaction with AlkB. Parameters derived from ITC showed that **3o** is a tight binding ligand for AlkB with a dissociation constant of 3.3 μ M. Analysis of thermodynamic parameters revealed that binding of **3o** resulted in favorable enthalpy change ($\Delta H < 0$) and unfavorable entropy change ($\Delta S < 0$). These results indicated favorable electrostatic, H-bonding and van der Waals interactions between the AlkB protein and the compound **3o**. The data for compounds **3a** and **3j** showed that these molecules did not bind to AlkB Fig.22(B and C).

The CD spectra of AlkB in presence of compound **3o** was also analyzed to determine if there are any changes in the local tertiary structure upon **3o** binding. The results of the CD spectroscopy are shown in Fig. 23. Comparison of the far-UV CD spectra of AlkB and AlkB-**3o** showed that the spectrum of AlkB-**3o** differed from that of AlkB with respect to CD signal at 208 nm and 222 nm which indicate a slight alteration in the alpha helix content of AlkB when **3o** was bound to AlkB. A reduction in positive signal at 195nm was also observed when **3o** was bound to AlkB which implied an alteration in the total beta helix content. These results indicated alterations in the characteristic jelly-roll fold formed by beta sheets. The near UV CD spectra of AlkB was also analyzed in the presence or absence of compound **3o**.

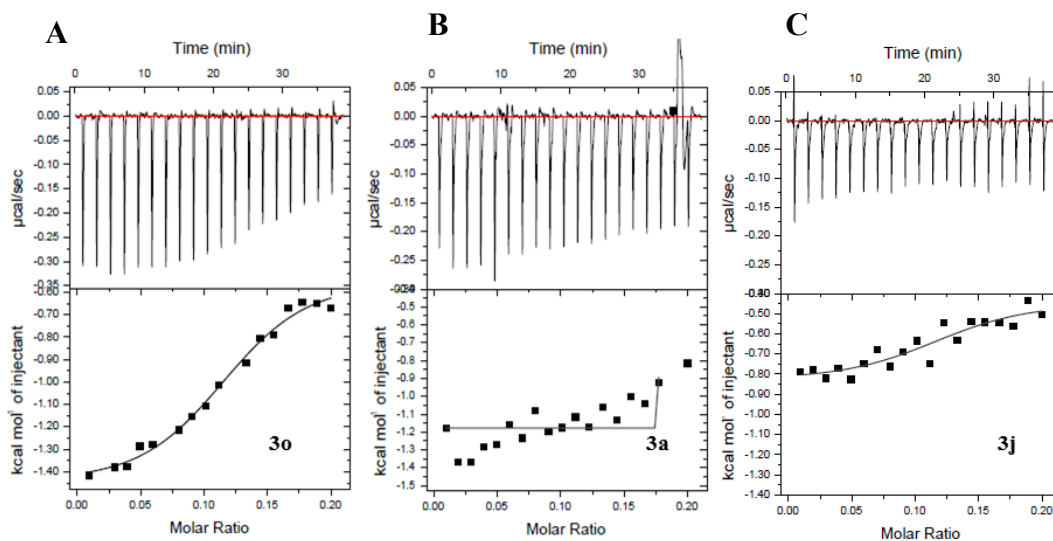


Figure 22: Binding analysis. (A) Isothermal titration calorimetry (ITC) to determine to bind of compound **3o**, (B) **3a** and (C) **3j** to recombinant AlkB. The top panel represents the raw data from the titration as a series of peaks corresponding to the heat change (μ calories/s) with each injection. The bottom panel is a plot of heat change on ligand addition (kcal/mole) against the compound/AlkB molar ratio. The data was fitted using one-site binding model in the microcal data analysis software package in Origin (origin labs).

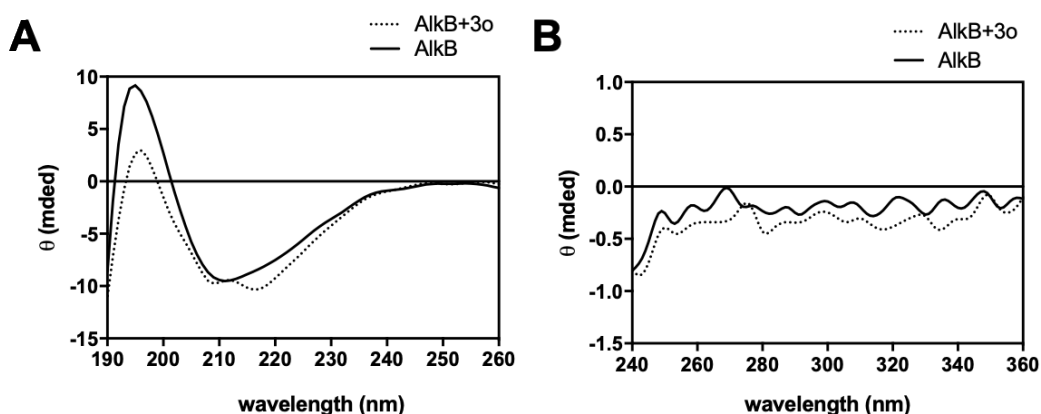


Figure 23: Conformational analysis of AlkBH3-3o interaction by circular dichroism (CD). (top) Far-UV CD spectra (between 190nm and 260nm) for AlkB (solid line)

or AlkB with compound **3o** bound (dotted line). (bottom) near-UV CD spectra (between 240nm and 360nm) for AlkB (solid line) or AlkB with compound **3e** bound (dotted line).

Analysis of near UV spectra revealed changes in the overall tertiary conformation of AlkB upon binding of compound **3o**. Since compound **3o** is an achiral molecule, no CD signal was observed from **3o** alone. Also, AlkB lacked disulfide bonds so, the near UV CD signal was obtained by aromatic amino acids tryptophan (290-300nm), tyrosine (270-280nm) and phenylalanine (250-270nm).

4.3.3. Mechanism of inhibition of AlkB

The IC₅₀ value was determined to assess the inhibitory potential of compound **3o**. Increasing concentration of the compound **3o** was added to the AlkB reaction mixture. The results are shown in Fig. 24. IC₅₀ value for compound **3o** was found to be 19.37μM.

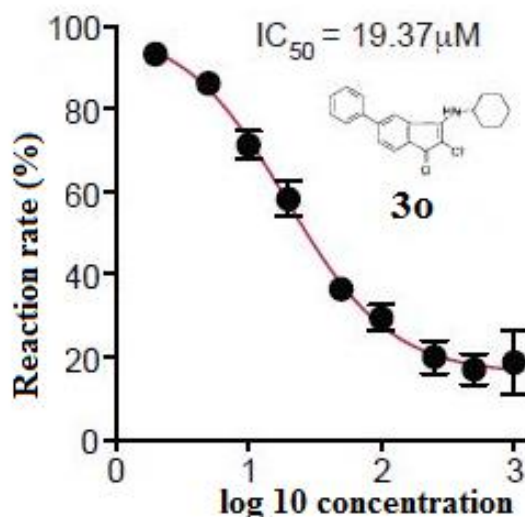


Figure 24: IC₅₀ data of compounds **3o** against AlkB.

The steady-state enzyme kinetics was performed next, to find out the mode of inhibition. The initial velocities of AlkB in presence of different concentrations of **3o** were determined and fitted to double reciprocal Lineweaver-Burk plot. It was found that the V_{max} remained unchanged in presence of **3o** which implied a competitive mode of inhibition (Fig. 25A). The initial velocities of AlkB were also analyzed by varying concentration of the co-substrate 2OG while keeping a fixed saturating concentration of DNA substrate. It was observed that there was a gradual decrease in V_{max} upon increasing the concentration of **3o**. Also, the intersection point of the lines corresponding to different concentrations of **3o** was above the y-axis in the Lineweaver-Burk plot (Fig. 25B). These results indicated that there is mixed inhibition with respect to co-substrate in presence of **3o**. The kinetics data strongly suggested that **3o** inhibited the AlkB repair activity by competing with the DNA substrate binding and indirectly affected 2OG catalysis.

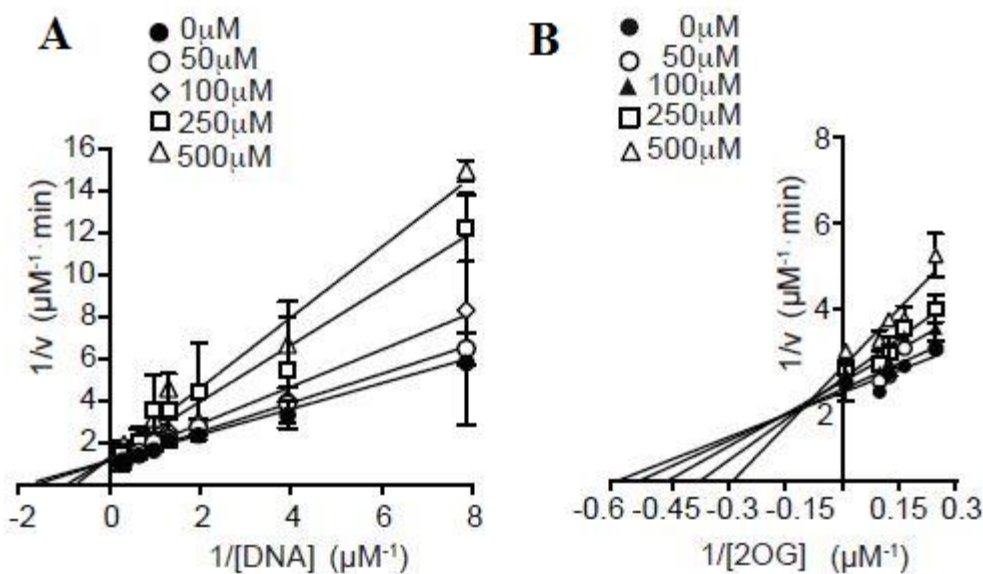


Figure 25: The effect of increasing concentrations of compound **30** over the rate of reaction of AlkB shown in Lineweaver-Burk plot of steady-state kinetics. Reactions were analyzed by quantification of formaldehyde released. (B) Lineweaver-Burk plot showing the effect of increasing concentrations of compound **30** over the rate of AlkB-catalyzed reaction with respect to 2OG. Error bars represent standard error from three independent experiments.

4.3.4. Prediction of binding pocket

The binding conformation of **30** and AlkB was further analyzed using molecular docking to predict the binding pocket. The active site Fe in AlkB is coordinated by the HDH triad formed by H131, D133, and H187. Single-stranded DNA is bound to active site via Nucleotide recognition lid formed by first 90 amino acids of the N terminal region. AlkB can bind to and repair many different kinds of damaged substrates viz. 1meA, 3meC, 1meG, etc but the binding mechanism remains the same for all. The damaged base is sandwiched between H131 and W69 by

hydrophobic interactions. Also, D135 forms a Hydrogen bond with the N6 position of 1-meA.

The target methylene group is bound by R210 via Vander wall interaction. The methylated nucleotide is recognized by the interaction of R161 with the phosphate of damaged nucleotide by the formation of a salt bridge. The nucleotide backbone of the substrate DNA is stabilized in Nucleotide recognition lid (NRL) via hydrogen bonding between phosphate groups and T51, Y76 and R161. Y76 plays an important role in DNA binding by hydrogen bonding network, providing hydrophobic interaction for base stacking and hydroxyl side chains interact with the phosphodiester backbone thus stabilizing the DNA. K127 and S129 also help in stabilizing phosphodiester backbone of DNA. Y55 interacts with the ribose sugar via hydrophobic interactions. 2OG is coordinated by binding motif R204xNxTxR210 which is conserved. C5 carboxylate of 2OG interacts with Arg204 by salt bridge formation and forms a hydrogen bond with N206 and Y122. The oxygen from C1 carboxylate group of 2OG forms hydrogen bond with N120 and R210 [10] . The docking data showed that compound **3o** interacted with AlkB by binding to the active site and blocking DNA binding. Compound **3o** formed direct pi-cation/anion interactions with the H131, D133 which are part of active site triad. Compound **3o** also formed a hydrogen bond with R210 which binds to the methylated nucleotide. These interactions were possibly inhibiting the binding of the damaged base as the key residues involved in substrate recognition and binding are obstructed. Compound **3o** also formed pi-pi stacking and pi- sigma stacking with Trp69 which is essential for catalysis. **3o** also blocked the nucleotide recognition lid (NRL) by forming pi-alkyl stacking with Met57 and Tyr76 which essentially provide

flexibility and interaction platform for accommodating DNA backbone [11, 12] (Fig. 26).

4.3.5. Inhibition of AlkB by 3o significantly enhances MMS-induced cell death

E. coli Alkb mutant strain (HK82), lacking functional AlkB is sensitive to MMS and fails to grow in media containing 0.01% MMS [13]. Based on these findings, it was hypothesized that the presence of a chemical inhibitor of AlkB will also cause normal cells to become sensitive to MMS and the cell survival would be inversely proportional to the degree of inhibition. It was examined whether the compound **3o** can inhibit *E. coli* AlkB function in vivo. To determine that wild-type *E. coli* cells were inoculated in media containing 0.01% MMS. *E. coli* strain with mutant alkb (HK82) was used as a control. It was found that the growth of wild-type *E. coli* was not affected by the presence of 0.01% MMS in the culture media due to active DNA repair by AlkB. However, alkb mutant strain (HK82) failed to grow under the identical condition suggesting the importance of repair for cell viability (Fig. 27A). Cells were grown in the media containing MMS in presence of each compound (**3a-3q**) independently and the rate of cell growth was analyzed. As shown in Figure 27A, no other compound except **3o** resulted any pronounced growth inhibition. We found that growth rate of wild-type *E. coli* in presence of **3o** was slow and comparable to *alkb* mutant strain HK82 (Figure 27A).

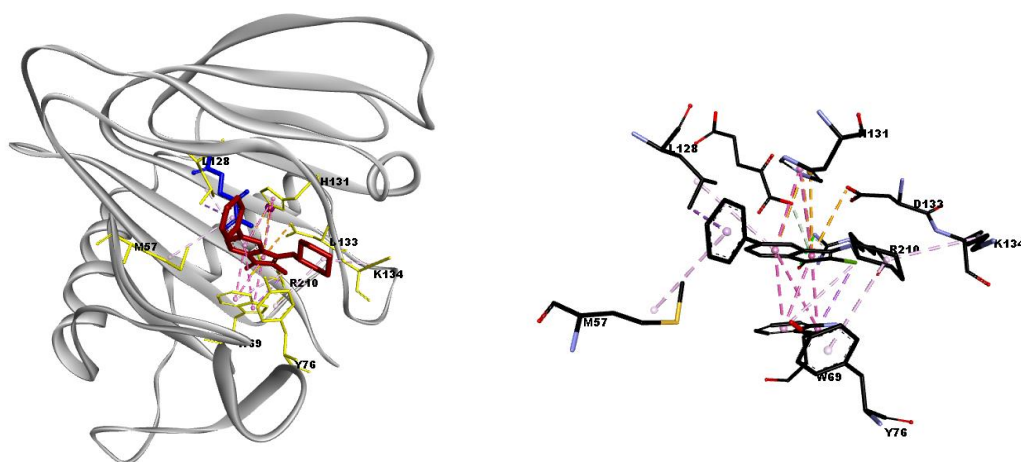


Figure 26: (A) Molecular docking analysis showing potential binding pocket of compound **3o**. (B) AlkB residues forming the binding pocket of compound **3o**.

Notably, compound **3n**, **3p** and **3j**, which showed some inhibition in the *in vitro* assay, failed to exhibit any growth inhibition, suggesting that these set of 2-Chloro-3-Amino indanone derivatives has no pleiotropic effect on the growth of *E. coli*. These results suggest that compound **3o** is cell permeable and could inhibit catalytic activity of AlkB.

In the subsequent experiment as shown in Fig. 27B, the *E. coli* cells were treated with increasing concentration of compound **3o**. It was observed that *E. coli* cells were becoming more sensitive to MMS upon increasing **3o** concentration. These results suggested that compound **3o** is cell permeable and could inhibit the bacterial AlkB *in vivo*. AlkB is well reported to repair N-alkylation damage caused the S_N2 type of methylating agents. MMS belongs to an S_N2 -type methylating agent that induces the formation of N1meA and N3meC lesions on DNA and repaired

specifically by AlkB. In summary Seventeen 2-Chloro-3-Amino indenone compounds were synthesized and evaluated as potential inhibitors of AlkB-catalyzed DNA demethylation. This study revealed the ability of one of the compounds **3o** to be competitive inhibitors of AlkB-catalyzed demethylation of DNA. This compound exhibited selective binding properties and was able to modulate the function of AlkB when present in the micromolar range of concentrations.

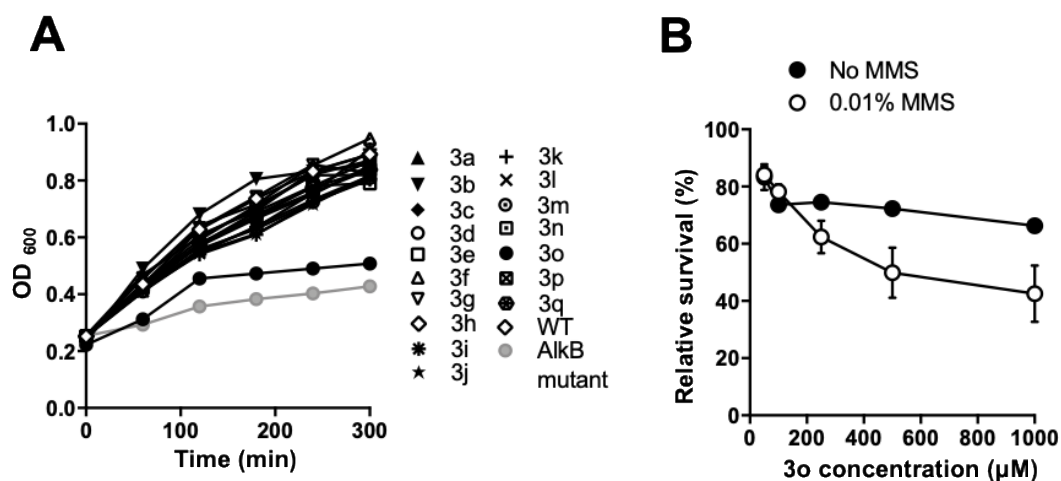


Figure 27: The inhibitory effect of **3o** on the *in vivo* repair activity. (A) Inhibition of repair was monitored by decreased cell survival upon exposure to compound **3a-3q** and DNA alkylating chemical MMS. Bacterial growth of wild-type *E. coli*, in presence of **3o** and the *alkb* mutant strain (HK82), was monitored as control. Compounds **3a-3q** (50μM) were dissolved in DMSO and added to the *E.coli* cells growing in LB media containing 0.01% MMS. Bacterial growth was monitored by OD₆₀₀ for 5h. The growth of cells in the absence of inhibitor was considered as 100%. The mean value of five independent experiments is plotted. (B) Effect of increasing concentration of compound **3o** on bacterial growth.

4.4. References

1. Mishina, Y. and C. He, *Oxidative dealkylation DNA repair mediated by the mononuclear non-heme iron AlkB proteins*. Journal of inorganic biochemistry, 2006. **100**(4): p. 670-678.
2. Fedeles, B.I., et al., *The AlkB family of Fe (II)/ α -ketoglutarate dependent dioxygenases: repairing nucleic acid alkylation damage and beyond*. Journal of Biological Chemistry, 2015, 290(34), p 20734-20742.
3. Kurowski, M.A., et al., *Phylogenomic identification of five new human homologs of the DNA repair enzyme AlkB*. BMC genomics, 2003. **4**(1):48.
4. Falnes, P.Ø., R.F. Johansen, and E. Seeberg, *AlkB-mediated oxidative demethylation reverses DNA damage in Escherichia coli*. Nature, 2002. **419**(6903): p. 178-182.
5. Trewick, S.C., et al., *Oxidative demethylation by Escherichia coli AlkB directly reverts DNA base damage*. Nature, 2002. **419**(6903): p. 174-178.
6. Nakao, S., et al., *Design and synthesis of prostate cancer antigen-1 (PCA-1/ALKBH3) inhibitors as anti-prostate cancer drugs*. Bioorganic & medicinal chemistry letters, 2014. **24**(4): p. 1071-1074.
7. Li, Q., et al., *Rhein inhibits AlkB repair enzymes and sensitizes cells to methylated DNA damage*. Journal of Biological Chemistry, 2016. 291(21), p. 11083-11093.
8. Mabuchi, M., et al., *Improving the bioavailability and anticancer effect of the PCA-1/ALKBH3 inhibitor HUHS015 using sodium salt*. In Vivo, 2015. **29**(1): p. 39-43.

9. Shivange, G., et al., *A role for Saccharomyces cerevisiae Tpa1 protein in direct alkylolation repair*. Journal of Biological Chemistry, 2014 289(52): p. 35939-35952.
10. Holland, P.J. and T.J.P.O. Hollis, *Structural and mutational analysis of Escherichia coli AlkB provides insight into substrate specificity and DNA damage searching*. 2010. **5**(1): p. e8680.
11. Yu, B., et al., *Crystal structures of catalytic complexes of the oxidative DNA/RNA repair enzyme AlkB*. Nature, 2006. **439**(7078): p. 879-884.
12. Yu, B. and J.F.J.P.o.t.N.A.o.S. Hunt, *Enzymological and structural studies of the mechanism of promiscuous substrate recognition by the oxidative DNA repair enzyme AlkB*. 2009. **106**(34): p. 14315-14320.
13. Lee, D.-H., et al., *Repair of methylation damage in DNA and RNA by mammalian AlkB homologues*. Journal of Biological Chemistry, 2005. **280**(47): p. 39448-39459.

Chapter 5: Screening and evaluation of indenone derivatives as potential inhibitors of human AlkBH3

5.1. Introduction

DNA methylation is an evolutionarily conserved mechanism of regulation present in the eukaryotic genome. DNA methylation at N-5 position of cytosine (N5meC) acts as epigenetic marker [1]. DNMT which is the enzyme responsible for N5meC methylation has also been known to methylate cytosine non-specifically at N3 position generating N3meC lesions which are mutagenic [2]. DNMT's have been found to be one of the major sources of endogenous N3meC generation in cells. In recent years, it has been found that DNMT's are overexpressed in several cancers such as breast cancer, prostate cancer, colon cancer [3]. Overexpression of DNMT's has been associated with promoting tumorigenesis in cancer cells [4]. These aberrant methyl adducts generated by DNMTs need to be repaired by AlkB homologs.

Human genome encodes nine homologues of AlkB (AlkBH1-8 and FTO) [5]. Human AlkB homolog-2 (AlkBH2) and AlkB homolog-3 (AlkBH3) have been known to repair N1meA and N3meC methylation damages in double- and single-stranded DNA and RNA [16]. Recent studies have suggested a direct role of AlkBH3 in cancer cell proliferation [6-18]. It has been reported that the proliferation of lung and prostate cancer cells is dependent on AlkBH3 expression [14, 15]. It has been shown that siRNA mediated knockdown of AlkBH3 in the human lung adenocarcinoma cell line A549 resulted in cell cycle arrest, senescence and strong suppression of cell growth [15]; prostate cancer cell line LNCap and PC3 overexpressed AlkBH3 and siRNA mediated knockdown of AlkBH3 resulted in reduced proliferation [19, 20]. AlkBH3 knockdown in another prostate cancer cell

line DU145 resulted in apoptosis [21]. Moreover, the high level of AlkBH3 expression is also found in non-small-cell lung cancer[15], pancreatic cancer,[22] and renal cell carcinoma [23]. Knockdown of AlkBH3 in these cells resulted in reduced proliferation [20]. Since overexpression of AlkBH3 is strongly linked to cancer, selective inhibitors for AlkBH3 are highly desirable.

The objective of this chapter was to test indenone derivatives for potential inhibition of AlkBH3.

5.2. Materials and method

5.2.1. Cloning

AlkBH3 was cloned into pTYB3 vector using NcoI and SalI sites. AlkBH2 was cloned into pET-28-a vector using EcoRI and SalI Sites.

Table 7: Cloning strategy for genes cloned in section 5.2.1.

Clone	Clone No.	Oligo Sequence (5' – 3')	Restriction sites
pTYB3-ABH3	254	Abh3-Tagless_R_SalI ATA AGT CGA CCC AGG GTG CCC CTC GAG GGT CTG G ABH3-BamH1-Nco1-sen CCT GGG ATC CAT GGA GGA AAA AAG ACG GCG AGC C	NcoI SalI
pET-AlkBH2	258	ABH2-EcoRI-sen TCG AGA ATT CAT GGA CAG ATT CCT GGT GAA AGG GG ABH2-SalI-Anti CAG CGC TAG CGT CGA CTT ATT TTT TAG TAA GCA AAA TTT TAC G	EcoRI SalI

5.2.2. Purification of proteins

Tagless AlkB, AlkBH3, and His-AlkBH2 proteins were expressed in BL-21(DE3)plysS cells by transformation of pTYB3-AlkB, pTYB3-AlkBH3, and

pET28a-AlkBH2 plasmids respectively. The purification protocol followed was same as discussed in section 2.2.1. The purified proteins were then dialyzed in a buffer containing 20mM Tris pH8.0 and 300mM NaCl.

5.2.3. Preparation of methylated DNA substrate

Desalted oligonucleotide 40mer polydT with single C (5' TTT TTT TTT TTT TTT TTT C TTT TTT TTT TTT TTT TTT TTT 3') was purchased from Imperial Lifescience. Methylation adducts were generated by treating the oligonucleotide with MMS (Sigma, 129925). The methylation protocol was same as discusses in section 4.2.2.

5.2.4. Preparation of double-stranded DNA substrate

Double-stranded DNA substrate was prepared by annealing MMS damaged 40mer polydTC DNA with 40mer polyA DNA. 250ng/ μ L of each of polyA and polyTC DNA were added to the annealing buffer containing 20mM Tris-HCl pH8.0 and 1mM EDTA. The annealing reaction was incubated at 37°C for 30 minutes followed by incubation on ice for 5minutes. The annealed DNA was then aliquoted and stored at -86°C.

5.2.5. *In vitro* screening

A library of indenone derivatives consisting of 27 compounds was screened for inhibition of AlkBH3 demethylation activity. 10mM stock of compounds was prepared by dissolving the desired amount in 100% DMSO. *In vitro* screening of compounds for their inhibition of demethylation activity was carried out with purified tag-less protein. 0.2 μ M of AlkBH3 was incubated with 50 μ M of different compounds dissolved in DMSO at 37°C for 1 h in demethylation reaction buffer (20mM Tris-HCl pH 8.0, 0.2mM 2OG, 20 μ M Fe(NH₄)₂(SO₄)₂, 2mM l-Ascorbate).

1 μ M of the substrate which was MMS damaged 40-mer oligonucleotide containing single N3meC was then added to initiate the AlkB catalyzed demethylation reaction. The released formaldehyde was quantified using direct repair assay as discussed earlier. To check the specificity of these compounds the assay was also performed with purified tagless AlkB and His-AlkBH2. Double-stranded DNA containing single N3meC (1 μ M) was used as a substrate for AlkBH2.

5.2.6. Determination of IC50

Different concentrations of indenone compounds **5a**, **5b**, and **5c** ranging from 0.5 μ M to 1000 μ M were dissolved in DMSO and added to AlkBH3 demethylation reaction mix. A 50 μ l reaction was set up with 1.5 μ l of 6.5 μ M AlkBH3 incubated in 5 μ l of 10X reaction buffer (20mM Tris-HCl pH 8.0, 0.2mM 2OG, 20 μ M Fe(NH₄)₂(SO₄)₂, 2mM L-Ascorbate) and incubated at 37°C for 60 min. The reaction was initiated by adding 5 μ l of the 10 μ M substrate followed by further incubation of 1hr at 37°C. The total reaction volume was 50 μ L. The formaldehyde generation was determined by using fluorescence-based method for direct detection of formaldehyde [156]. The initial velocity V_o was measured for each reaction and plotted against compound concentrations in order to determine the IC₅₀ values using GraphPadPrism software.

5.2.7. CD-spectroscopy

The protein AlkBH3 was prepared for CD experiment by dialyzing in low salt buffer containing 10mM Tris-HCl pH 7.4 and 50mM NaCl. The ligand compound **5c** was diluted in DMSO to the final DMSO concentration of 0.1%. 1:1 ratio of AlkBH3 and the compound **5c** was used for the CD spectroscopy. 12 μ M of AlkBH3 and 12 μ M of compound **5c** were mixed in assay buffer comprising 10mM Tris-HCl, pH

7.4 and 50mM NaCl at room temperature. CD spectra were recorded for both far UV CD in the wavelength range of 190nm to 160nm and near UV CD in the wavelength range of 240-360nm using a 1mm path length quartz cell. AlkBH3 (12 μ M) and the compound **5c** (12 μ M) was mixed 1:1 molar ratio for 1h. CD spectra were also recorded for the protein AlkBH3 and compound **5c** individually. Since the compounds were dissolved in DMSO, it was added in all the three samples i.e. AlkBH3/compound**5c**/AlkBH3+compound **5c** to the final concentration of 0.1%. CD spectroscopy was done using JASCO J-1500 instrument. The CD parameters were kept same as described in section 4.2.5.

5.2.8. Isothermal titration calorimetry (ITC)

ITC was done using Microcal 200 (GE Healthcare). The sample cell was filled with Purified AlkBH3 10 μ M and the compound **5c** was added to the syringe at the concentration of 100 μ M. The experiments were carried out with 20 consecutive injections (2 μ l) of compound **5c** (100 μ M) to mix with the AlkBH3 (10 μ M) with 2 min intervals between successive injections. The rotation speed of the syringe was maintained at 600 rpm. The integration of the heat pulses obtained from each titration was fitted using MicroCal Origin 7.0 software to determine the site-binding model and to obtain the corresponding dissociation constant.

5.2.9. Enzyme kinetics

Purified recombinant AlkBH3 (0.2 μ M) was mixed with the eight different concentration of 40-mer internal N3me-oligo-dC (ranging from 0.12-3.8 μ M) in reaction buffer (20mM Tris-HCl pH 8.0, 0.2mM 2OG, 20 μ M Fe(NH₄)₂(SO₄)₂, 2mM L-Ascorbate). Reactions were also performed in presence of 50, 100, 250 and 500 μ M of compound **5c**. The enzyme was mixed with compounds for 1h and the

reaction started by adding the substrate. The amount of formaldehyde released at different time point was quantified using direct repair assay where formaldehyde released was detected by converting it into a fluorescent product. The initial velocities after addition of the compounds were calculated by the analysis of the slopes of time course reactions. The initial velocity data were then fit to the Michaelis-Menten equation to calculate V_{max} (maximal velocity), K_M (Michaelis constant) using GraphPad Prism 7.0 (GraphPad Software, Inc., San Diego, CA). Transformation of Michaelis-Menten to Lineweaver-Burk plot was also carried out by GraphPad Prism 7.0.

5.2.10. Molecular docking

Autodock-4.0 was used for docking **5c**, **5b** and **5a** to and AlkBH3 using structure 2IUW from protein data bank. 3D structure of the ligands was prepared using the MarvinSketch software. The geometry optimization and energy minimization of ligands were carried out using an MM94 force field. The protein structure was prepared by adding Hydrogen atoms followed by removal of all the water molecules, using Autodock-4.0. Kollman charges were added to protein prior to docking using Autodock tools. The compounds **5a**, **5b**, and **5c** were docked to AlkBH3 blindly using the grid box of dimensions $126 \times 126 \times 126$ with grid box center at (14.268, 3.335, -7.861) and spacing of 0.5 \AA . Analysis of the docked structures and evaluation of binding energy was done using analysis tool of Autodock suite. Visualization of the docked structure of protein-ligand and comparison of the docked positions of different ligands was done using Discovery studio visualizer.

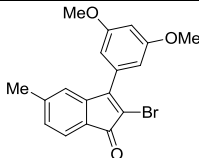
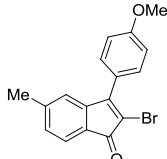
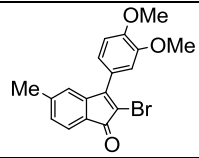
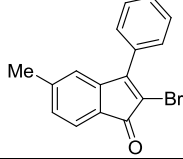
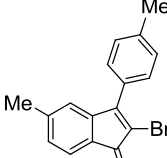
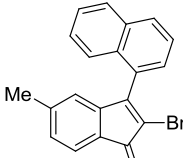
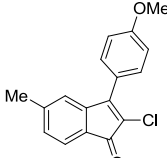
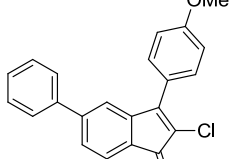
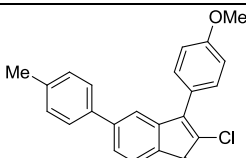
5.2.11. Cytotoxicity analysis

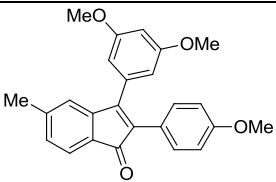
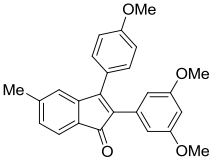
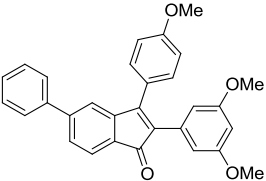
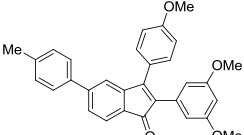
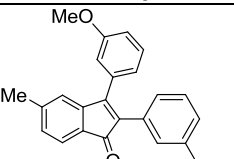
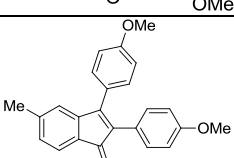
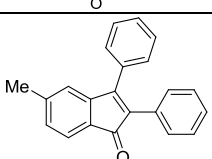
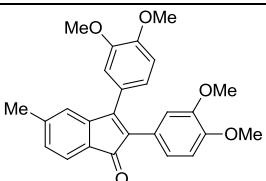
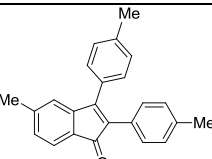
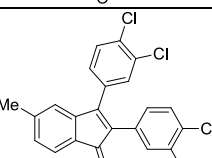
For analysis of toxicity of the indenone compounds, A549 cells were studied. A549 cell line is non-small cell lung cancer cell line derived from Human adenocarcinoma. Mice model studies have shown that siRNA mediated knockdown of AlkBH3 in A549 cell line leads to cell cycle arrest and suppression of cell growth [15]. Cells were seeded in 96 well plates (2000 cells/well) and cultured in DMEM media (Himedia cat. No. AL219A) supplemented with 10% v/v fetal bovine serum (Genetix brand cat.No. CCS-500-SA-U) and incubated overnight at 37°C, 5% CO₂. A range of concentration (0.01–200 µM) of compounds **5a/5b/5c** was added in four replicates to the cells in 96-well plate and incubated at 37°C, 5% CO₂ for 48–72 h. After the incubation period, cells viability was analyzed using the MTT assay. MTT assay was done using EZcount MTT cell assay kit, Himedia. For MTT assay, first, the media was removed from the wells of 96-well plate. The cells were then washed with PBS twice and 100µL of colorless DMEM media (Himedia cat no. AL264A). 10µL of MTT reagent was added to the wells and plate was incubated in dark at 37°C, 5% CO₂ for 4 hours. After the incubation period, 100µL of solubilization solution was added to the plate and it was incubated on a gyratory shaker for 15mins. The absorbance was measured at 570nm using Multimode reader, Biotek Instrument.

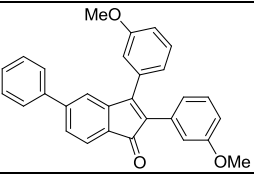
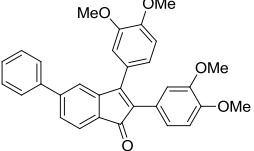
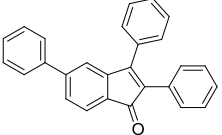
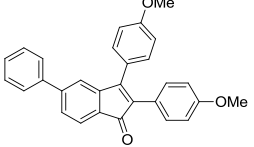
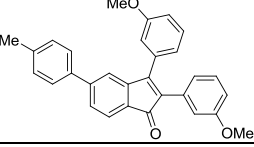
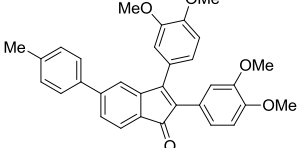
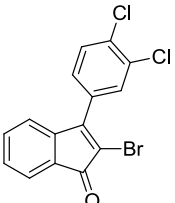
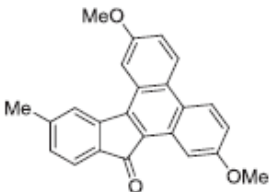
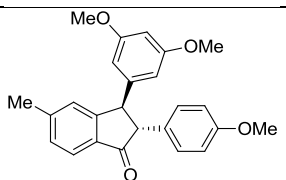
5.2.12. Effect of AlkBH3 inhibition on cell proliferation:

The effect of inhibition of AlkBH3 on the proliferation of A549 cells was studied. A549 cells were seeded in 96 well plates at the density of 1000 cells/ well and cultured

Table 8. Library of 22 indenone compounds screened for AlkBH3 inhibition

Structure	Molecular weight	Compound No.
	359.2139	4a
	329.1879	4b
	359.2139	4c
	299.1619	4d
	313.1885	4e
	349.2206	4f
	284.7369	5a
	346.8063	5b
	360.8329	5c

	386.4398	6a
	386.4398	6b
	448.5092	7a
	462.5357	7b
	356.4138	8a
	356.4138	8b
	296.3618	8c
	416.1624	8d
	324.4150	8e
	434.1421	8f

	418.4832	9a
	478.1780	9b
	358.1358	9c
	418.4832	9d
	432.5098	10a
	492.5617	10b
	354.0255	13
	363.45	14
	388.4557	15

in DMEM media (Himedia cat. No. AL219A) supplemented with 10% v/v fetal bovine serum (Genetix brand cat.No. CCS-500-SA-U). The cells were allowed to

adhere by overnight incubation at 37°C, 5% CO₂. Then the cells were treated with 1µM of compound **5a**, **5b** or **5c** in presence of MMS 1mM over a period of 60 hours. A parallel control experiment was set up where cell proliferation was monitored without any treatment. The cell density was determined after every 12-hour treatment using MTT assay. The protocol for MTT assay was same as discussed in section 5.2.10. The resulting cell number was plotted with respect to time.

5.2.13. MMS sensitivity of A549 cells

A549 cells were seeded in 96 well plates (2000 cells/well) and cultured in DMEM media supplemented with 10% v/v fetal bovine serum and incubated overnight at 37°C, 5% CO₂. A549 cells were exposed to various concentrations of MMS from 0-400µM (0, 10, 50, 100, 200, 300 and 400µM) for 48 hours. The cells were also treated with 1µM of compound **5a**, **5b** or **5c** to determine the effect of AlkBH3 inhibition on MMS sensitivity of A549 cells. After 48 hours, the cell viability at each MMS concentration with or without treatment with the compound was determined using the MTT assay. The protocol for MTT assay was same as discussed in section 5.2.10.

5.3. Results and discussion

5.3.1. Evaluation indenone compounds as an inhibitor of DNA repair by human AlkBH3

In order to screen compounds for their inhibitory effect on the activity of human AlkBH3, a robust assay that directly monitors formaldehyde release over time was used. The assay is based on the reaction of acetoacetanilide with formaldehyde in

presence of ammonium acetate and formation of a fluorescent dihydropyridine derivative with peak emission at 465 nm. Formaldehyde concentration was detected from a standard plot of formaldehyde. To carry out in vitro DNA repair reaction, purified *E. coli* AlkB, human AlkBH2, and AlkBH3 proteins were used. Recombinant proteins were purified without any affinity tag. MMS-damaged 40-mer oligonucleotide (T20 3meC T19) consisting of single N3meC was used as the substrate. For the screening of compounds, confirmed it was first confirmed that the DMSO concentration of 10% (the final concentration used for screening) did not affect the AlkB or AlkBH3 activity. In vitro DNA repair reactions (50 μ l) were performed at pH 8.0 for 1 h by using a purified enzyme (0.2 μ M) and 40-mer oligo-N3me-C (1 μ M) as substrate. All the in vitro assays were performed in parallel and the results were obtained with the same batch of the methylated oligonucleotide. Recombinant AlkB, AlkBH2, and AlkBH3 showed comparable repair as evident from the similar absorption at 465 nm (Fig. 28A and B). As a control to indicate no DNA repair reaction, catalytically dead mutant AlkB was used. In vitro screening was performed using 50 μ M of each of the compounds. To allow binding, the enzyme was mixed with compounds for 1 h before adding the substrate to the reaction. Representative results of the initial screening are shown in Fig. 31A. A compound was considered to have an inhibitory effect when the measured formaldehyde release was less than 10% of the DMSO control. As a result of the initial screening of 27 compounds, three compounds, namely **5c**, **8f** and **10a** displayed significant inhibitory effect on the human AlkBH3 activity. In order to find the selectivity of the compounds, the effect of **5c** was tested on the activity of *E. coli* AlkB and human AlkBH2. As shown in Fig. 31B AlkBH3 activity was

significantly affected by **5c** but AlkB and AlkBH2 activity remained unchanged. Next, the IC50 values of the compound **5c**, **8f** and **10a** were determined in vitro. As shown in Fig. 32, the IC50 value of the **5c** was found to 9.84 μ M. Although the IC50 values of **8f** and **10a** were also close, the compound with the lowest IC-50 was selected for further screening.

5.3.2. Conformational and binding analysis of AlkBH3 inhibitor 5c

The potent inhibitory activity of **5c** suggested that it might directly interact with AlkBH3. To test this hypothesis, the ability of the compounds to form complex was tested by using circular dichroism (CD) spectroscopy and isothermal titration calorimetry (ITC). Chiral molecules exhibit CD spectra when chromophore groups absorb light in the specific wavelength regions. Far-UV (190–260 nm) CD spectroscopy of proteins is characteristic of backbone folding whereas the near-UV (260–310 nm) CD spectroscopy gives information about the local tertiary structure of the aromatic side-chain residues such as tryptophan, tyrosine and phenylalanine, and disulfide bonds. The far-UV CD spectra of AlkBH3 and **5c**-bound AlkBH3 revealed that the **5c** binding resulted in alteration of CD signal at 195 nm, characteristic double-stranded β - helix conformation of AlkBH3 (Fig. 33). This indicated that the conformational change induced by binding of **5c** might involve only a few residues from a larger and structured domain, most probably the jelly roll fold where active site is located. near-UV CD-spectra of AlkBH3 in the presence and absence of **5c** was also analyzed. As shown in Fig. 33, near-UV CD spectra of the **5c**-bound AlkBH3 were different from the free protein. The compound **5c** being achiral molecule did not exhibit any CD signal. Since AlkBH3 lack disulfide bond, near-UV CD spectroscopy only.

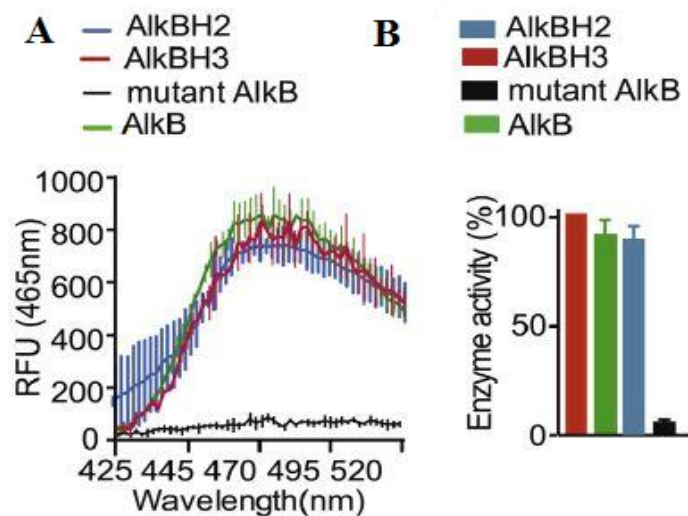


Figure 28: (A) Fluorescence emission spectra of recombinant AlkB, AlkBH2, AlkBH3 and mutant AlkB for comparing enzyme activity. (B) Bar graph representation of AlkB, AlkBH2, AlkBH3 and mutant AlkB activity quantified by measuring released formaldehyde. Error bar depicts the standard error from three independent experiments.

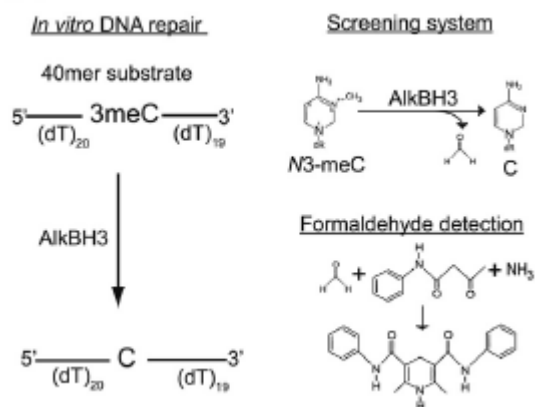


Figure 29: Inhibitor screening assay

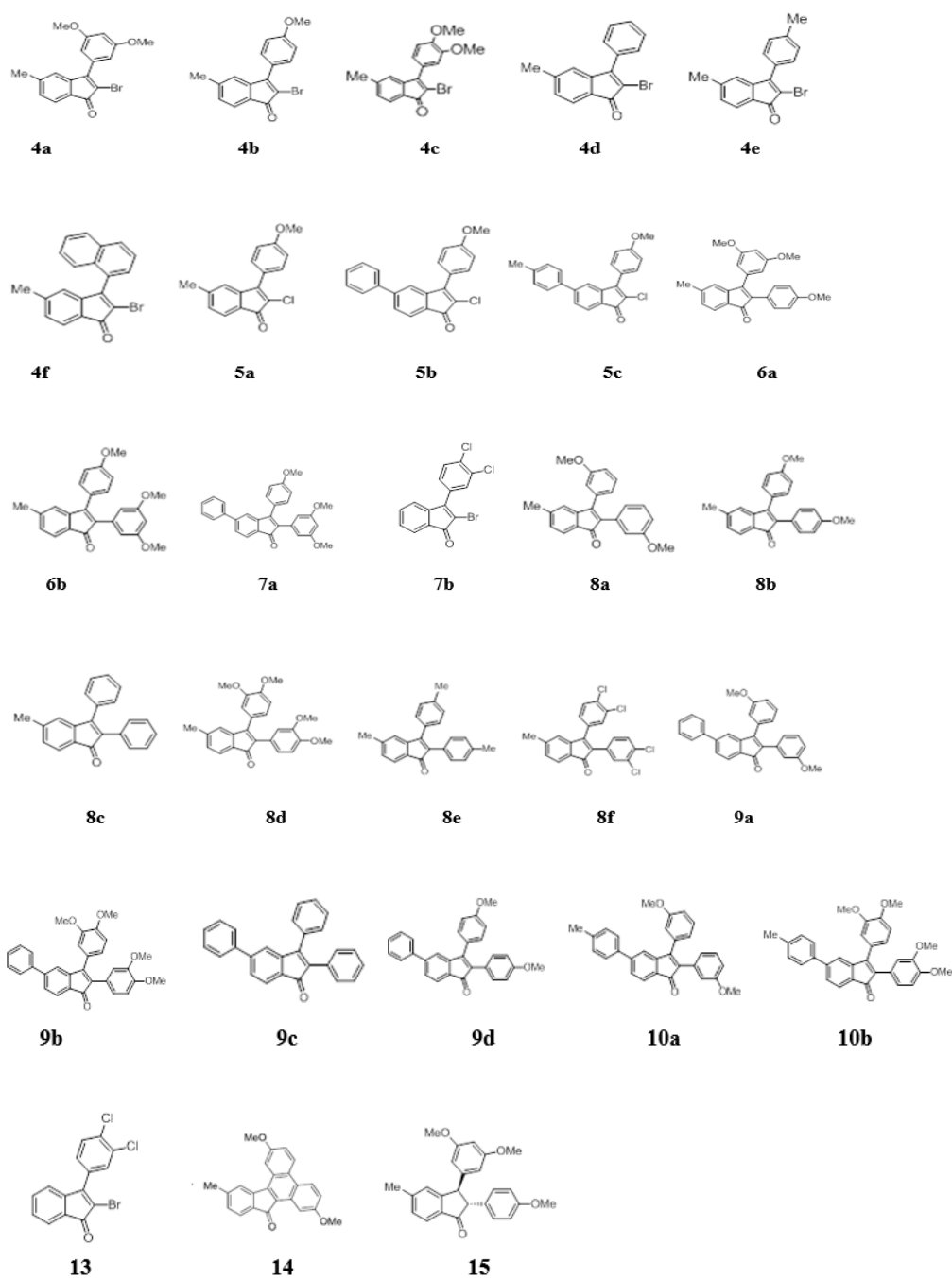


Figure 30: Library of 27 indenone analogs screened for inhibition of AlkBH3 demethylation activity.

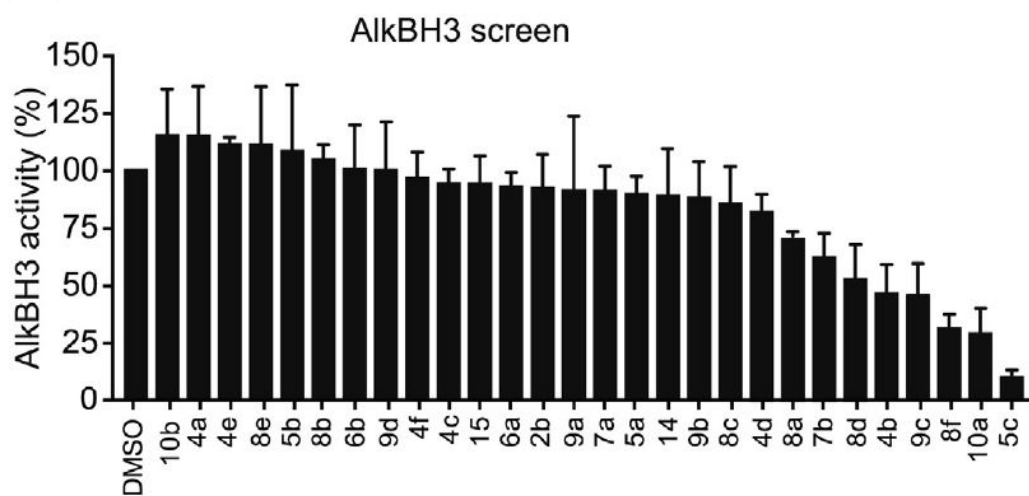
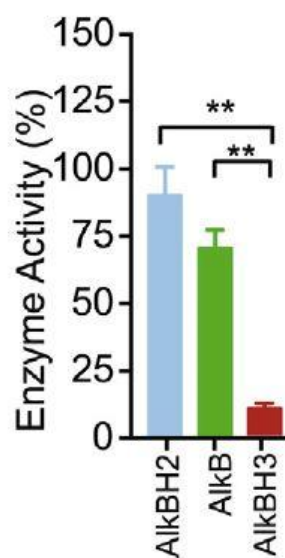
A**B**

Figure 31: (A) screening for inhibition of AlkBH3 activity with 27 indenone (B) Effect of AlkBH3 inhibitor 5c on the activity of AlkB and AlkBH2. Error bars represent \pm SEM (n=5). **P < 0.01; Student's t-tests.

depicted asymmetry surrounding the aromatic residues and any associated tertiary structure perturbations in the microenvironment. As Shown in Fig. 33, near UV CD spectrum of AlkBH3- **5c** indicated the variation of the chiral environment of aromatic amino acid residues, tryptophan (290–300 nm), tyrosine (270–280 nm) and phenylalanine (250–270 nm). Together, the CD spectroscopy data strongly suggested subtle structural changes of AlkBH3 molecule upon **5c** binding. Next, the binding of AlkBH3 to **5c** was validated by quantifying the corresponding thermodynamic parameters by ITC. The ITC data were fitted to a one-binding site model and the derived parameters are shown in Fig. 34. The data revealed that the binding between **5c** and AlkBH3 were tight ($K_d=7.81 \mu\text{M}$) and binding resulted in an unfavorable entropy change ($\Delta S < 0$) and a favorable enthalpy change ($\Delta H < 0$). ΔS and ΔH both being negative signified favorable non-covalent interactions, including electrostatic, H-bonding and van der Waals interactions between the AlkB/AlkBH3 protein and the compound.

5.3.3. Mechanism of inhibition of AlkBH3

Steady-state enzyme kinetics was performed to study the mechanism of inhibition of the compounds. For this, the initial velocity of AlkBH3 was determined in the presence of increasing concentrations (50–500 μM) of compound **5c**. The variable concentration of substrate and fixed saturating concentration of co-substrate 2OG (200 μM) was used. The initial velocities of AlkBH3 in presence of increasing concentration of compound **5c** resulted in unchanged V_{max} , a feature characteristic of competitive inhibitor (Fig. 35A). It was speculated that **5c** might bind close to the catalytic site of AlkBH3. The initial velocities of AlkBH3 were also analyzed by the

variable concentration of co-substrate (2OG) and fixed saturating concentration of substrate DNA (1.5 μM) and increasing concentration of **5c**. As shown in Fig. 35B, with AlkBH3 and a variable concentration of 2OG, Lineweaver-Burk plot revealed a concomitant decrease of V_{max} with increasing concentration of **5c** and the intersection of the lines were above the y-axis, which suggested the compound **5c** to be mixed type inhibitor with respect to 2OG cosubstrate. Such mixed-type inhibition against 2OG substrate of AlkBH3 by **5c** might be indicated that these compounds bind to a site different from the 2OG-binding site and thus influence the binding of 2OG by indirect competition. Taken together, these results provided evidence that indenone- derived compound **5c** can inhibit DNA repair activity by directly competing with the substrate binding and indirectly affecting 2OG binding.

To gain further insight into the mechanism of **5c**, the binding efficiency of **5c** to the target molecule AlkBH3 was analysed by molecular docking studies. Notably, **5c** differs structurally from **5a** and **5b** by an aromatic ring and methyl group, respectively. The docking analysis demonstrated that **5c** forms pi-sigma bond with His 191, which is part of the active site iron coordination triad that forms the characteristic HD...H motif. The carbonyl group of **5c** makes hydrogen bond with Arg131 via side chain amino group of present at a distance of 3.10 Å. It also interacts with Arg 131 via pi-cation bonding. Interestingly, Arg 131 is important for binding of in-coming damaged

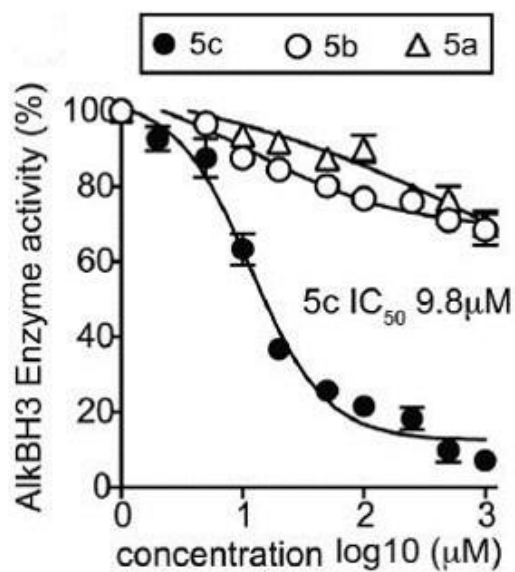


Figure 32: IC₅₀ data of compounds **5a**, **5b** and **5c** against AlkBH3

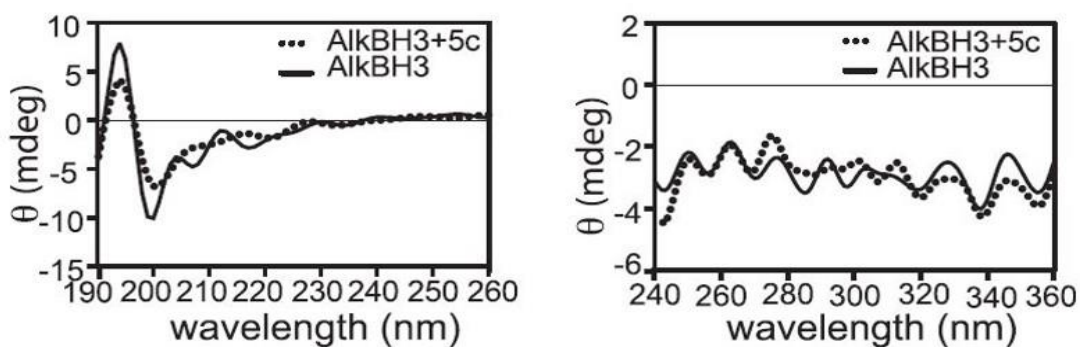


Figure 33: Conformational analysis of AlkBH3-5c interaction by circular dichroism (CD). Far-UV CD spectra (between 190 nm and 260 nm) for AlkBH3 or AlkbH3 with compound 5c bound; near-UV CD spectra (between 240 nm and 360 nm) for AlkBH3

base to the pocket. **5c** also interacts with Tyr 143 by pi-pi stacking and Arg 275 by pi-cation interaction. Agr275 is involved in 2OG binding via coordination with C1

of 2OG. Overall, most of the **5c** interacting residues are of catalytic importance to AlkBH3. Mutational studies have shown that point mutation of any of these of residues makes AlkBH3 inactive [25]. On the other hand, docking analysis of **5b** showed that it interacts with Tyr 143 by forming pi-pi stacking but unlike **5c**, it does not interfere with either the DNA binding residues or the 2OG coordination residues. Similarly, docking analysis of **5a** showed that it binds to a different location further away from the DNA binding pocket via interaction with Ile 203. Taken together, molecular docking analysis revealed structure-activity relationship of AlkBH3 inhibition by 5c and suggested that binding of 5c to the close proximity of the active site might affect the catalytic activity of AlkBH3. 3d-Graphical representation of docked position of **5c**, **5b** and **5a** on AlkBH3 molecule is shown in Fig. 36. The ligand binding residues for compound **5c**, **5b** and **5c** and the bonds formed between these molecules and amino acid residues from AlkBH3 are shown 2d-diagram in Fig. 37.

5.3.4. Compound 5c inhibits proliferation of human lung carcinoma A549 cells in a dose-dependent manner and sensitizes to alkylating agent MMS

Human AlkBH3 is overexpressed in non-small cell lung adenocarcinoma cell line A549 and AlkBH3 gene silencing was reported to inhibit A549 cell survival. In order to test if **5c** can affect the viability of A549 cell line under the culture condition, these cells were examined in the presence of increasing concentration of **5c** using the MTT assay. It was evident that higher concentrations of **5c** in the culture medium inhibited the viability of A549 cells in a dose-dependent manner (Fig. 38). The concentration of **5c** to inhibit 50% cell growth (EC50) was estimated to be around 18.7 μ M. Since **5c** is structurally similar to **5a** and **5b**, cell viability was

also tested in the presence of 5a and 5b. EC50 of **5b** was much larger than **5c** (369.7 μM). A similar result was also obtained with compound 5a, which did not show any sensitivity even at 500 μM . Based on this result, it was concluded that only **5c** could affect the A549 cell viability and **5a** and **5b**, though structurally similar, had much less effect on cell viability. Next, the effect of AlkBH3 inhibition on cell proliferation was studied. It was found that exposure to low concentration of **5c** is sufficient to significantly suppress cell growth (Fig. 39).

As expected, compound **5b** and **5a** had no effect on cell proliferation. AlkBH3-deficient primary MEFs (mouse embryonic fibroblasts) are at least twice as sensitive to SN2-type alkylating agents MMS compared to wild-type MEFs. The objective was to see if **5c** can potentiate the cytotoxic effect of the mono-functional alkylating agent MMS. MMS is a classic SN2 type alkylating compound which produces mainly N-alkylated base damage and AlkBH3 protects from MMS-induced cytotoxicity. It was found that **5c** treatment significantly increased MMS sensitivity compared to the control (DMSO) in A549 cell (Fig. 40). On the contrary, compound **5b** and **5a** did not cause any MMS sensitivity. Collectively, the result demonstrated that **5c** prevented the growth of lung cancer cell line A549 and enhanced sensitivity to alkylating agent MMS. Although AlkBH3 knock-down was reported to inhibit A549 cell proliferation,^{3,9} it remains unclear whether the growth inhibition is directly due to defect of AlkBH3-mediated DNA repair. As AlkBH2-mediated DNA

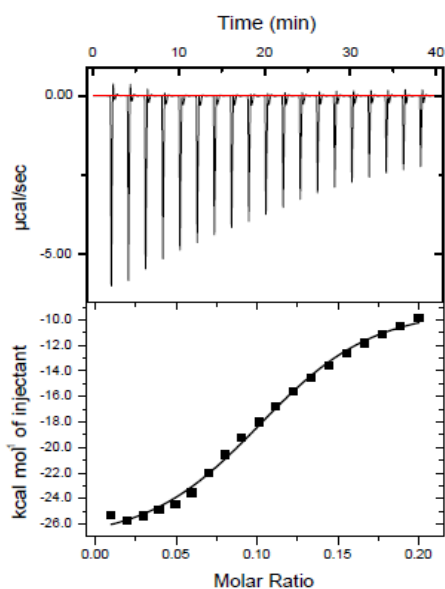


Figure 34: Binding analysis of AlkBH3-5c by isothermal titration calorimetry (ITC). Binding of compound 5c to recombinant AlkBH3. The top panel represents the raw data from the titration as a series of peaks corresponding to the heat change (μ calories/s) with each injection. The bottom panel is a plot of heat change on ligand addition (kcal/mol) against the 5c/AlkBH3 Molar ratio.

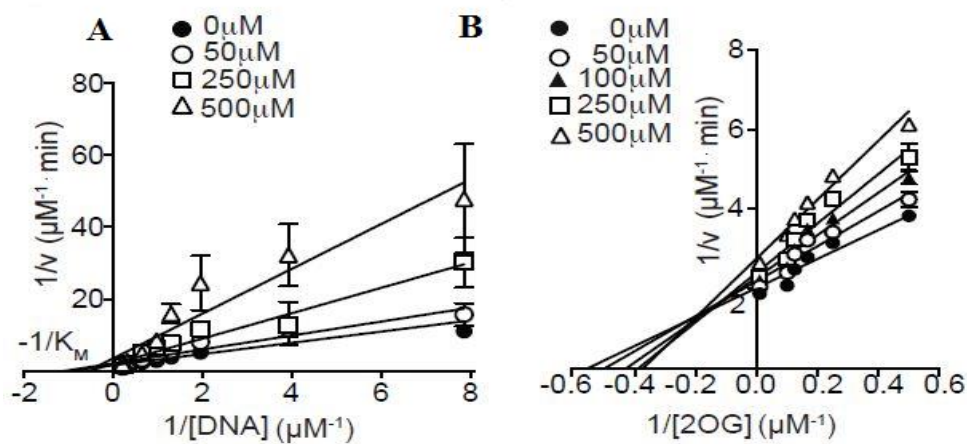
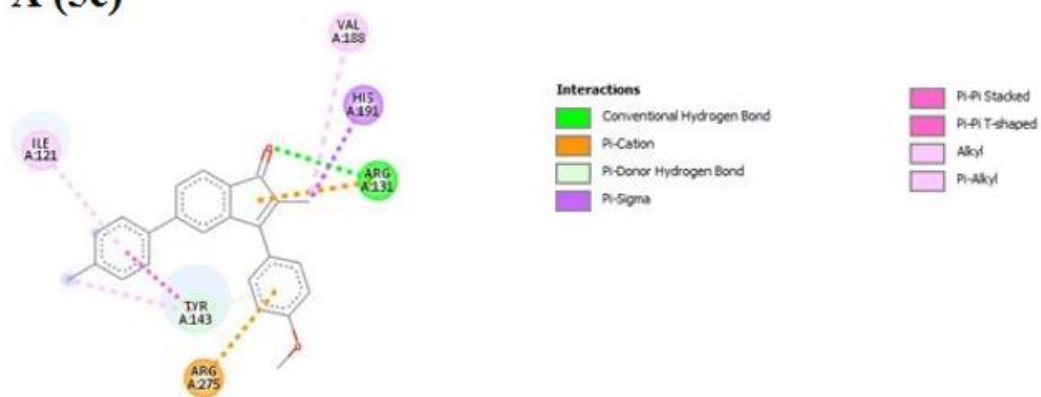


Figure 35: Mechanism of catalytic inhibition. (A) The effect of increasing concentrations of compound 5c over the rate of reaction of AlkBH3. (B) The effect of increasing concentrations of compound 5c over the rate of AlkBH3- catalyzed reaction with respect to 2OG. Error bars represent standard error from three independent experiments.

repair remains unaltered, it can be speculated that some unique DNA damage signaling pathway operates in A549 cells that causes inhibition of cell proliferation. Therefore, attributing the MMS sensitivity of A549 cells solely to AlkBH3 inhibition may not be accurate. Furthermore, **5c** might also have pleiotropic effects and target some DNA damage response pathways or AlkB homologues in living cells as the specific functions of these homologues are not completely understood. Several indenone compounds were evaluated as potential inhibitors of AlkBH3 catalyzed DNA demethylation. The primary screens, based on in vitro inhibition of the demethylase activity of AlkBH3 using single-base methylated DNA substrate and purified enzyme, resulted in one inhibitor against human AlkBH3. The compound **5c** exhibited modest binding properties and was able to inhibit the function of AlkBH3 in vitro. Addition of **5c** also abrogated lung cancer cell line A549 growth and enhanced sensitivity to DNA alkylating agent MMS in the micromolar range of concentrations. Determining the precise mechanism of the inhibitors will require further investigation, including solving the structure with the inhibitors. The multitude of reports implicating AlkBH3 activity to the proliferation of cancer cells reflects the need for potent and selective inhibitors of AlkBH3 so that its pathobiology can be further explored and validated.

A (5c)



B(5b)



C(5a)

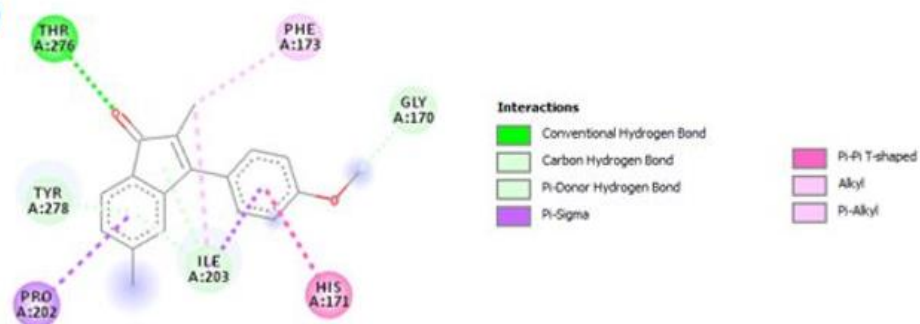


Figure 37: 2D interaction diagram of docked conformation showing interaction diagram of (A) 5c (B) 5b (C) 5a with AlkBH3.

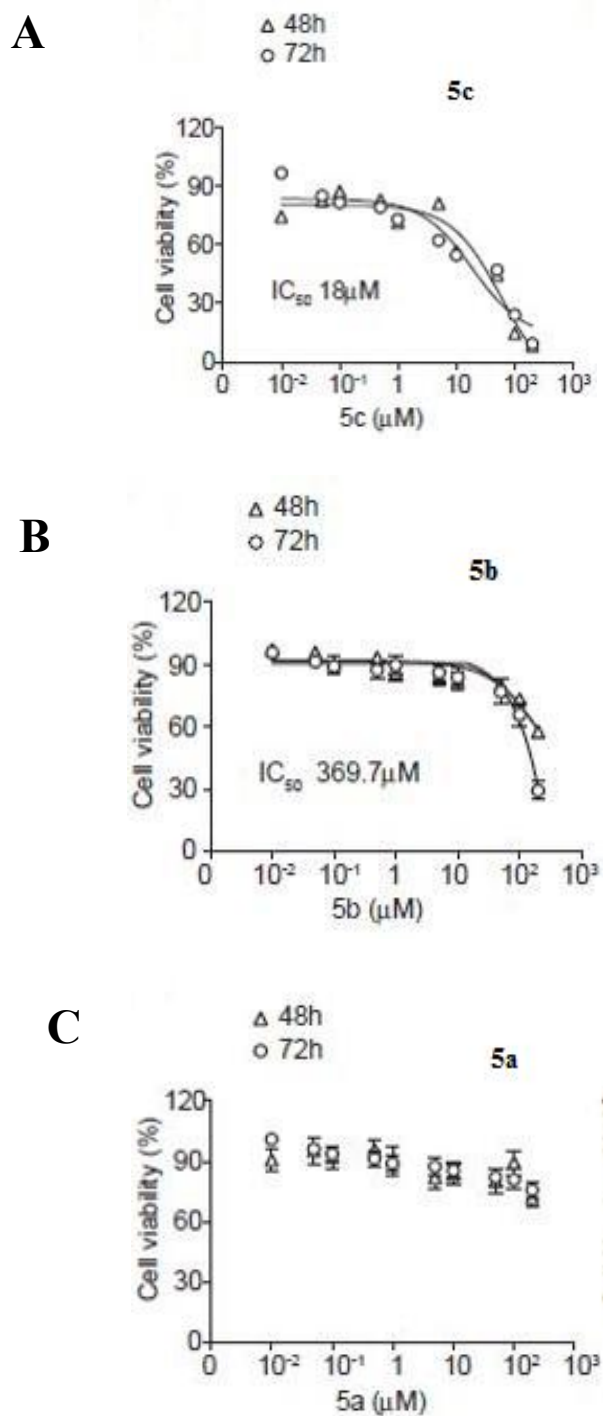


Figure 38: (A) cytotoxic/cytostatic effect of **5c**, (B) **5b**, (C) **5a**, respectively, evaluated by MTT assay. A549 cells were plated into 96-well plates, and cultured for 48–72 h in varying concentrations (0–200 μM) of compounds.

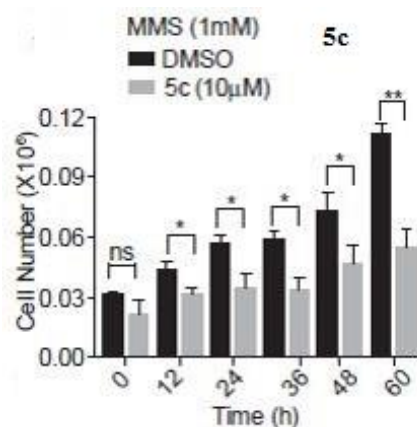
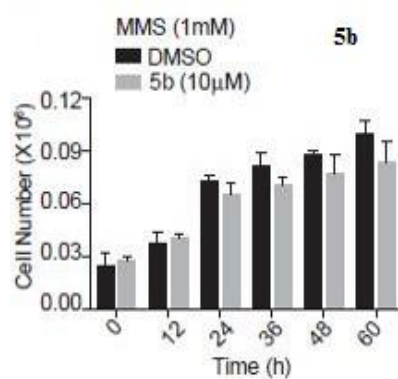
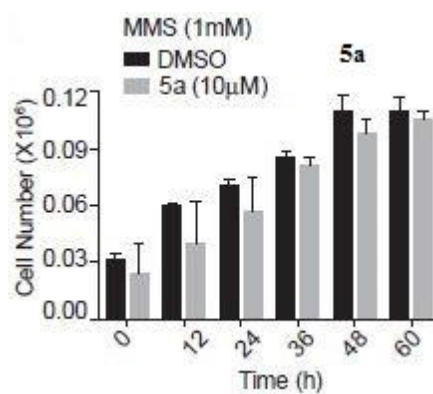
A**B****C**

Figure 39: Inhibition of A549 cell growth by **5c** (A), **5b** (B) **5a** (c), respectively, during a time course. 12 h after seeding, the cells were exposed for two doubling time continuously to the fixed concentrations (1 µM) of compounds. Each bar represents results of four independent experiments.

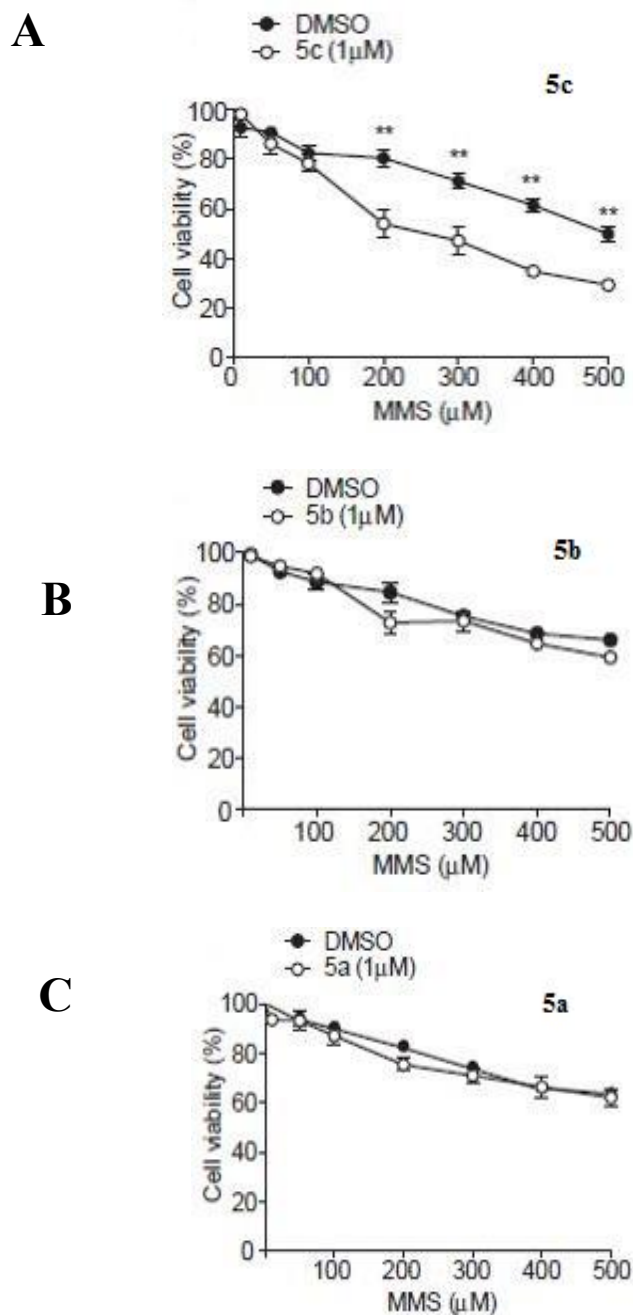


Figure 40: A549 cells were exposed to MMS at various concentrations (0, 10, 50, 100, 200, 300 and 400 μM) for 48 h; then cell viability was evaluated by MTT assay. Error bar represent the SEM of replicates from four representative experiment that was repeated two times. *P < 0.05; **P < 0.01; Student's t-tests, ns, not significant.

There were a few other limitations of this study. Firstly, the results were presented based on a small set of compounds. Further synthetic efforts are required to validate the SAR of this compound. Secondly, IC₅₀ of the compound **5c** was estimated to be 9.8 μM. Although this is close to known AlkBH3 inhibitor Rhein (5.3 μM), future efforts will be directed to obtain a compound with sub-micromolar IC₅₀. The fact that at least one hit had been found out of 27 compounds, suggests that indenone derivatives could provide a platform for generating inhibitor against Fe(II)/2OG-dependent dioxygenases. It could be anticipated that these compounds might provide a framework from which second-generation indenone derivatives may be developed. The future challenge includes the development of a more potent indenone-derived AlkBH3 inhibitor, which may be exploited as a combination therapy for cancer treatment. These results might also help in finding potential pharmaceutical applications of indenone derivatives as inhibitors of other human 2OG/Fe(II)-dependent oxygenase and overcoming resistance to alkylating agents used in cancer therapy.

5.4. References

1. Moore, Lisa D et al. "DNA methylation and its basic function" *Neuropsychopharmacology : official publication of the American College of Neuropsychopharmacology* vol. 38,1 (2012): 23-38.
2. Rošić, Silvana et al. "Evolutionary analysis indicates that DNA alkylation damage is a byproduct of cytosine DNA methyltransferase activity" *Nature genetics* vol. 50,3 (2018): 452-459.
3. Subramaniam, Dharmalingam et al. "DNA methyltransferases: a novel target for prevention and therapy" *Frontiers in oncology* vol. 4 80. 2014, doi:10.3389/fonc.2014.00080
4. Zhang and Xu *Biomarker Research* (2017) 5:1 DOI 10.1186/s40364-017-0081-z
5. Falnes, P.Ø., et al., *Substrate specificities of bacterial and human AlkB proteins*. *Nucleic acids research*, 2004. **32**(11): p. 3456-3461.
6. Cetica, V., et al., *Pediatric brain tumors: mutations of two dioxygenases (hABH2 and hABH3) that directly repair alkylation damage*. *Journal of neuro-oncology*, 2009. **94**(2): p. 195-201.
7. Choi, S.-y., J.H. Jang, and K.R. Kim, *Analysis of differentially expressed genes in human rectal carcinoma using suppression subtractive hybridization*. *Clinical and experimental medicine*, 2011. **11**(4): p. 219-226.
8. Kogaki, T., et al., *TP53 gene status is a critical determinant of phenotypes induced by ALKBH3 knockdown in non-small cell lung cancers*. *Biochemical and biophysical research communications*, 2017. **488**(2): p. 285-290.

9. Koike, K., et al., *anti-tumor effect of AlkB homolog 3 knockdown in hormone-independent prostate cancer cells*. 2012. **12**(7): p. 847-856.
10. Konishi, N., et al., *High expression of a new marker PCA-1 in human prostate carcinoma*. 2005. **11**(14): p. 5090-5097.
11. Liefke, R., et al., *The oxidative demethylase ALKBH3 marks hyperactive gene promoters in human cancer cells*. *Genome medicine*, 2015. **7**(1): p. 66.
12. Müller, R., et al., *Targeting proliferating cell nuclear antigen and its protein interactions induces apoptosis in multiple myeloma cells*. *PloS one*, 2013. **8**(7): p. e70430.
13. Shimada, K., et al., *ALKBH3 contributes to survival and angiogenesis of human urothelial carcinoma cells through NADPH oxidase and tweak/Fn14/VEGF signals*. *Clinical Cancer Research*, 2012: p. 5247-5255.
14. Shimada, K., et al., *Prostate cancer antigen-1 contributes to cell survival and invasion through discoidin receptor 1 in human prostate cancer*. 2008. **99**(1): p. 39-45.
15. Tasaki, M., et al., *ALKBH3, a human AlkB homologue, contributes to cell survival in human non-small-cell lung cancer*. *British journal of cancer*, 2011. **104**(4): p. 700-706.
16. Ueda, M., et al., *Novel Metabolically Stable PCA-1/ALKBH3 Inhibitor Has Potent Antiproliferative Effects on DU145 Cells In Vivo*. *Anticancer research*, 2018. **38**(1): p. 211-218.
17. Wang, Q., et al., *Association of AlkB homolog 3 expression with tumor recurrence and unfavorable prognosis in hepatocellular carcinoma*. *Journal of gastroenterology and hepatology*, 2018. doi: 10.1111/jgh.14117.

18. Yamato, I., et al., *PCA-1/ALKBH3 contributes to pancreatic cancer by supporting apoptotic resistance and angiogenesis*. 2012; 72 p.4829-4839.
19. Dango, S., et al., *DNA unwinding by ASCC3 helicase is coupled to ALKBH3-dependent DNA alkylation repair and cancer cell proliferation*. *Molecular cell*, 2011. **44**(3): p. 373-384.
20. Ueda, Y., et al., *AlkB homolog 3-mediated tRNA demethylation promotes protein synthesis in cancer cells*. *Scientific reports*, 2017. **7**: 42271.
21. Koike, K., et al., *anti-tumor effect of AlkB homolog 3 knockdown in hormone-independent prostate cancer cells*. *Current cancer drug targets*, 2012. **12**(7): p. 847-856.
22. Hotta, K., et al., *Clinical significance and therapeutic potential of prostate cancer antigen-1/ALKBH3 in human renal cell carcinoma*. *Oncology reports*, 2015. **34**(2): p. 648-654.
23. Shivange, G., et al., *A role for Saccharomyces cerevisiae Tpa1 protein in direct alkylation repair*. 2014, 289: p. 3389-97.
24. Sundheim, O., et al., *Human ABH3 structure and key residues for oxidative demethylation to reverse DNA/RNA damage*. 2006. **25**(14): p. 3389-3397.

List of publications

1. **Richa Nigam**, Roy Anindya. Escherichia coli single-stranded DNA binding protein SSB promotes AlkB-mediated DNA dealkylation repair, *Biochemical and Biophysical Research Communications* (2018), 496, (2), 274-279. Doi:10.1016/j.bbrc.2018.01.043
2. **Richa Nigam**, Monisha Mohan, Gururaj Shivange, Pranjal Kuamr Dewangan, Roy Anindya, Escherichia coli AlkB interacts with single-stranded DNA binding protein SSB by an intrinsically disordered region of SSB, *Molecular Biology Reports* (2018). Doi:10.1007/s11033-018-4232-6
3. **Richa Nigam**, Kaki Raveendra Babu, Topi Ghosh, Bhavini Kumari, Deepa Akula, Subha Narayan Rath, Prolay Das, Roy Anindya, Faiz Ahmed Khan, Indenone derivatives as inhibitor of human DNA dealkylation repair nzyme AlkBH3, *Bioorganic & Medicinal Chemistry* (2018),26, (14), 4100-4112, Doi: 10.1016/j.bmc.2018.06.040
4. **Richa Nigam**, Monisha Mohan, Roy Anindya, Escherichia coli single-stranded DNA binding protein SSB binds to AlkB and promotes DNA repair. *FEBS Open Bio*, 8: 28135 . [Doi:10.1002/2211-5463.12453](https://doi.org/10.1002/2211-5463.12453)
5. Gururaj Shivange, Monisha Mohan, **Richa Nigam**, Naveena Kodipelli, Roy Anindya, RecA stimulates AlkB-mediated direct repair of DNA adducts, *Nucleic Acids Research*, (2016), 44, (18), 8754-8763. Doi:10.1093/nar/gkw611.